To the Graduate Council:

I am submitting herewith a thesis written by Naveen Bhojraj entitled "Structure and Properties of Oriented films Prepared from Styrene-Maleic Anhydride Copolymers and Polystyrene." I have examined the final copy of this thesis for form and content and recommend that it be accepted in partial fulfillment of the requirements for the degree of Master of Science, with a major in Polymer Engineering.

Joseph E. Spruiell, Major Professor

We have read this thesis
and recommend its acceptance:

John F. Fellers

Accepted for the Council:

Associate Vice Chancellor
and Dean of the Graduate School

STATEMENT OF PERMISSION TO USE

I am presenting this thesis in partial fulfillment of the requirements for a Master's degree at The University of Tennessee, Knoxville, I agree that the Library shall make it available to borrowers under the rules of the Library. Brief quotations from this thesis are allowable without special permission, provided that accurate acknowledgement of the source is made.

Permission for extensive quotation from or reproduction of this thesis may be granted by my major professor, or in his absence, by the Head of Interlibrary Services when, in the opinion of either, the proposed use of the material is for scholarly purposes. Any copying or use of the material in this thesis for financial gain shall not be allowed without my written permission.

Signature N Duncan

Date July 10, 1992

STRUCTURE AND PROPERTIES OF ORIENTED FILMS PREPARED FROM STYRENE-MALEIC ANHYDRIDE COPOLYMERS AND POLYSTYRENE

A Thesis
Presented for the
Master of Science
Degree
The University of Tennessee, Knoxville

Naveen Bhojraj
August 1992

ACKNOWLEDGEMENTS

I would like to express my appreciation to my advisor Professor Joseph E. Spruiell for his contributions and guidance during the course of this work. I would also like to acknowledge ARCO Chemical Company for providing the financial support and technical support for this project. My special thanks are due to Dr. Steven A. Schwartz for coordinating this project and for his helpful suggestions.

I also wish to express my acknowledgements to my advisory committee Dr. Donald C. Bogue and Dr. Jack F. Fellers for their support and help during the project.

ABSTRACT

A study was carried out to determine processing parameters and to characterize oriented films prepared from copolymers of styrene maleic anhydride (S/MA) with 8 % and 14 % maleic anhydride. The purpose of this study was to investigate the potential of these films for packaging applications that would withstand the temperatures of foods being heated in microwave ovens. Studies on the pure homopolymer of polystyrene were also done in order to provide comparison of the S/MA material to that of a similar material of known properties. Oriented films from uniaxial to biaxial nature were prepared for each grade under a range of process conditions using a biaxial stretching apparatus. The resulting films exhibited a range of molecular orientations and mechanical properties.

In general the molecular orientation increased with increase in the stretch ratio and strain rate. Films prepared from compression molded plaques had more uniform and reproducible properties than the same films produced from plaques cut from extruded sheets. Thus residual orientation in the sheet prior to stretching plays an important role in successfully orienting and predicting the properties of S/MA films prepared from extruded sheets.

The optimum process temperatures for S/MA 3000FG (14 % MA) was 170°C while S/MA 2000 FG (8 % MA) and PS (0% MA) processed at the lower temperatures of 155°C and 140°C, respectively. The differences in processing temperatures reflects the

variation of the Tg of the polymer with increase in the maleic anhydride content.

The degree of molecular orientation for all the grades investigated was found to be very sensitive to the stretch temperature. Increase in the stretch temperature sharply decreased the final orientation in the films.

For the optimum process temperature range, for a common stretch ratio and strain rate, the tensile strengths of these polymers in decreasing order were S/MA 3000FG > S/MA 2000FG > PS.

Films of polystyrene prepared under identical conditions but three different starting thicknesses of 14 mils, 21 mils and 26 mils gave maximum strengths and molecular orientation in films prepared from plaques of 21 mils starting thickness.

TABLE OF CONTENTS

CHAPTER **PAGE**

1. INTRODUCTION....1

2. BACKGROUND AND LITERATURE REVIEW

2.1 GENERAL CONSIDERATIONS....3

2.1.1 Copolymerization....3

2.1.2 Basic Structure of S/MA....5

2.1.3 Cast Film and Tenter Frame Process....9

2.1.4 Vacuum Forming Process....11

2.2 MOLECULAR ORIENTATION IN POLYMERS....11

2.2.1 Introduction....11

2.2.2 Orientation Development in Flowing Melts and Its Relation to Stress....13

2.2.3 Representation of Orientation in Crystalline and Amorphous Polymers....14

2.2.4 Methods for Detecting Molecular Orientation....22

3 EXPERIMENTAL

3.1 MATERIALS....39

3.2 PROCESSING....39

3.2.1 Preparation of Initial Samples....39

3.2.2 Prepration of Biaxially Stretched Films....42

3.3 CHARACTERIZATION....42

3.3.1 Tensile Testing....43
3.3.2 Dynamic Mechanical Analysis....43
3.3.3 Birefringence....43
3.3.4 Shrinkage Measurements....51

4 RESULTS AND DISCUSSIONS
4.1 GENERAL CHARACTERIZATION AND COMPARISON OF RESINS....52
4.1.1 Glass Transition Temperatures....52
4.1.2 Tensile Properties of Unoriented Resins....54
4.1.3 Preliminary Determination of Processing Window....54
4.1.4 Estimation of Intrinsic Birefringences....57
4.2 MOLECULAR ORIENTATION OF FILMS PREPARED FROM COMPRESSION MOLDED PLAQUES....58
4.2.1 Birefringence of S/MA 3000 (14% MA) Films....59
4.2.2 Birefringence of S/MA 2000 (8% MA) Films....68
4.2.3 Birefringence of Polystyrene 8G (0% MA) Films....71
4.2.4 Comparison of Orientation Developed in the Three Resins....75
4.3 MECHANICAL PROPERTIES OF FILMS PREPARED FROM COMPRESSION MOLDED PLAQUES....84
4.3.1 S/MA 3000 (14% MA) Films....84
4.3.2 S/MA 2000 (8% MA) Films....88
4.3.3 Polystyrene 8G (0% MA) Films....88
4.3.4 Comparison of the Three Resins....100
4.4 EFFECT OF INITIAL PLAQUE THICKNESS ON THE ORIENTATION DEVELOPMENT IN FILMS OF POLYSTYRENE....100

4.5 SHRINKAGE BEHAVIOR OF S/MA AND PS FILMS.....111
4.6 STRETCHING TO FILMS FROM EXTRUDED SHEETS.....120
5 SUMMARY AND CONCLUSIONS.....140
REFERENCES.....143
VITA.....148

LIST OF TABLES

TABLE **PAGE**

2.1 Styrene comonomer reactivity ratios.....6

2.2 White-Spruiell orientation factors for different types of orientation in a film.....18

2.3 Values of intrinsic birefringence of fully oriented polystyrene in literature.....38

3.1 Material specifications of S/MA and Polystyrene.....40

3.2 Parameter settings for compression molding of S/MA and Polystyrene plaques.....41

4.1 Optimum stretch temperatures for stretching in the T.M. Long stretcher.....56

4.2 Values calculated for the intrinsic birefringence of S/MA and PS.....60

LIST OF FIGURES

FIGURE **PAGE**

2.1 Random copolymer of Styrene Maleic Anhydride....8

2.2 Tenter frame process for continuous oriented polystyrene making process....10

2.3 Schematic diagram of a vacuum forming process....12

2.4 Different states of orientation in films showing White and Spruiell biaxial orientation factors....19

2.5 Graphical representation of orientation in the orientation triangle diagram....21

2.6 Refractive index ellipsoid: (a) Optically isotropic medium. (b) Optically anisotropic medium....30

2.7 Film strip showing the projections of the refractive index ellipsoid on the three sides of the polymer film and the definition of these birefringence values....31

2.8 Coordinate reference axis for the calculation of intrinsic birefringence....35

3.1 Schematic diagram of Garetner plane polariscope for determining birefringence....44

3.2 Reference directions for stretching: 1 is the machine direction, 2 is the transverse direction and 3 is the direction normal to the plane of the sheet....47

3.3 Babinet compensator showing wedge movement and direction of optic axis....48

3.4 Optical bench with compensator and rotating stage to determine in-plane and out-of plane birefringences.....50
4.1 Plots of linear tan delta as a function of temperature for S/MA and PS measured at 1.1 Hz in dynamic mechanical measurements.....53
4.2 Room temperature stress strain curves for PS and S/MA polymers (The numbers on the curves indicate the tensile modulus in psi.....55
4.3 Birefringence for unconstrained uniaxial stretching of S/MA 3000 at 2000 %/min-(compression molded).....61
4.4 Birefringence for equal biaxial stretching of S/MA 3000 at 2000 %/min (compression molded) 62
4.5 Effect of stretch temperature on orientation for films made from compression molded S/MA 3000 (2.5 MD x 2.0 TD, 2000 %/min)..... 64
4.6 Effect of Strain rate on a 3000 S/MA film stretched to a 3 x 2 ratio at 168 C.....65
4.7 Birefringence vs. uniaxial stretch ratio for films from compression molded S/MA 2000 (2000 %/min and 155 C).....69
4.8 Birefringence vs. biaxial stretch ratio for films from compression molded S/MA 2000 (2000 %/min and 155 C).....70
4.9 Effect of stretch temperature on orientation for films made from compression molded S/MA 2000. (2.5 MD x 2.0TD Stretch Ratio, 2000%/min).....72

4.10 Strain rate effect for S/MA 2000 stretched to a 3 x 2 ratio at 155 C....73
4.11 In-plane birefringence for PS for several biaxial stretch ratios....74
4.12 Out of-plane birefringence for PS for several biaxial stretch ratios....76
4.13 Birefringence data for equal biaxial stretch of polystyrene films made from compression molded plaques (2000 %/min, 140 C)....77
4.14 Effect of stretch temperature on orientation for films made from compression molded PS....78
4.15 Effect of birefringence on strain rate for films stretched from 26 mils plaques of PS to a 3 x 2 stretch ratio, 140 C....79
4.16 Effect of the stretch temperatures on the orientation of films made from compression molded polystyrene and S/MA copolymers (2.5MDx2.0TD, 2000 %/min)....81
4.17 Orientation diagram for biaxially stretched films of polystyrene and S/MA copolymers and the indicated stretch temperatures for a strain rate of 2000 %/min....82
4.18 Orientation factors for PS and S/MA stretched to a ratio of 4 MD x 2.5 TD at 2000 %/min....85
4.19 Tensile strength for compression molded S/MA 3000 equal biaxial stretch at 2000 %/min....86
4.20 Elongation to break for compression molded S/MA 3000 equal biaxial stretch at 2000 %/min....87

4.21 Tensile strength for compression molded S/MA 2000 equal biaxial stretch at 2000 %/min....89
4.22 Elongation to break for compression molded S/MA 2000 equal biaxial stretch at 2000 %/min....90
4.23 Effect of temperature on the stress at break for compression molded S/MA 2000 and 2.5 MD x 2.0 TD stretch ratio....91
4.24 Effect of temperature on the strain at break along and transverse to the machine direction for compression molded S/MA 2000 and 2.5 MD x 2.0 TD stretch ratio....92
4.25 Stress at break for films of PS with a fixed stretch ratio of 1.5 along the TD and tested along the MD (26 mils thk, 140 C and 2000 %/min)....93
4.26 Elongation to break for films of PS with a fixed stretch ratio of 1.5 along the TD and tested along the MD (26 mils thk, 140 C and 2000 %/min)....95
4.27 Stress at break for films of PS with a fixed stretch ratio of 2.0 along the TD and tested along the MD (26 mils thk, 140 C and 2000 %/min)....96
4.28 Elongation to break for films of PS with a fixed stretch ratio of 2.0 along the TD and tested along the MD (26 mils thk, 140 C and 2000 %/min)....97
4.29 Stress strain curves for PS showing change from brittle to ductile failure with increase in stretch ratio....98
4.30 Orientation factors for PS showing stress at break for several biaxial stretch ratios....99

4.31 Tensile strengths for S/MA and PS samples that were compression molded and stretched biaxially at 2000%/min and tested along the MD.....101
4.32 Orientation factors vs. equal biaxial stretch ratio at 2000%/min showing percentage elongation to break for PS and S/MA tested along the MD.....102
4.33 Effect of plaque thickness on the in-plane birefringence for films of PS stretched with a fixed ratio of 1.5 along the TD. (140 C and 2000 %/min).....104
4.34 Effect on the out of-plane birefringence with change in plaque thickness for films of PS stretched with a fixed ratio of 1.5 along the TD. (140 C and 2000 %/min).....105
4.35 Effect of the stress at break with change in the initial sample thickness for films of PS stretched with a fixed ratio of 1.5 along the TD. (140 C and 2000 %/min).....106
4.36 Effect on the elongation to break with change in the initial sample thickness for films of PS stretched with a fixed ratio of 1.5 along the TD. (140 C and 2000 %/min).....108
4.37 Stress at break vs. birefringence for films made from different plaque thicknesses of PS. (2000 %/min, 140 C).....109
4.38 Percent elongation vs. birefringence for films made from different plaque thicknesses of PS (2000 %/min and 140 C) 110
4.39 Unrestrained shrinkage of S/MA 3000 as a function of stretch ratio showing MD orientation factors (165 C for 8 min).....113

4.40 Unrestrained shrinkage of S/MA 2000 as a function of stretch ratio showing MD orientation factors. (165 C for 8 min).....114
4.41 Unrestrained shrinkage of PS as a function of stretch ratio showing MD orientation factors (165 C for 8 min).....115
4.42 Recovery as a function of temperature for 3 x 3 films of PS and S/MA.....116
4.43 Percent recovery as a function of (T-Tg).....118
4.44 Arrhenius type plots for PS and S/MA copolymers.....119
4.45 Grid depiction for the identification of extruded samples of S/MA copolymers.....121
4.46 Variation in In-plane birefringence across the width of extrusion of S/MA 3000 lhhp- 1e. Different curves represent variations with grid location along the extrusion direction.....123
4.47 Low initial orientation areas of S/MA 3000 LHHP-1e extruded sheet biaxially stretched at 3000 %/min and 170 °C.....124
4.48 High initial orientation areas of S/MA 3000 LHHP-1E extruded and biaxially stretched at 3000 %/min and 170 C.....125
4.49 Orientation factors of biaxially stretched films from high and low initial oriented areas of S/MA 3000, (3000 %/min,168 +/- 2 C).....128
4.50 In-plane birefringence variation across the width of extrusion for S/MA 2000 run 5 trial 10. Different curves represent variations with grid location along the extrusion direction.....129

4.51 In-plane birefringence variation across the width of extrusion of S/MA 2000 fgx run 9 trial 12. Different curves represent variations with grid location along the extrusion direction.....130
4.52 Variation in In-plane birefringence across the width of extrusion of S/MA 2000 hhp21-b. Different curves represent variations with grid location along the extrusion direction.....131
4.53 Variation inIn-plane birefringence across the width of extrusion for S/MA 2000 hhp21-a. Different curves represent variations with grid location along the extrusion direction.....132
4.54 In-plane birefringence variation across the width of extrusion of S/MA 2000 run 11 trial 9. Different curves represent variations with grid location along the extrusion direction.....133
4.55 Birefringence vs. biaxial stretch ratio for low initial orientation areas of extruded S/MA 2000 (Run 5, Trial 10) sheet biaxially stretched at 3000 %/min.....134
4.56 Birefringence vs. biaxial stretch ratio for high initial orientation areas of extruded S/MA 2000 (Run 9, Trial 12) sheet biaxially stretched at 3000 %/min.....135
4.57 Birefringence vs. stretch ratio for extruded 2000 S/MA- llhp-1a at 165 C and 3000 %/min.....137
4.58 Effect of stretch temperature on relaxation of residual orientation of extruded sheet llhp-21a- S/MA 2000.....138

CHAPTER 1

INTRODUCTION

Polymer films are planar forms of plastic(< 0.25 mm)[1] that are thick enough to be self supporting but thin enough to be flexed and folded without cracking. Thermoplastic films have been the subject of extensive research efforts due to their commercial success in the packaging of food and other items. These films make use of a combination of properties like low thickness, exceedingly good flex characteristics, clarity, low or selective permeability to gases, good resistance to service temperatures and high surface area to cost ratio.

In 1991 the U.S. consumption of polymer resins for packaging was 15,087 million lbs[2] of which more than a third was for film applications. This included HDPE, LDPE, OPP, OPS, PET and PA. Meat, poultry, snack food, cheese, confectionery, baked goods, dried fruits and nuts and frozen food are some of the examples of packaging applications using these polymers.

An important aspect for the success of films for packaging applications is the ability to impart the right amount of molecular orientation. Molecular Orientation plays an important role in determining the mechanical, physical and transport properties of polymers.

Establishment of the processing window for orientation and

characterization of the resulting oriented films gives an idea about the behavior of these materials during stretching on a commercial scale or even post stretching operations like vacuum forming, printing and heat sealing.

Polystyrene is a standard and conventional material for packaging, but its maleic anhydride copolymer is relatively new in this market segment. Styrene/maleic anhydride (S/MA) polymers, with or without glass reinforcement, have been long used for automotive interior applications; they are known for their good creep and impact resistance and for their dimensional stability at temperatures somewhat greater than for polystyrene.(3) These polymers when converted into films have very good clarity and show exceptionally good temperature resistance compared to polystyrene homopolymer and other conventional packaging materials. These films can also be toughened by the addition of impact modifiers like graftable rubber during the reaction stage or even by melt blending of butadiene.

The main aim of this thesis was to establish the suitability of two grades of S/MA with two different levels of maleic anhydride for stretch orientation and mechanical property improvements. The molecular orientation induced due to different stretch ratios for a given set of processing conditions and its effect on the mechanical and physical properties have been investigated. In order to compare the copolymer to the pure homopolymer, similar experiments have been done for polystyrene.

CHAPTER 2

BACKGROUND AND LITERATURE REVIEW

2.1 GENERAL CONSIDERATIONS

2.1.1 Copolymerization

Copolymerization is a useful technique to make improvements in polymer properties. Copolymerization produces changes in properties like melting point, glass transition temperature, solubility etc. In this method two or more structurally different monomers are incorporated into the growing polymer chain. Major classes of copolymers are random, alternate, block or graft depending on how the addition of the monomers occurs during the polymerization process.

The terminal model of 1944[4] developed by Mayo and Lewis gives a model for a process in which the rate constant for the addition of each monomer is dependent on the identity of the terminal unit on the growing chain. They considered four possible chain extension reactions when monomers M1 and M2 were present in the feed. Two of these equations are homopolymerizations or self propagating steps while the other two are heteropolymerizations or cross propagating steps.

$$M_1 + M_1^{\bullet} \xrightarrow{k_{11}} M_1^{\bullet}M_1$$
$$M_1 + M_2^{\bullet} \xrightarrow{k_{21}} M_1^{\bullet}M_2$$
$$M_2 + M_2^{\bullet} \xrightarrow{k_{22}} M_2^{\bullet}M_2$$
$$M_2 + M_1^{\bullet} \xrightarrow{k_{12}} M_2^{\bullet}M_1 \qquad \ldots 2.1.1$$

The ratio of the propagating rate constants are expressed as monomer reactivity ratios where

$$r1 = \frac{k11}{k12}$$

$$r2 = \frac{k22}{k21} \qquad \ldots 2.1.2$$

The rate of disappearance of the monomers M1/M2 is described by the equation

$$\frac{d[M_1]}{d[M_2]} = \frac{[M_1]\, k_{11}[M_1^{\bullet}] + k_{21}[M_2^{\bullet}][M1]}{k_{12}[M1^{\bullet}] + k_{22}[M_2]\,[M2^{\bullet}]} \qquad \ldots 2.1.3$$

substitution of r1 and r2 in the above equation gives the copolymerization equation

$$n = \frac{d[M_1]}{d[M_2]} = \frac{r_1([M_1]/[M_2]) + 1}{r_2([M_2]/[M_1]) + 1} \qquad \ldots 2.1.4$$

$$= \frac{r1x + 1}{r2/x + 1} \qquad \ldots 2.1.5$$

This equation may be used to show the effect of the composition of feed x on the composition of the copolymer (n). The values of these two parameters are equal in azeotropic copolymerization (composition of the copolymer is the same as that of the feed) but are different in most types of copolymerizations. Hence, to produce copolymers of uniform composition, the monomers are added continually to the feed.

The reactivity ratios may be determined by an analysis of the change in the composition of the feed during the very early stages of polymerization.

if r1 > 1 then M1 tends to homopolymerize or form block copolymers. when the product of r1 and r2 is close to 1 an ideal and random copolymer is produced.

When the product of the reactivity ratios approaches 0, an alternating copolymer is produced. The value of r1 and r2 for most copolymerizations is between 1 and 0, and this value must be used with discretion for estimating the randomness in a copolymer. Table 2.1 gives the reactivity ratios[5] for styrene as M1 (monomer 1). The r values for S/MA copolymerization suggests the formation of an alternating copolymer. However, the S/MA used in the present study is a random copolymer manufactured by a proprietary process of ARCO Chemical Company.

2.1.2 Basic Structure of S/MA

As discussed in the above section, copolymerization of styrene and maleic anhydride by conventional techniques yields a perfectly

Table 2.1

Styrene comonomer reactivity ratios†

Monomer 2	r_1*	r_2#	Temp.oC
acrylonitrile	0.4	0.04	60
butadiene	0.5	1.40	50
maleic anhydride	0.014	0.0	80
methyl methacrylate	0.52	0.46	60
m-divinyl benzene	0.65	0.60	60

† Styrene is monomer 1.

* $r_1 = k_{11}/k_{12}$

$r_2 = k_{22}/k_{21}$

alternating copolymer of S/MA. Because of the high level of maleic anhydride incorporated into the main chain, the polymer would be too brittle for any significant commercial use. To be viable for product applications, maleic anhydride is randomly incorporated into the growing polystyrene chain by free radical polymerization using special processes in continous stirred tank reactors with very efficient heat removal systems to yield styrene/maleic anhydride. The chemical structure of this polymer is presented in Figure 2.1. The presence of the maleic anhydride group on the backbone of the chain increases the rigidity of the chain, in comparison to polystyrene, and thus increases the glass transition temperature. Depending on the amount of maleic anhydride content, there is a proportional increase in the Tg of the polymer. These polymers are stable to processing temperatures up to 550°F (287°C). Moore(6) has prepared a series of maleic anhydride copolymers from 0-33% maleic anhydride content, each at different molecular weights and has characterized them with regard to Tg, HDT, thermal stability and melt viscosity. In his study the Tg appeared to increase linearly with increase in MA at 2.76°F/added % of maleic anhydride. A schematic diagram for the synthesis of these copolymers is also given in reference(6).

Toughness can be incorporated into the polymer during the reaction stage using graftable rubber or even by melt blending with butadiene. However impact modified S/MAs have lower heat resistance than their unmodified S/MA counterparts.

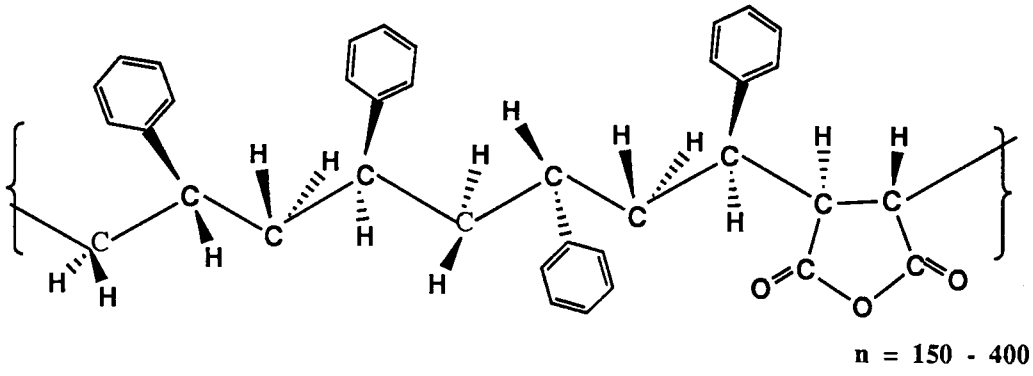


Figure 2.1
Random Copolymer of Styrene Maleic Anhydride

2.1.3 Cast-Film and Tenter Frame Process

A schematic diagram of a cast film line with a tenter frame is shown in Fig. 2.2.(7) In the first stage, not shown, the polymer melt is extruded from a slit die onto an internally cooled highly polished chill roll. Polystyrene casting equipment typically uses a three roll "stack" arrangement for the cooling or casting rolls.(8) Since the material is amorphous, it is cooled more gradually. Semicrystalline materials are often quenched to impede crystallization and to retain optical properties. The sheet then passes through a set of heating rolls to establish the desired temperature for machine direction orientation. The number of preheat rolls in an oriented polystyrene system to accommodate 4000 lbs./hr. can be as low as four. A 2.5 machine direction stretch is common for polystyrene.

The sheet now having been cast and stretched in the machine direction is ready to be stretched laterally. The most common method of producing transverse or lateral orientation is by means of a tenter frame. The sheet is passed through a tenter having two horizontal chain systems so that the base sheet is stretched in the direction normal to the machine direction as the clamps separate from one another along the divergence rail. The width of the tenter frame is adjustable throughout the total length, making it possible to obtain the desired lateral stretch ratio. If a simultaneous stretch along the MD and TD are needed, then the speed of the take up roll is kept at a higher rpm than that of the feed roll. Films progress

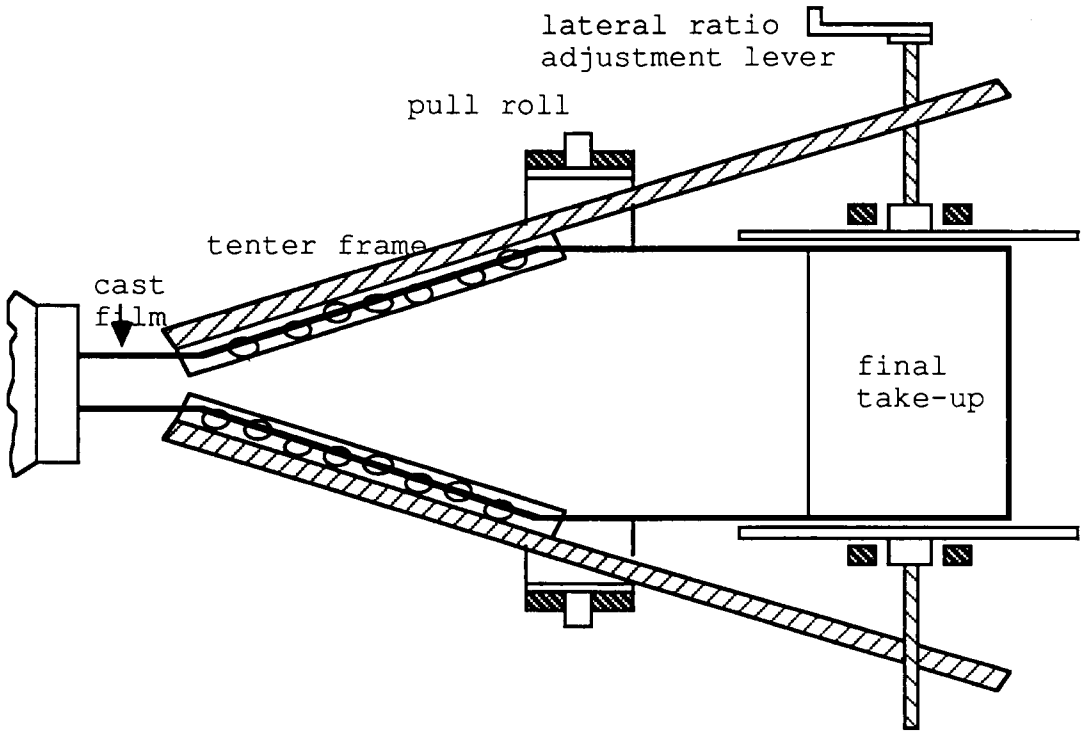


Figure 2.2. Tenter frame process for continuous oriented polystyrene making process (7)

through the system at roughly 1000 feet/min., while the temperature is closely monitored and controlled.

This process produces the MD and TD orientation needed to get the desired strength, shrinkage and clarity in the film.

2.1.4 Vacuum Forming Process

A thermoplastic sheet, preoriented in the tenter frame, is converted into simple shapes by this process.(9) A sheet is supported over a mold and heated to a temperature, above the Tg or below the Tm (for semi crystalline polymers), at which it can be reshaped. The mold is provided with multiple holes so that vacuum may be drawn that will pull in the softened sheet to the mold contour where it hardens to the desired shape. There are many variations to this process; one general case is illustrated in Fig.2.3

2.2 MOLECULAR ORIENTATION IN POLYMERS

2.2.1 Introduction

Broadly speaking, orientation is a preferential alignment of the crystal axes of a semicrystalline polymer or the chain axis in an amorphous polymer with respect to a coordinate system fixed in the sample (10).

Polymer processing operations frequently result in molecular orientation. The level of orientation developed is unique to the

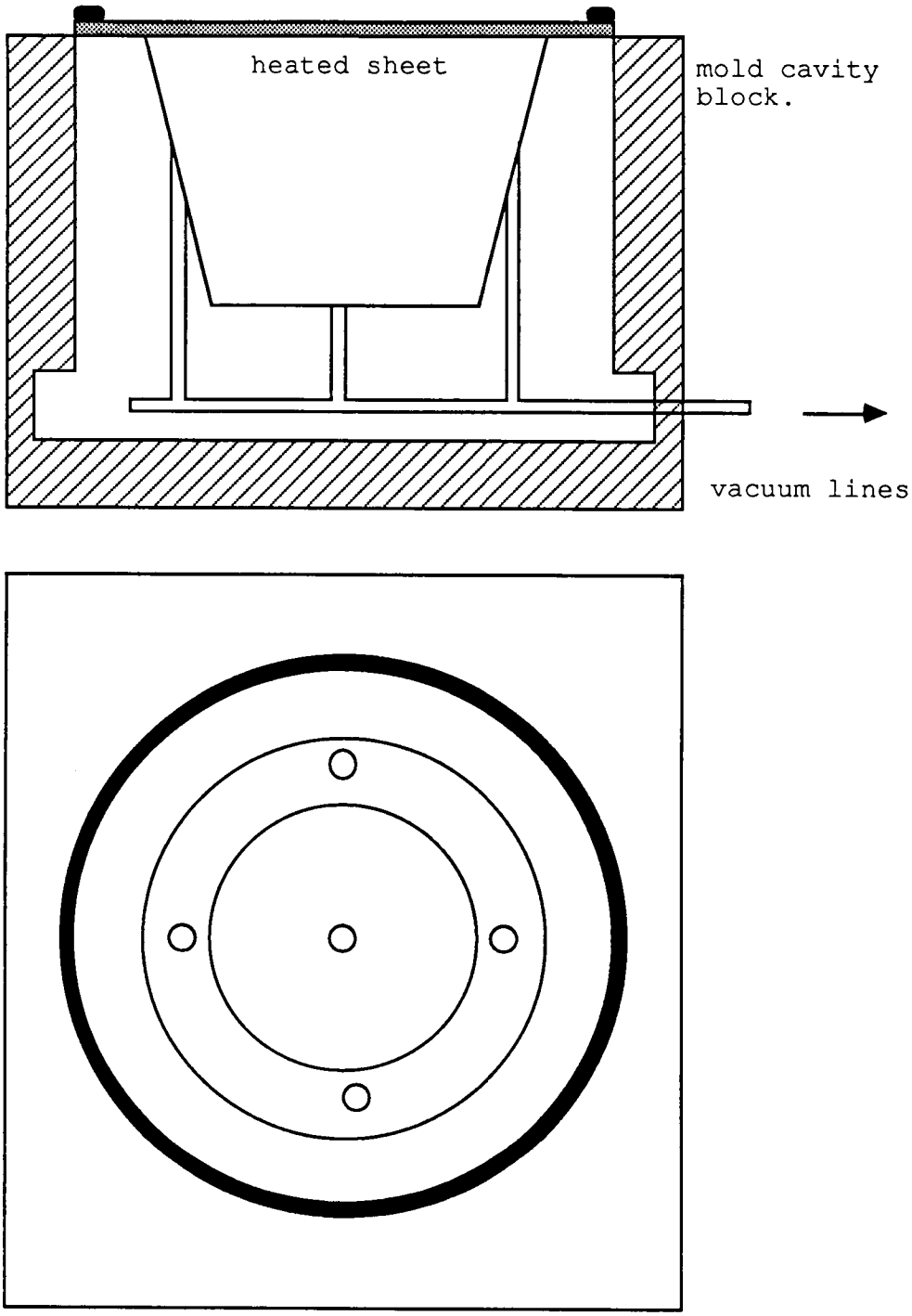


Figure 2.3 Schematic diagram of a vacuum forming process(9)

chemical composition of the material, process parameters and the geometry of the mold or die forming the product. The inherent anisotropy in the bonding of polymer molecules can be used to an advantage by appropriate selection of process parameters to induce and freeze this orientation to enhance overall properties like tensile strength and toughness. Fiber spinning and uniaxial film drawing tend to align the molecules parallel to the length of the fiber or film. This produces desirable properties along the stretch direction due to the presence of strong covalent bonds along the polymer chain but poor properties across the stretch direction due to weaker Van der Waals forces. Stretching a film biaxially allows the production of films with balanced properties in the plane of the film. By determining the level and distribution of orientation, which is a direct result of the processing conditions, it is possible to determine the processing parameters that produce an optimum product.

2.2.2 Orientation Development in Flowing Melts and Its Relation to Stress.

When molten glassy polymers are stressed, as is the case in most processing operations, there is a preferential alignment of the chains. Depending on the nature of the stress field, various orientation modes are induced in the polymer material. Experiments of Brewster(11) showed that application of stress produced birefringence. Newmann and Maxwell and later authors hypothesized the existence of the stress-optical law as

$$\Delta n_{12} = n_1 - n_2 = C(\sigma 1 - \sigma 2) \qquad ...2.2.1$$

where $\Delta n12$ is the birefringence, n is the refractive index in the 1 and 2 directions, and $\sigma 1$ and $\sigma 2$ are the principal stresses along the 1 and 2 directions.

A detailed experimental verification of this relationship for polystyrene under non-isothermal conditions is given by references (12) (13) and (14). Oda, White and Clark (15) show that birefringence in filaments is proportional to the difference in principal stresses in the samples at the point of vitrification and that the coefficient in the melt phase is the stress optical coefficent. Values for the stress optical coefficent reported in the literature can be found in (16). Oda, White and Clark have verified the stress optical coefficient and used it to predict birefringence in fabricated polystyrene parts. This concept has been used to predict birefringence distributions in injection molded parts, blown bottles and melt spun fibers(17),(18), (19).

2.2.3 Representation of Orientation in Crystalline and Amorphous Polymers

By 1930 it was well known that both X-ray diffraction and birefringence could quantitatively determine the degree of orientation in fibers (20). Pole figures from wide angle X-ray diffraction could give the preferential distribution of the normal to

the crystal plane in the crystalline regions of the polymer. Birefringence measured the total orientation in the amorphous as well as the crystalline regions of the polymer. Sisson and Clark (21) defined types of orientation in terms of pole figures. This was extended by Heffelfinger (22) to explain orientation induced during the processing of PET films.

Hermanns and Platzek (23) proposed a function f_H to define the level of uniaxial orientation for a fiber with cylindrical symmetry. This function is

$$fH = \frac{(3<Cos^2\Phi>-1)}{2} \qquad ...2.2.2$$

where Φ is the angle between the molecular chain axis and the fiber axis (uniaxial symmetry) and $<Cos^2\Phi>$ is the average value of the cosine squared of Φ averaged over all molecular segments in the sample. According to equation 2.2.2, f=1.0 if the molecular chain axes are perfectly aligned parallel to the fiber axis. The value of f = 0 for random orientation and -0.5 if the chain axes are aligned perpendicular to the fiber axis.

In 1958 Stein (24) defined uniaxial orientation of the crystallographic a, b and c axes for crystalline filaments relative to the fiber axis. They are given by the Hermans-Stein orientation factors.

$$fj = \frac{(3<Cos^2\phi_{j1}>-1)}{2} \qquad ...2.2.3$$

where $<Cos^2\phi_j>$ is the average value of the cosine squared of the angle between the fiber axis and the a, b or c crystal axes.

In an attempt to define biaxial orientation factors, using Eulers angles of spherical coordinates, Stein defined 6 orientation factors for the three crystallographic axes. These are given by equation 2.2.4

$$f2j = 2\cos^2\delta j - 1 \qquad ...2.2.4$$

where j represents one of the crystallographic axes and j= a,b or c. δj, is the Eulerian longitude between the j crystal axis and an axis in the plane of the film.

The range of values of Stein's biaxial orientation factors is +1 to -1 for each given crystal axis. When all the crystal axes lie in the plane of the film it gives a value of +1. A value of 0 means that the axes are random with respect to the plane of the film (uniaxial). A value of -1 indicates that the crystal axis lie in the plane perpendicular to the plane of the film.

Later, White and Spruiell (25) proposed biaxial orientation factors based upon the anisotropy of the polarizability tensor. They employed angles between the chain axes or the crystal axes with respect to the machine direction, transverse direction and normal directions.

For orthorhombic crystals the White-Spruiell orientation factors can be written as

a axis:

$$f1B = 2\langle Cos^2\phi_{a,1}\rangle + \langle Cos^2\phi_{a,2}\rangle - 1$$

$$f2B = 2\langle Cos^2\phi_{a,2}\rangle + \langle Cos^2\phi_{a,1}\rangle - 1$$

b axis

$$f1B = 2\langle Cos^2\phi_{b,1}\rangle + \langle Cos^2\phi_{b,2}\rangle - 1$$

$$f2B = 2\langle Cos^2\phi_{b,2}\rangle + \langle Cos^2\phi_{b,1}\rangle - 1$$

c axis

$$f1B = 2\langle Cos^2\phi_{c,1}\rangle + \langle Cos^2\phi_{c,2}\rangle - 1$$

$$f2B = 2\langle Cos^2\phi_{c,2}\rangle + \langle Cos^2\phi_{c,1}\rangle - 1 \qquad ...2.2.5$$

where a, b and c refer to the crystallographic axes. Only 4 are independent since

$$\langle Cos^2\phi_{a,j}\rangle + \langle Cos^2\phi_{b,j}\rangle + \langle Cos^2\phi_{c,j}\rangle = 1$$

j = 1,2 or 3 or the MD, TD or ND.

Depending on the type of orientation in the film, these factors have a range from -1 to +1 as seen from the Table 2.2 and Fig.2.4 For the uniaxial case the orientation factors reduce to the Hermanns orientation factor. For planar orientations f_1^B and f_2^B may vary from 0 to 1. As the chains tend to be oriented into the plane of the film, f1B and f2B become negative.

For amorphous polymers the White-Spruiell functions can be

Table 2.2
White-Spruiell orientation factors for different types of orientation in a film.†

Orientation	f1B	f2B
isotropic	0	0
uniaxial MD	$\frac{3\overline{\cos^2\Phi_{c1}}-1}{2}$	0
chains parallel to MD	+1	0
uniaxial TD	0	$\frac{3\overline{\cos^2\Phi_{c2}}-1}{2}$
chains parallel to TD	0	+1
Equal Biaxial or planar	$\frac{1-3\overline{\cos^2\Phi_{c3}}}{2}$	$\frac{1-3\overline{\cos^2\Phi_{c3}}}{2}$
Chains parallel to ND	-1	-1
Planar	$\cos^2\Phi_{c1}$	$\cos^2\Phi_{c2}$
Planar equal biaxial	+1/2	+1/2

†$\cos^2\Phi_{c1} + \cos^2\Phi_{c2} + \cos^2\Phi_{c3} = 1$

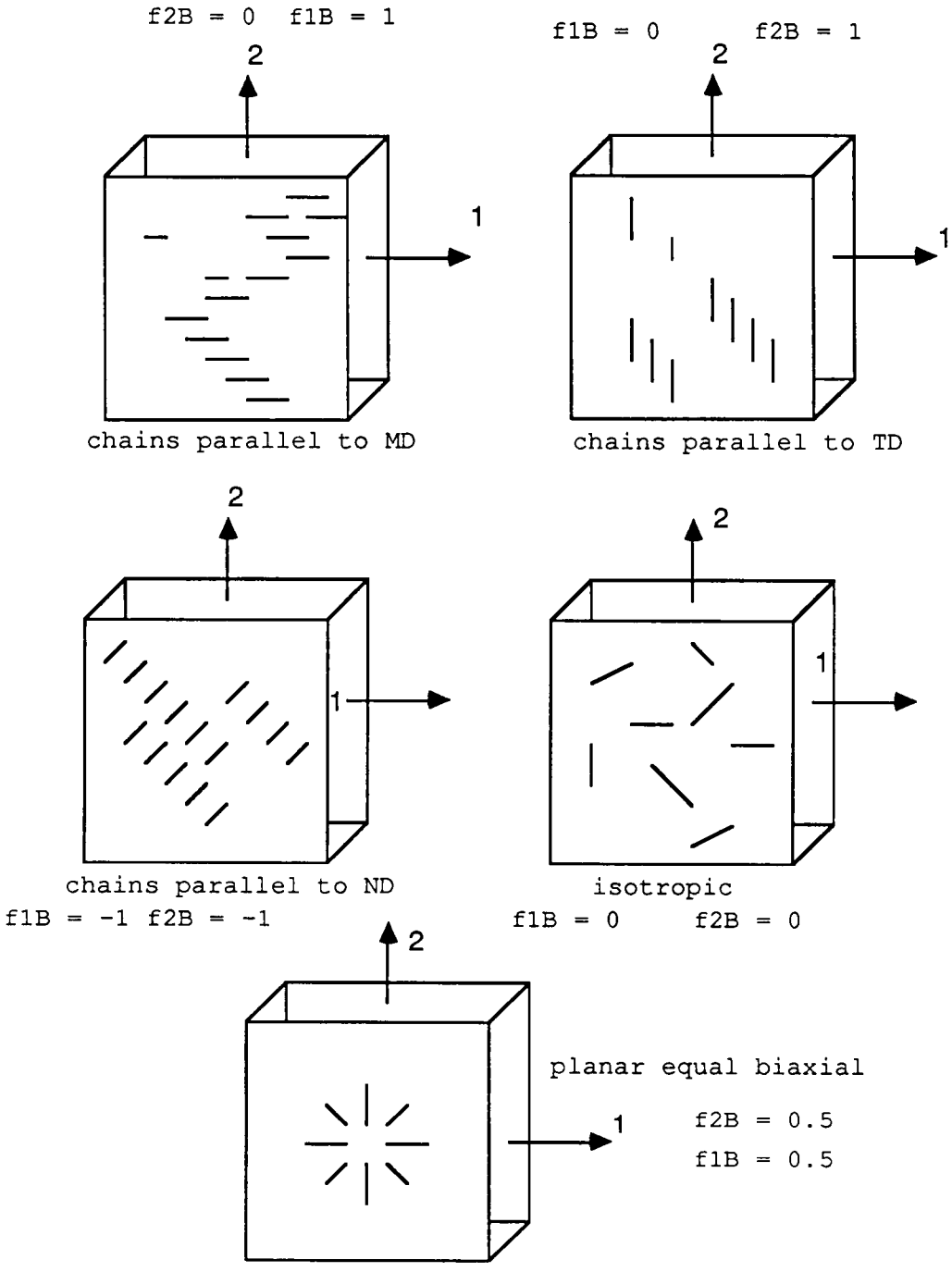


Figure 2.4 Different states of orientation in films showing White and Spruiell biaxial orientation factors

written as

$$f1_B = 2\langle Cos^2\phi_{c,1}\rangle + \langle Cos^2\phi_{c,2}\rangle - 1$$
$$f2_B = 2\langle Cos^2\phi_{c,2}\rangle + \langle Cos^2\phi_{c,1}\rangle - 1 \qquad ...2.2.6$$

where c is the axis along the polymer chain and 1 and 2 refer to the machine and transverse direction, respectively. These orientation functions are symmetric with respect to the machine and transverse directions, unlike the Stein and Nomura and Kawai (26) factors which are defined in terms of Eulers angles and are biased in favor of a single specific direction in the material. Almost all modern film processing operations involve orientation along the machine as well as the transverse direction. The White-Spruiell functions give a complete and unbiased specification of biaxial orientation.

White and Spruiell (25) describe an orientation function triangle diagram to illustrate the state of relative orientation of different samples by plotting these orientation factors graphically in an "orientation triangle diagram." The advantage of using the orientation factors is that the nature and magnitude of molecular orientation can be determined at a glance for films processed under different conditions. The two orientation factors defined in earlier sections and given by f1B and f2B (chain axis orientation factors relative to the machine and transverse directions, respectively) are plotted as shown in Fig.2.5. All the states of orientation lie within an isosceles orientation triangle. The origin of this plot represents the

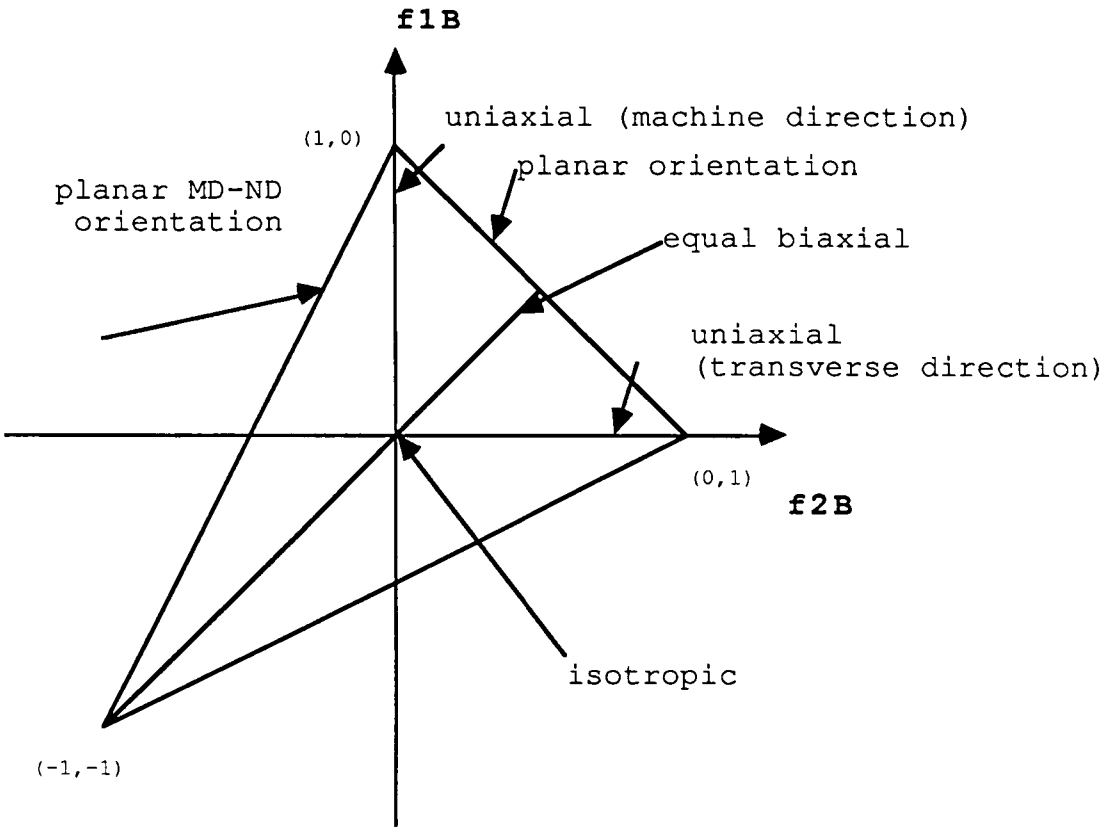


Figure 2.5 Graphical representation of orientation in the orientation triangle diagram

isotropic state (no preferred orientation). (In our study, the orgin represents the orientation level of compression molded specimens before stretching). States of uniaxial orientation with respect to the MD or TD lie along the 1 or 2 axes, respectively. The three vertices of this isosceles triangle represent states of perfect uniaxial orientation along any of the 3 reference directions; (1,0) and (0,1) represent perfect alignment of the chains with the MD and TD, respectively, while (-1,-1) represents the state of perfect orientation perpendicular to the plane of the film or in the ND (normal direction). States of equal biaxial orientation with respect to the MD and TD lie on the altitude of the triangle; the special point represented by (1/2,1/2) corresponds to all chains lying in the MD-TD plane.

2.2.4 Methods for Detecting Molecular Orientation

The orientation of macromolecules that exists in fabricated products, plays an important role in determining mechanical and optical characteristics of the product. Thus in order to evaluate a polymeric product and the relationship of its performance to processing conditions, it is important to measure molecular orientation.

Molecular orientation can be determined using a variety of experimental techniques like optical birefringence, infrared dichroism, Wide angle X-ray diffraction (WAXD)- pole figure analysis, sonic modulus etc. Each method has its own limitations relative to the type and level of orientation being measured. Since semicrystalline

polymers exist in crystalline and amorphous phases, different orientation distributions can exist in the two phases. WAXD - pole figure analysis provides a measure of molecular orientation only in the crystalline phase, while infrared dichroism can measure orientation selectively in the crystalline or the amorphous phase or even the average orientation in the sample. Birefringence and sonic modulus on the other hand is a measure of the total average orientation in both the phases. The principles behind these methods are briefly outlined in subsequent sections. For amorphous polymers, as is the case in our present study with S/MA and PS, optical birefringence is a quick way to measure and represent the total molecular orientation in the polymer. Since this is the method used in the present study, this method is described in greater detail.

Wide Angle X-ray Diffraction

This method is popularly used to specify orientation distribution for crystalline or semicrystalline materials. Pole figure analysis gives the spatial distribution of the poles (normals to the diffraction crystal planes projected on to a sphere). Due to the diffuseness of scattering from amorphous regions, this method is only useful for crystalline materials. Details of this technique can be found in (27).

Dichroism

When polarized radiation is passed through an anisotropic

solid, the absorption of certain wavelengths occurs and may depend on the direction of the electric vector (28). This phenomena is known as dichroism and is used to obtain structural information about polymers.

The dichroic ratio D is defined as

$$D = \frac{A11}{Apb} \qquad ...2.2.7$$

Where A_{11} is the absorbance measured with the electric vector parallel to the primary reference direction in the sample and α_{pb} is the absorbance measured perpendicular to the reference direction. Samuels (29) gives the general relationship between D and $\langle Cos^2\phi \rangle$ for uniaxial orientation.

$$\frac{1}{2}(3\langle Cos^2\phi \rangle - 1) = f = \frac{D-1}{D+2}\,\frac{Do+2}{Do-1} \qquad ...2.2.8$$

where Do is the dichroic ratio for $\langle Cos^2\phi \rangle = 1$. If the transition moment α is known, then Do can be found from the relationship

$$Do = 2\,Cot^2\alpha \qquad ...2.2.9$$

Dichroism in the infra red region is applicable to many polymers. If the polymer consists of one phase then the above equation can be used conveniently. For a semicrystalline material the

above equation can be applied separately to crystalline and amorphous dichroic bands. The use of this method for biaxial orientation was done by Schmidt (30), Koenig (31), Cornell (32) and Nomura et al. (33).

Sonic Measurements

The relationship between molecular orientation and Young's modulus E (34) is expressed by the equation

$$\frac{1}{E} = \frac{1}{\rho v^2} = 1 - \frac{\langle \cos^2\Phi \rangle}{E_{ot}} \qquad \ldots 2.2.10$$

where v is the sonic velocity

Eot is the intrinsic lateral modulus

ρ is the polymer density

Φ is the angle between the chain axis and direction of sound propagation. For a two phase system Samuels (35) derived the relationship

$$\frac{1}{E_{or}} = \frac{X}{E_{t,oc}} (1 - \langle \cos^2\Phi \rangle_c) + \frac{1-X}{E_{t,A}} (1 - \langle \cos^2\Phi \rangle_A) \qquad \ldots 2.2.11$$

where E_{or} is the modulus for the oriented polymer, and X is the fraction of crystallinity. C and A refer to the crystalline and amorphous components, respectively.

The intrinsic lateral modulus is related to Eu, the experimentally measured modulus for the unoriented polymer by the equation(28)

$$\frac{3}{2E_u} = \frac{X}{E_{otc}} + \frac{1-X}{E_{ot,A}} \qquad ...2.2.12$$

For a one phase system, the orientation parameter can be evaluated by equation 1, However, when crystallites are present, the degree of crystallinity must be known. The crystalline orientation from X-ray diffraction may be used so that the amorphous orientation can be determined.

Optical Birefringence

The velocity of light in a medium depends on the polarizability and hence the index of refraction of the medium through which it travels. There are substances for which the index of refraction is different for light linearly polarized in one direction and linearly polarized in another. Due to the anisotropic nature of bonding in polymer molecules, the polarizability parallel to the chain will differ from that perpendicular to it. Hence, the refractive index with respect to a light wave with its electric vector parallel to an assembly of chains will differ from that for a wave with its electric vector perpendicular to it. In other words, polymer chains are intrinsically birefringent or exhibit the phenomena of double refraction. By definition, birefringence is the difference in refractive indices along two principal directions. The level of birefringence for a particular polymer chain will depend on the chemical composition

and the arrangement of atoms in the chain. The latter is closely dependent on the processing history of the polymer in question. If the refractive index is larger along the molecule than along it, the polymer will exhibit a positive birefringence. In some instances like PS and S/MA, the polarizability (or refractive index) is larger perpendicular to the chain with the result that these polymers exhibit a negative value of birefringence.

For randomly oriented polymer molecules, the differences in polarizabilities will average out and the index of refraction of the assembly will be the same in all directions; hence the birefringence will be zero (i.e., the specimen is optically isotropic). If, however, all of the chains are fully aligned, the birefringence will be maximum, equal to the intrinsic birefringence of the molecule. If the molecules are partially aligned, then the measured birefringence will lie between these two extreme values and can be used as a measure of orientation.

A uniaxially oriented sample such as a fiber or uniaxially oriented film, can be characterized by two principal refractive indices: one parallel to the axis and the other in a plane normal to it. Hence the orientation can be characterized by a single value of birefringence, i.e., the difference of these two principal refractive indices. In the general case as in biaxially oriented films, there are three principal refractive indices in mutually perpendicular directions, and complete characterization of orientation requires measurement of two independent values of birefringence.

The birefringence of a sample gives the overall molecular orientation in the crystalline and amorphous phases. The total birefringence of a semi crystalline polymer is related to the birefringence in the amorphous and crystalline regions by the equation

$$\Delta n = X\Delta^{o}_{c}f_{c} + (1-X)\Delta^{o}_{am}f_{ham} + \Delta n_{f} \quad ...2.2.13$$

where X is the crystalline fraction and f_{hc} and f_{ham} are the Hermanns orientation factors in the crystalline and amorphous phases, respectively. Δ^{o}_{c} and Δ^{o}_{am} are the intrinsic birefringences of the fully oriented crystalline and amorphous phase. Here Δn_{f} is the form birefringence in voids or phase boundaries of incompatible blends where the phases exhibit a large difference in refractive index.

In order to get a clearer understanding of the physical meaning of the values of birefringence, the variation in the refractive index with respect to a chosen set of reference coordinates can be used to represent a refractive index ellipsoid. For materials that are optically isotropic, the optical indicatrix is a sphere. If n1, n2 and n3 are the refractive indices in the three principal directions then for isotropic materials:

n1 = n3 = n2 (see Figure 2.6)

and the birefringence is zero.

The material is said to be optically uniaxial if variation of the

refractive index is an ellipsoid of revolution with

$$n1 \neq n2 = n3$$

and for the general biaxial case,

$$n1 \neq n2 \neq n3$$

With the above understanding, we can define three values of birefringence (one in-plane and two out-of-plane) in the case of biaxially oriented films. These are schematically illustrated in Figure 2.7

$\Delta 12 = n1\text{-}n2 =$ in-plane birefringence

$\Delta 13 = n1\text{-}n3 =$ out-of-plane birefringence

$\Delta 23 = n2\text{-}n3 = \Delta 13\text{-}\Delta 12 =$ out-of-plane birefringence

Therefore birefringence is an indicator and measure of the level of molecular orientation in polymers, that is related to the anisotropy in the bulk material when the molecules are not randomly oriented in space. However such comparisons are limited to birefringences of the same polymer because birefringence is dependent on the chemical composition of the polymer. Normalizing the birefringence values with the maximum possible value of the birefringence for the same polymer will permit comparison between two or more polymers with different chemical compositions. This maximum value of the birefringence is known as the intrinsic birefringence and is calculated from theory assuming a fully extended chain.

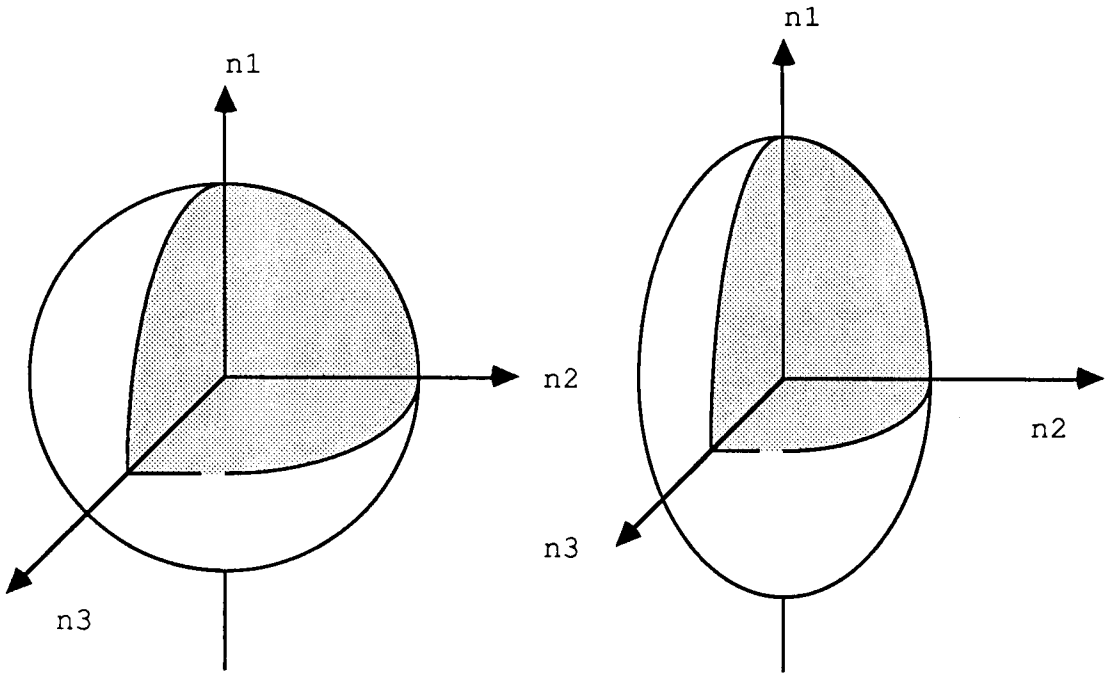
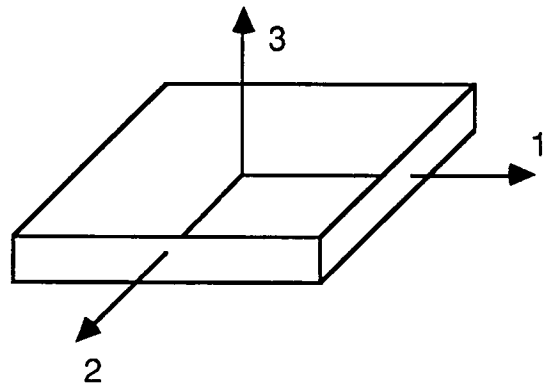


Figure 2.6 Refractive index ellipsoid: (a) Optically isotropic medium (b) Optically anisotropic medium.(36)



$\Delta 12 = n1-n2$
$\Delta 13 = n1-n3$
$\Delta 23 = n2-n3$

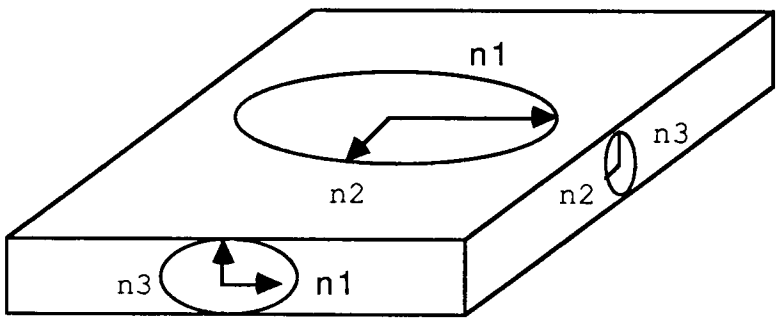


Figure 2.7 Film strip showing the projections of the refractive index ellipsoid on the three sides of the polymer film and the definitions of these birefringence values

Intrinsic Birefringence

The intrinsic birefringence of a polymer chain is defined as the birefringence of the polymer if all the chains were extended and perfectly oriented along a single direction. Though theoretically sound, in practice it is impossible to orient 100% of the chains along the stretch axis. So in order to evaluate the intrinsic birefringence the bond polarizabilities must be summed parallel (α_{11}) and perpendicular (α_{pb}) to a fully extended chain model.

In general the polarizability of a chemical bond is anisotropic, i.e., it is greater along the bond than it is at an angle to it with the result that the refractive indices are different in different directions. Under the influence of an electric field, the electrons in the chemical bonds of a polymer chain slightly shift their average positions. Both the electric field E and the induced dipole P are vector quantities linearly related by the polarizability α, which is a second order tensor

$$P = \alpha E \qquad \ldots 2.2.14$$

The polarizability is related to the refractive index 'n' through the Lorentz-Lorenz equation (37) (38) by equation 2.2.3. This is strictly true for isotropic systems

$$\frac{n^2-1}{n^2+2} = \frac{4\Pi N\rho\alpha}{3M} \qquad \ldots 2.2.15$$

However, the above equation has been extended to anisotropic systems where it has been assumed that the above equation remains valid along the principal axes of polarizability and refractive index ellipsoids. Writing equation 2.2.15 for an ith bond of a chain we have

$$\frac{n_i^2-1}{n_i^2+2} = \frac{4\Pi N\rho\alpha_i}{3M} \qquad \ldots 2.2.16$$

where ρ is the density

N is the Avagadro number

M is the molecular weight of the repeat unit

α_i is the polarizability of the i^{th} kind of chemical bond.

If n11 and npb are the refractive index along the principal directions, then equation 2.2.16 can be written as

$$\frac{n_{11}^2-1}{n_{11}^2+2} - \frac{n_{pb}^2-1}{n_{pb}^2+2} = \frac{4\Pi N\rho(\alpha_{11}-\alpha_{pb})}{3M} \qquad \ldots 2.2.17$$

$$\text{Also } \frac{\alpha_i-\alpha_j}{\alpha_{11}-\alpha_{pb}} = \frac{n_{11}-n_{pb}}{\Delta^o} \qquad \ldots 2.2.18$$

For small values of $(n_{11}-n_{pb})$, the equation 2.2.17 may be reduced to

$$\frac{6n}{(n^2+2)^2}(n_{11}-n_{pb}) = \frac{6n}{(n^2+2)^2}\Delta^o = \frac{4\Pi N\rho(\alpha_{11}-\alpha_{pb})}{3M} \qquad \ldots 2.2.19$$

where n is the mean refractive index. Then

$$\Delta^{\circ} = \frac{2\Pi N\rho}{9M} \frac{(n2+2)^2}{n} (\alpha_{11}-\alpha_{pb}) \qquad ...2.2.20$$

Polarizability(39) is a second order tensor and its component $\alpha_{st}{}^{i}$ in the coordinate reference frame with axes along and perpendicular to the chain backbone are related to those in the coordinate frame of the bond $\alpha_{ab}{}^{i}$ by

$$\alpha_{st}{}^{i} = \Sigma_a \Sigma_b \; l_{sa}{}^{i} \, l_{tb}{}^{i} \; \alpha_{ab}{}^{i} \qquad ...2.2.21$$

where the $l_{st}{}^{i}$ are cosines of the angles between the axes defining the i^{th} bond and the extended macromolecule. (Fig.2.8) For a structural unit with n bonds

$$\alpha_{st} = \Sigma \, \alpha_{st}{}^{i} = \Sigma \; \Sigma_a \Sigma_b \; l_{sa}{}^{i} \, l_{tb}{}^{i} \, \alpha_{ab}{}^{i} \qquad ...2.2.22$$

Introducing the matrix representation $\alpha_{ab}{}^{i}$ in the bond

$$\alpha^{i} = \begin{vmatrix} \alpha_{b}{}^{i} & 0 & 0 \\ 0 & \alpha_{pb}{}^{i} & 0 \\ 0 & 0 & \alpha_{pb}{}^{i} \end{vmatrix} \qquad ...2.2.23$$

where $\alpha_{b}{}^{i}$ is along bond i and $\alpha_{pb}{}^{i}$ is perpendicular to the bond i. The components α_{st} can be written as

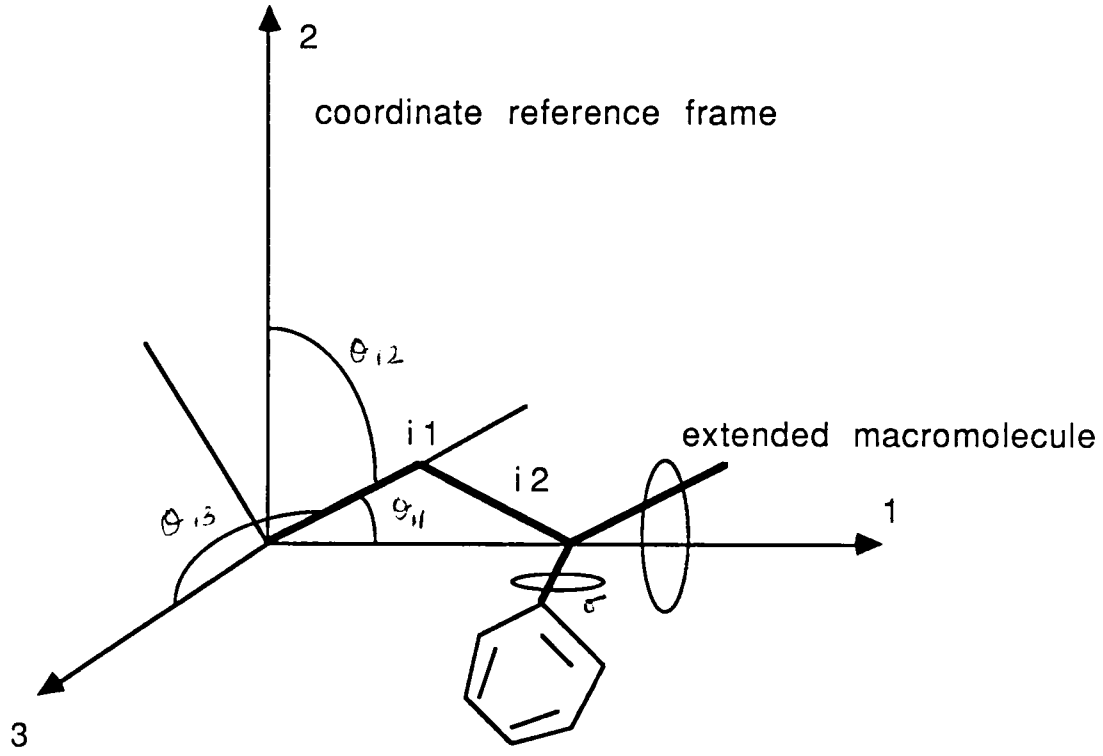


Figure 2.8 Coordinate reference axis for the calculation of intrinsic birefringence

$$\alpha_{11} = \Sigma \left[\alpha_b{}^i \, Cos^2\theta_{11}{}^i + \alpha_{pb}{}^i \left(Cos^2\theta_{12}{}^i + Cos^2\theta_{13}{}^i \right) \right]$$
$$= \Sigma \left[\alpha_b{}^i \, Cos^2\theta_{11}{}^i + \alpha_{pb}{}^i \, Sin^2\theta_{11}{}^i \right]$$

$$\alpha_{22} = \Sigma \left[\alpha_b{}^i \, Cos^2\theta_{21}{}^i + \alpha_{pb}{}^i \left(Cos^2\theta_{22}{}^i + Cos^2\theta_{23}{}^i \right) \right]$$
$$= \Sigma \left[\alpha_b{}^i Sin^2\theta_{11}{}^i Cos^2\theta^i + \alpha_{pb}{}^i \left(Sin^2\Phi^i Cos2\Phi^i Cos^2\theta_{11} \right) \right]$$

$$\alpha_{33} = \Sigma \left[\alpha_b{}^i Sin^2\theta_{11}{}^i Sin^2\Phi^i + \alpha_{pb}{}^i \left(Cos^2\Phi^i + Cos^2\theta_{11}{}^i Sin^2\Phi^i \right) \right]$$

...2.2.24

where Φ^i is the azimuthal angle between the 2 axis in the chain coordinate frame and the longitude defined by the i^{th} bond axis. α_{11} and α_{pb} are given by

$$\alpha_{11} = \alpha_{11}$$

$$\alpha_{pb} = \frac{\alpha_{22} + \alpha_{33}}{2} \qquad \text{...2.2.25}$$

The estimation of the intrinsic birefringences has many practical limitations for full accuracy in its calculation (39). The main reason is that the values of the bond polarizabilities are not known accurately. The values reported by Denbigh (40) differ from those of Bunn and Daubney (41) and Wang (42). The orientations of the substituent groups like the benzene ring in polystyrene is not known accurately. Also all the bond angles for the calculation have to be

assumed based on a fully extended model. Stein (43) has discussed problems of this type in the evaluation of the intrinsic birefringence. Literature values for intrinsic birefringence of polystyrene are given in Table 2.3. These values illustrate the wide variety of results obtained, depending on the assumptions used in the calculation and the values of the bond polarizabilities used.

With the knowledge of the intrinsic birefringence and the measured birefringence of a particular polymer, we can make comparisons between two or more polymers with different chemical compositions. This is done using orientation functions and it allows an absolute measure of orientation to be obtained. The White-Spruiell functions f_1^B and f_2^B can be related to the refractive index in the three directions, or the out of plane birefringences by

$$\Delta_{13} = n_1 - n_3 = f^1_B \, \Delta^o$$
$$\Delta_{23} = n_2 - n_3 = f^2_B \, \Delta^o \qquad \text{...2.2.26}$$

Where Δ^o is the intrinsic birefringence and f^1_B, f^2_B are the machine direction and transverse direction orientation factors, respectively.

Table 2.3.
Values of intrinsic birefringences of fully oriented polystyrene in literature.

Model		$(\alpha 1-\alpha 2)E24$ cc.	Δo
Gurnee(38)			-0.3
Choi Spruiell(44)			-0.125
Matsumoto and Fellers(45)			-0.14
Stein(46)			-0.276
Miligan(47)			-0.012
Matsumoto(48)			-0.0125
Gurnee			
Free rotation		-2.54	-0.141
Fixed phenyl	$\theta = 0$	-7.17	-0.399
group	$\theta = \pi/2$	+2.10	+0.118
Restricted rotation			
	$\theta = 0$	-7.17	-0.399
	$\theta = 15$	-6.97	-0.388
	$\theta = 30$	-6.37	-0.355
	$\theta = 45$	-5.49	-0.306
	$\theta = 60$	-4.46	-0.248
	$\theta = 75$	-3.43	-0.191
	$\theta = 90$	-2.54	-0.141
Muller(49)		-0.30	
Khun and Grun(50)		-18.0	

CHAPTER 3

EXPERIMENTAL

3.1 MATERIALS

Three polymers were used in this study. A polystyrene, Dylene® 8G and two S/MA copolymers with the trade names Dylark®2000FG and Dylark®3000FG. The Dylark®2000FG contains about 8% (by weight) maleic anhydride while Dylark®3000FG contains about 14% maleic anhydride. These materials were supplied by ARCO Chemical Company in the form of pellets. The S/MA grades were also supplied in the form of 12.5" wide extruded sheets prepared under a variety of extrusion conditions.

The detailed characteristics of these materials taken from ARCO technical specification sheets (51) are presented in Table 3.1

3.2 PROCESSING

3.2.1 Preparation of Initial Samples

Square plaques 59mm wide were prepared by compression molding with a 25 mil thick spacer. Employing a 12 ton compression force in the Wabash hydraulic press, two samples were made during one molding cycle. Polyimide films 4 mils thick were placed to prevent the melt from touching the aluminum cover plates. Use of polyimide films for molding gave good plaques with no undulations on the

Table 3.1

Material specifications of S/MA and Polystyrene

Resin properties	ASTM method	S/MA 2000 (8% MA)	S/MA 3000 (14% MA)	PS (0%MA)
spc. gravity (23°C)	D-792	1.08	1.10	1.05
MFI gms/10 min	D-1238	1.7	1.9	1.8
Water absorbtion	D-570	0.10	0.10	----
Tensile strength (psi)	D-638	7000	7000	----
Tensile elongation (%)	D-638	1.8	----	2.8
Flexural Modulus (psi)	D-790	524,000	530,000	450,000
Izod impact (J/m) (ft.lbs/inch of notch)	D-256	0.2	0.2	0.5
Vicat softening (°C)	D-1525	118	130	108
HDT (°C) @ 18.6 kg/cm2	D-648	96	107	94
Refractive index	D-542	1.583	1.581	----
Haze % (0.125")	D-1003	<2	<2	----

Table 3.2

Parameter settings for compression molding of S/MA and polystyrene plaques.

Parameter	Setting		
	2000 FG	3000FG	8G
Temperature oC	200	220	200
Preheat time min.	3	3	3
Compression time min.	2	2	2
Pressure tons (4" dia. ram)	12	12	12
Cooling time min.	5	5	5

surface and free from variations in thickness. The parameter settings for compression molding of Dylark®2000FG, 3000FG and Dylene®8G are shown in Table 3.2. The compression molding temperatures were measured at the extremities of the face of the platens using an iron constantan thermocouple. Unless stated otherwise, the initial thickness of the compression molded specimens was 26 mils.

3.2.2 Preparation of Biaxially Stretched Films

The 59 mm square molded plaques were stretched using the T.M.Long extensional tester to prepare oriented films with different stretch ratios in the machine and transverse direction. The optimum processing window was arrived at after several experiments on the effect of stretch ratio, stretch temperature and the strain rate. The plate temperatures in the biaxial stretching apparatus were measured from the control panel of the T.M. Long tester and the temperature of the hot air from the blower was measured using a thermometer at the blower exit.

These experiments and the results will be discussed in subsequent chapters. Thickness measurements on the films were made using a digital micrometer with a least count of 0.001 mm.

3.3 CHARACTERIZATION

The characterization techniques and procedures used during the study are briefly described below.

3.3.1 Tensile Testing

Mechanical testing was done using a table model of the Instron Mechanical Tester, model 1122. The procedures outlined in ASTM-D 882, for use to determine the tensile properties of plastics in the form of thin sheeting or film were followed. A cross head separation rate of 5 mm/min was employed. The samples were cut from oriented films along the MD or TD using a circuit board cutter and utmost care was taken to cut parallel edges on the sample.

3.3.2 Dynamic Mechanical Analysis

Dynamic mechanical analysis was done on samples using an automated Rheovibron model DDV-11C. The glass transition temperature was determined at a frequency of 1.1 Hz. The dimensions of the samples were in accordance to the standards outlined in the operating manual. The tension applied to the samples during testing was 20 grams. while the heating rate was kept constant at 1 degree C/min.

3.3.3 Birefringence

The birefringence values of the oriented films were measured by means of a compensator and the tilting technique developed by Stein (52). The schematic of this apparatus is shown in Fig. 3.1. It consists of an optical bench with a Gaertner plane polariscope, babinet compensator and a polarized light source.

There are several types of compensators available depending

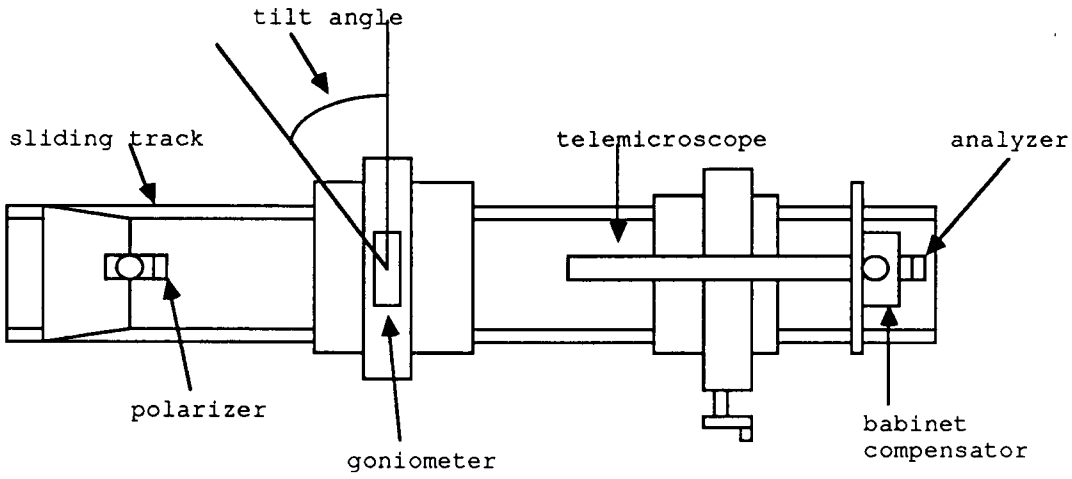


Figure 3.1 Schematic diagram of Garetner plane polariscope for determining birefringence.

on the degree of retardation being measured. Compensators interpose a variable optical path difference into the light beam passing through the microscope. It can be arranged that the high and low refractive directions of the compensator are superimposed on the low and high index directions of the specimen. The result is the subtraction of the optical path differences. When the optical path difference produced by a variable compensator is identical to that of the specimen, a zero path difference results. The compensated part of the image appears black. The compensators design is such that this occurs only in a band across the field of view. This band is referred to as a zero order fringe. On either side of the fringe will be a sequence of colored fringes.

If the orientation of the compensator is such that its higher refractive index is aligned with that of the specimen, no compensation can occur since the optical path differences are added.

It is necessary for the specimen and the compensator to be used with well crossed polars and with the specimen in its position of maximum brightness. This will occur midway between, or at 45 degrees to, the positions in which the specimen extinguishes between crossed polars. In practice, the specimen is rotated to extinction without the compensator in place and then rotated by 45 degrees. On inserting and adjusting the compensator the zero order fringe is sought. The optical path difference generated by the compensator is obtained by reading the dial on the micrometer. This reading can be converted into an optical path difference with reference to

manufacturer's tables.

The designated reference directions are shown in Fig.3.2 Directions 1 and 2 are in the plane of the film with 1 as the machine direction and 2 as the transverse or cross machine direction. In the case of extruded sheet the direction of extrusion is maintained as the machine direction for stretching. To measure birefringence the apparatus was arranged with the analyzer and the polarizer set 90 degrees apart. Plane polarized light striking an anisotropic film splits into two components, with one component of the wave retarded with respect to the other. The birefringence can be related to this retardation by the equation:

$$\Delta 12 = \frac{R\,\lambda}{d} \qquad \ldots 3.3.1$$

where $\Delta 12$ is the birefringence in the plane of the film, λ is the wavelength of the light used (546 nm), R is the retardation in units of number of waves and d is the sample thickness. The retardation was measured by means of a Babinet compensator which consists of two crystalline quartz wedges, with the optic axis of each wedge set in the plane of the face but 90 degrees apart. (Fig. 3.3) One wedge is stationery has a set of black lines or bifilars scribed on it. The other wedge is moveable with a calibrated screw and can therefore be used to quantify the retardation by bringing the components of the split wave into phase. Zero retardation is seen as a black band in white light. When the black band is adjusted to the scribed line the

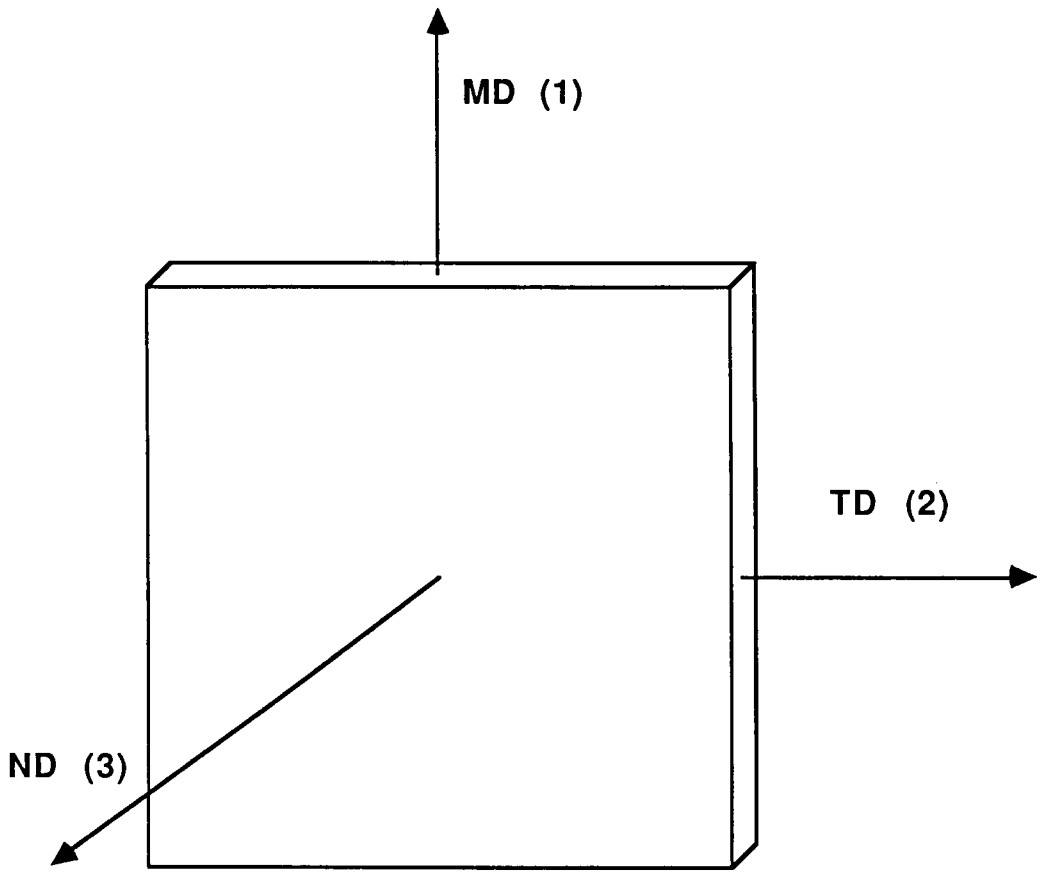


Figure 3.2 Reference directions for stretching: 1 is the machine direction, 2 is the transverse direction and 3 is the direction normal to the plane of the sheet. For extruded samples, the extrusion direction was always parallel to the MD

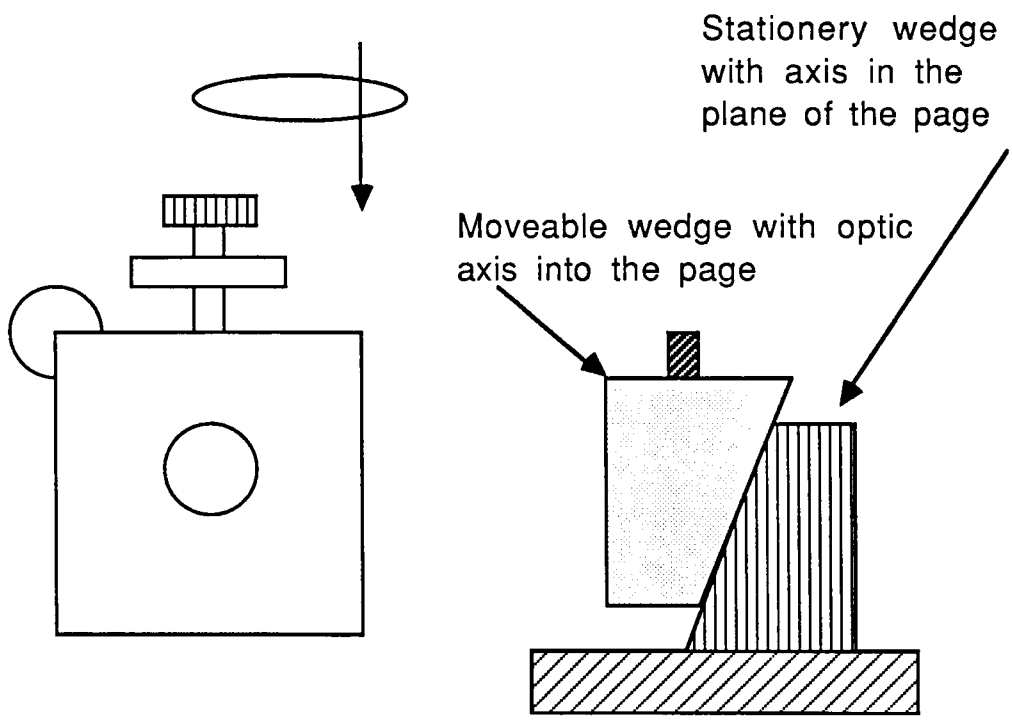


Figure 3.3 Babinet compensator showing wedge movement and direction of optic axis

amount of retardation, which is proportional to the thickness of the wedge, can be measured.

Measuring the retardation was accomplished by first finding the position of the wedge without a sample (baseline compensator reading) and then with a sample at 0 and 90 degree positions. The difference in the base line and the average reading at 0 and 90 was used to find the retardation R by the following equation

$$R = (+/-)\ (\text{Sample reading} - \text{Average reading})\ \frac{[\text{wave/turn}]}{k} \quad \ldots 3.3.2$$

where wave/turn is the amount of retardation of the compensator per turn of the micrometer and k is the compensator constant. For the compensator used in this study k is 0.998 and there are 0.1891 waves per turn. The in-plane birefringence was then calculated by equation 3.3.1

For equal biaxial orientation the "in-plane" birefringence is zero, but the difference in the refractive index in the plane of the film and normal to the film or the "out-of plane" birefringence is non zero. This quantity can be used as a measure of the level of biaxial orientation.

To measure the "out-of plane" birefringence a tilting technique developed by Stein(53) as seen in Fig.3.4 was used. In this technique

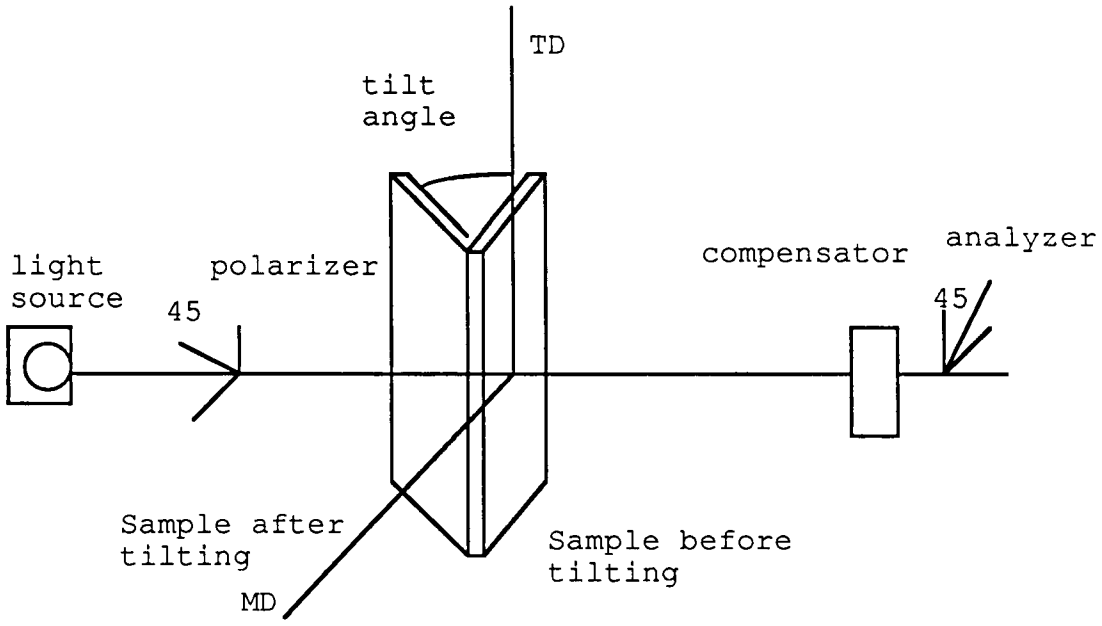


Figure 3.4 Optical bench compensator and rotating stage to determine in-plane and out-of plane birefringences. (Sample tilting is about TD)

a compensator is used to measure the retardation as described before, but at several angles of the film with respect to the incident light. The Δ13 birefringence can be then determined by the following equation

$$\Delta_{13} = \frac{\lambda}{t} \left\{ \frac{R_o - R\Phi(1 - \mathrm{Sin}^2\Phi/n2)^{0.5}}{\mathrm{Sin}^2\Phi/n^2} \right\} \qquad \ldots 3.3.3$$

where λ is the wavelength of light used, Φ is the angle of tilt, t is the film thickness, Ro is the retardation for normal incidence, RΦ is the retardation at angle Φ and n is the average refractive index of the polymer. The Δ23 birefringence of the film can be found by the equation

$$\Delta_{23} = \Delta_{13} - \Delta_{12} \qquad \ldots 3.3.4$$

3.3.4 Shrinkage Measurements

In order to measure shrinkage oriented specimens 3" square were laid flat on a sheet of paper of the same size and kept in an oven at a constant temperature.

The final dimensions were measured to the nearest mm and the percent shrink was calculated as the ratio of the change in dimensions to the original dimension along the MD or the TD. The percent recovery was calculated by dividing the percent shrink by the ratio of the difference between the final draw length and the initial length before draw to the final draw length.

CHAPTER 4

RESULTS AND DISCUSSIONS

4.1 GENERAL CHARACTERIZATION AND COMPARISON OF RESINS.

4.1.1 Glass Transition Temperatures

The three resins have been preliminarily classified according to their glass transition temperatures by dynamic mechanical analysis. Based on the DMA data an idea of the processing temperatures was obtained. Fig.4.1 presents the plot of the loss tan delta as a function of temperature. Styrene/maleic anhydride with 14% maleic anhydride content gave a maximum in Tan δ at 142°C supporting the expectation that increase in the stiffness of the chain backbone contributes to the increase in the glass transition temperature. S/MA with 8% maleic anhydride has a loss peak associated with the glass transition temperature at 130°C and pure homopolymer polystyrene gave a maximum in the loss peak at 117°C.

These results are in reasonable agreement with the literature which indicate that an increase in 1% of maleic anhydride contributed to about 1.7°C increase in the glass transition temperature.

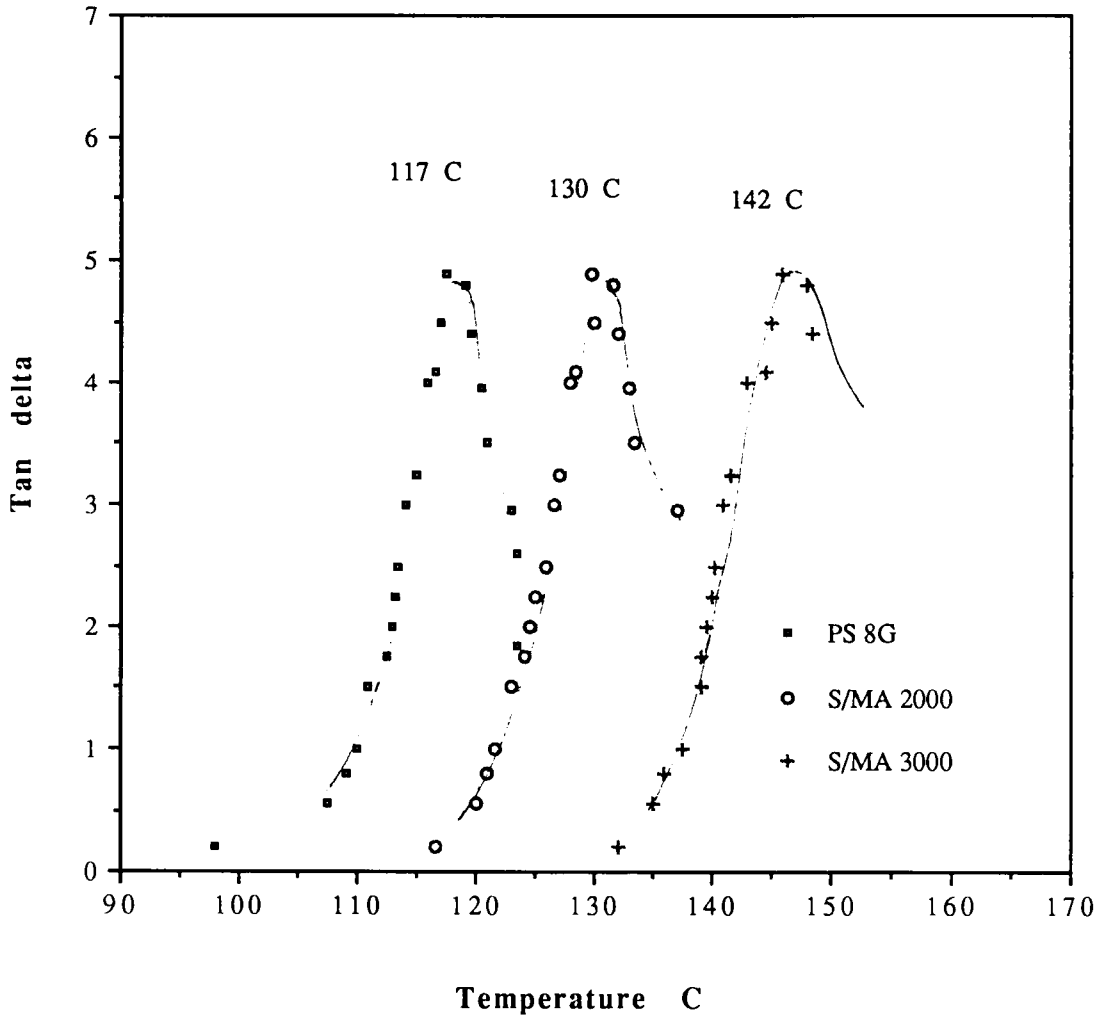


Figure 4.1 Plots of linear tan delta as a function of temperature for S/MA and PS measured at 1.1 Hz in dynamic mechanical measurements

4.1.2 Tensile Properties of Unoriented Resins

The room temperature tensile tests on compression molded samples are shown in Fig.4.2. These results show that all grades are basically brittle glassy polymers in the unoriented state at room temperature. The tensile modulus recorded for S/MA 3000 (14% MA), S/MA 2000 (8% MA) and PS (0% MA) were 200,000 psi, 172,000 psi and 120,000 psi respectively. They show that copolymerization with maleic anhydride increases the elastic modulus and tensile strengths of unoriented sheets of these polymers

4.1.3 Preliminary Determination of Processing Window

Several experiments were conducted to stretch the three polymers in a range of temperatures, stretch ratios and strain rates. The optimum processing temperatures for the three resins investigated are given in Table 4.1. It was generally observed that use of lower stretch temperatures than those mentioned in Table 4.1 put too low a limit on the stretch ratio that could be obtained. Although higher temperatures than given in the table did increase the capacity of the material to be stretched to greater stretch ratios, there were numerous occurrences of sample failure and thin spots close to the blower plate. Based on these preliminary results a strain rate of 2000%/min was chosen for studying orientation development.

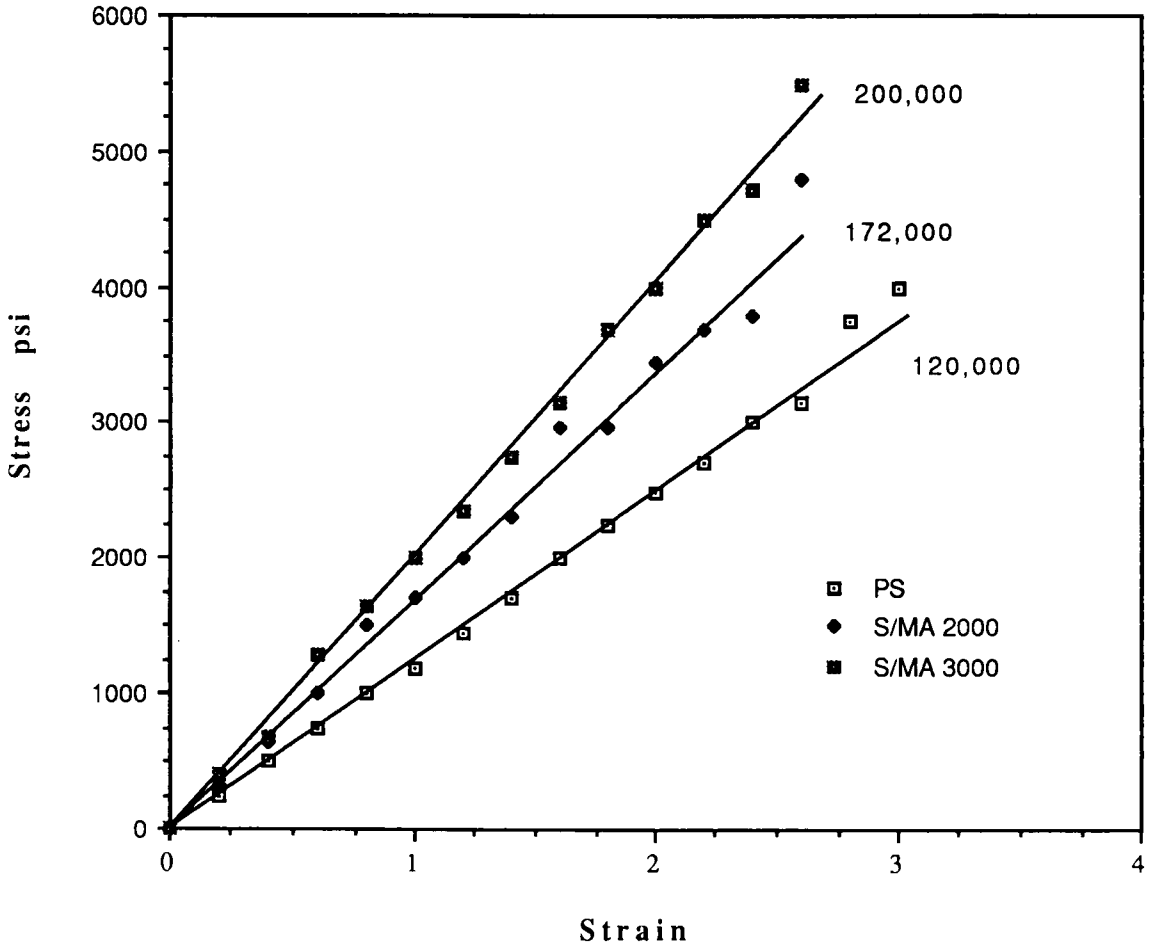


Figure 4.2: Room temperature stress strain curves for PS and S/MA polymers (The numbers on the curves indicate the tensile modulus in psi)

Table 4.1

Optimum stretch temperatures for stretching in the T.M. Long stretcher

Grade	Tg °C		Stretch
	DMA	DSC	Temperature oC
Dylark 3000 FG (S/MA)	142	131	168 +/-3
Dylark 2000 FG (S/MA)	130	118	155 +/-3
Dylene 8G (PS)	117	105	140 +/-3

4.1.4 Estimation of Intrinsic Birefringences

As mentioned in earlier sections, we have used birefringence as a primary tool to follow the development of orientation. The observed birefringence is a function of both the degree of orientation and the intrinsic birefringence of the material. For a given composition of polymer, the birefringence is directly proportional to the level of molecular orientation. But, since the values of intrinsic birefringences are different for different materials, a comparison of the level of orientation developed in different polymers will not be possible until the birefringences are normalized by the intrinsic birefringence. The following assumptions were made in the calculation of the intrinsic birefringences of the present polymers.

1. A fully stretched model conformation of the repeat unit is assumed, which is presumably comparable to the maximum possible anisotropy. The monomer unit of a PS/MA molecule was located by means of a coordinate system represented in Fig.2.8. The 1 axis is the chain axis or the chain direction of the extended macromolecule and it bisects the carbon-carbon bond of the main chain of PS at an angle $(180-\theta)/2$ where θ was chosen as 112^{o}. The 2 axis is the transverse direction and is coplanar with the 1 or the machine direction. The 3 axis is perpendicular to the 1 and 2 axes and forms a right handed coordinate system. σ is the angle characterizing the state of rotation of the benzene ring about the carbon-carbon bond that links it to the main chain, or in this case it is the angle made by the plane of the ring with the plane defined by the 1 and 2 axes. Only one such

conformation where the benzene ring is in the 1-2 plane was chosen and rotation of this group was not taken into consideration. Likewise, the maleic anhydride molecule was also assumed to be in the 1-2 plane.

2. The values of bond polarizabilities chosen were those reported by Denbigh (40)

3. The Lorentz-Lorenz equation was used to calculate the polarizability differences in the principal directions.

4. Using the equation for the intrinsic birefringence of a blend developed by Stein (52) the relationship for S/MA copolymer can be given as

$$\Delta o_{\text{copolymer}} = \Delta^{o*} w_{1(PS)} + \Delta^{o*} w_{2(MA)} \qquad ...4.1.1$$

The values suggested by our calculations for the intrinsic birefringences of S/MA and PS are given in Table.4.2

4.2 MOLECULAR ORIENTATION OF FILMS PREPARED FROM COMPRESSION MOLDED PLAQUES

Compression molding of pellets into plaques for stretching yields specimens that have a random distribution of chains in the bulk of the material. We have seen that the speed of light waves passing through the three principal directions will be governed by the three principal refractive indices in the material. Now due to the

random distribution of chains in the bulk of the material, the speed in all the three principal directions will be the same. This means that the refractive indices in all the three directions will be identical. This results in a zero value of the starting birefringence for both, in the plane and out of the plane of the film and gives the opportunity to fundamentally investigate the development of orientation as a function of process variables like temperature, strain rate and stretch ratio.

4.2.1 Birefringence of S/MA 3000 (14% MA) Films

Effect of Stretch Ratio

Figure 4.3 gives the birefringence vs. the unconstrained stretch ratio for samples stretched uniaxially without any constraints in the width direction. These experiments were conducted at a stretch temperature of 165°C and a strain rate of 2000 %/min. For uniaxially stretched films, the stretch direction was labeled the "1" direction, the transverse direction as the "2" direction and the direction normal to the plane, the "3" direction.

As seen from the figure, the $\Delta 12$ and $\Delta 13$ birefringences are almost equal and gradually increase with increase in stretch ratio, while $\Delta 23$ remains approximately equal to zero. This produces a state of orientation in the films similar to that developed in stretched fibers.

Figure 4.4 gives birefringence as a function of equal biaxial

Table 4.2

Values calculated for intrinsic birefringence of S/MA and PS

Grade	MA content	Δ^o
Maleic anhydride	100 %	-0.2669
Dylene 8G (PS)	0 %	-0.3043
Dylark 2000 FG (S/MA)	8 %	-0.3013
Dylark 3000 FG (S/MA)	14 %	-0.2990

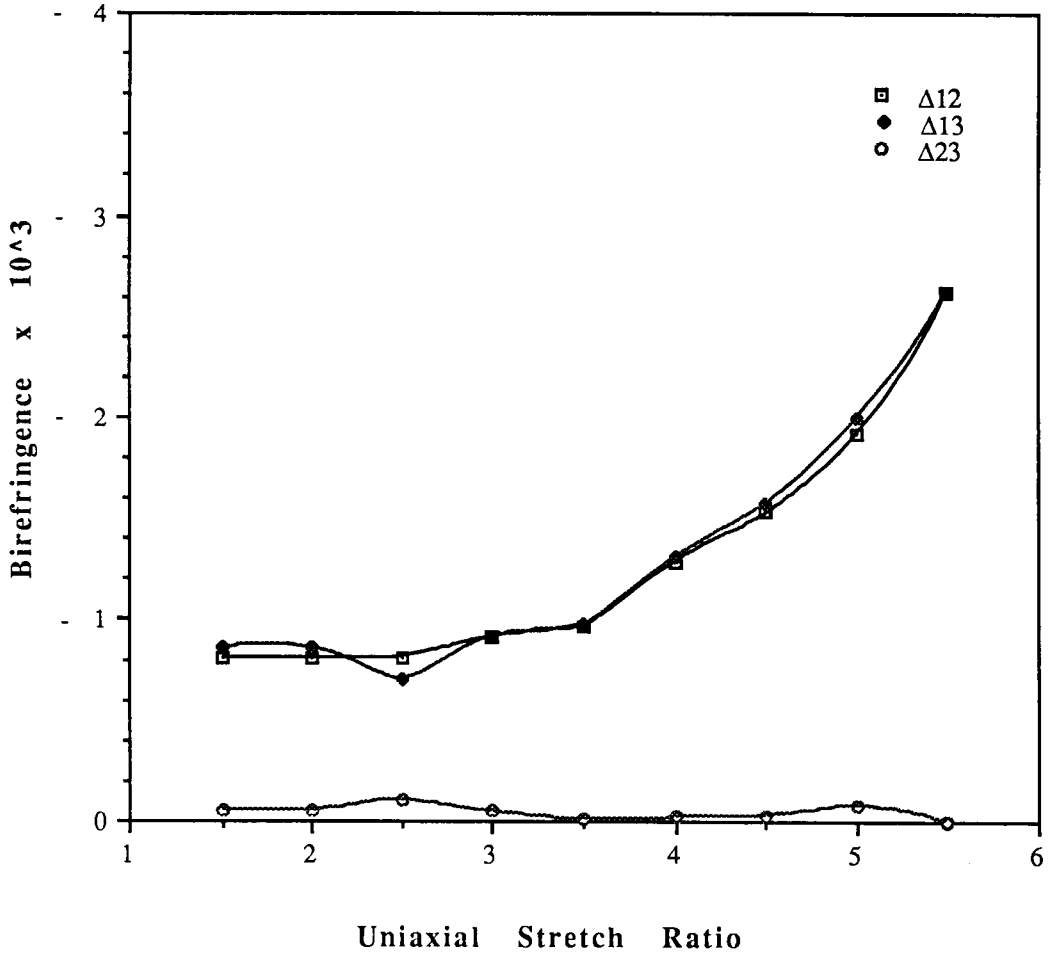


Figure 4.3 Birefringence for unconstrained uniaxial stretching of S/MA 3000 at 2000%/min-(compression molded)

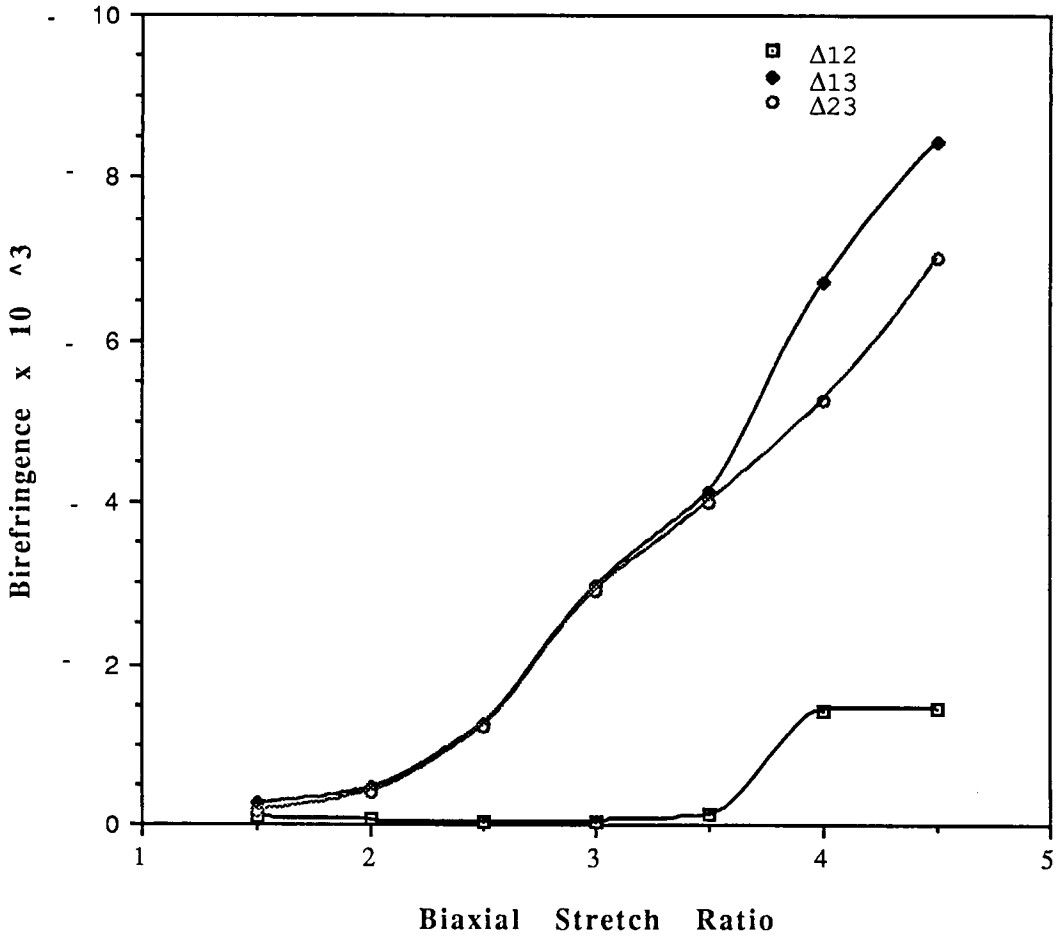


Figure 4.4 Birefringence for equal biaxial stretching of S/MA 3000 at 2000%/min (compression molded)

stretch ratio for the same set of samples processed at the same temperature and strain rate. As seen from the figure, the $\Delta 13$ and $\Delta 23$ values of birefringence increase steadily with an increase in the stretch ratio. However, the $\Delta 12$ value remains approximately equal to zero, irrespective of the stretch ratio. The small degree of unevenness at higher stretch ratios is probably due to errors in precise control of process parameters like strain rate and cooling rate. Although there is an increase in the orientation of the chains along the MD and TD with increase in stretch ratio, the magnitude of increase is the same. This explains the zero value of the in-plane or $\Delta 12$ birefringence.

Effect of Stretch Temperature

The orientation representation for a 2.5 x 2.0 stretch ratio as a function of stretch temperature is shown in Figure 4.5 As expected, we see a decrease in the birefringence with increase in the stretch temperature. The data in the plot reveals two related aspects of processing of oriented films. Firstly, for the stretch ratio investigated, S/MA 3000 can be processed in the temperature range of 165-210^{o}C. Secondly, the choice of temperature is dependent on the level of final orientation that is desired. Temperatures between 165-175^{o}C would be best suited for high levels of orientation in the final film.

Effect of Strain Rate

Figure 4.6 gives the development of birefringence as a function of strain rate. These results indicate an almost linear

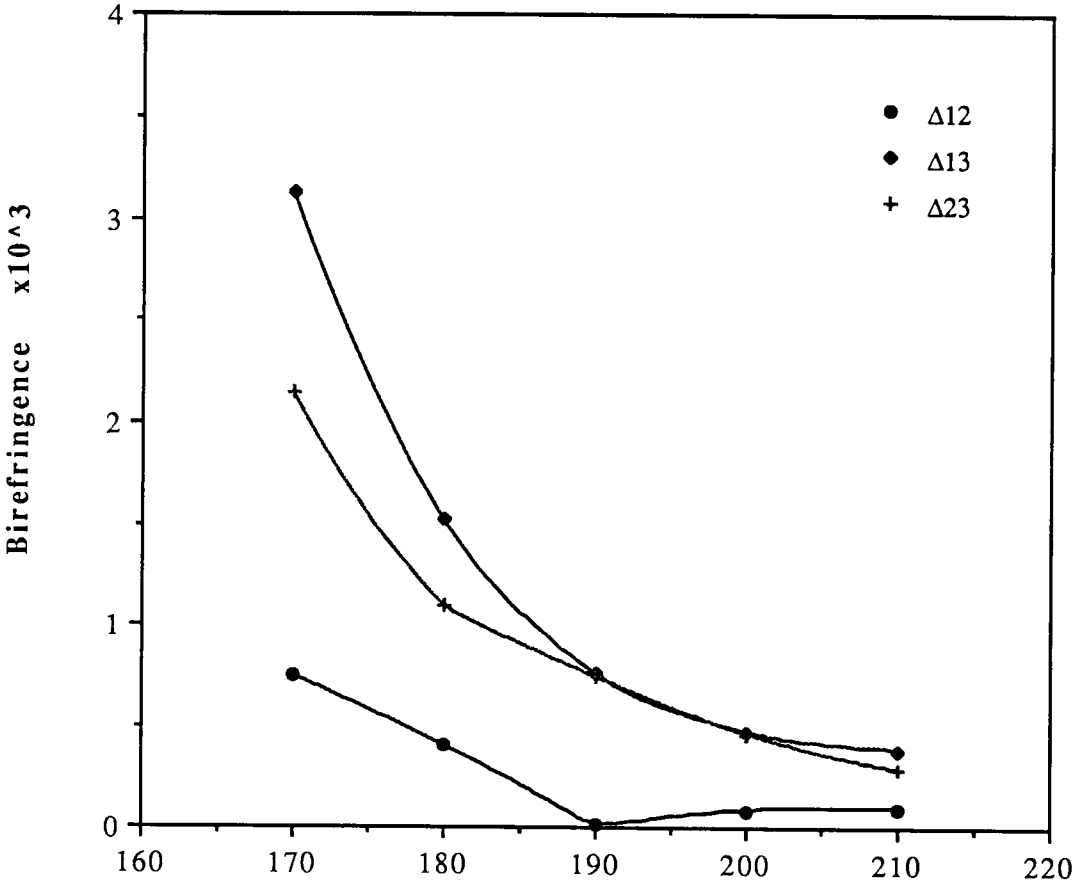


Figure 4.5 Effect of stretch temperature on orientation for films made from compression molded S/MA 3000 (2.5 MD X 2.0 TD, 2000 %/min)

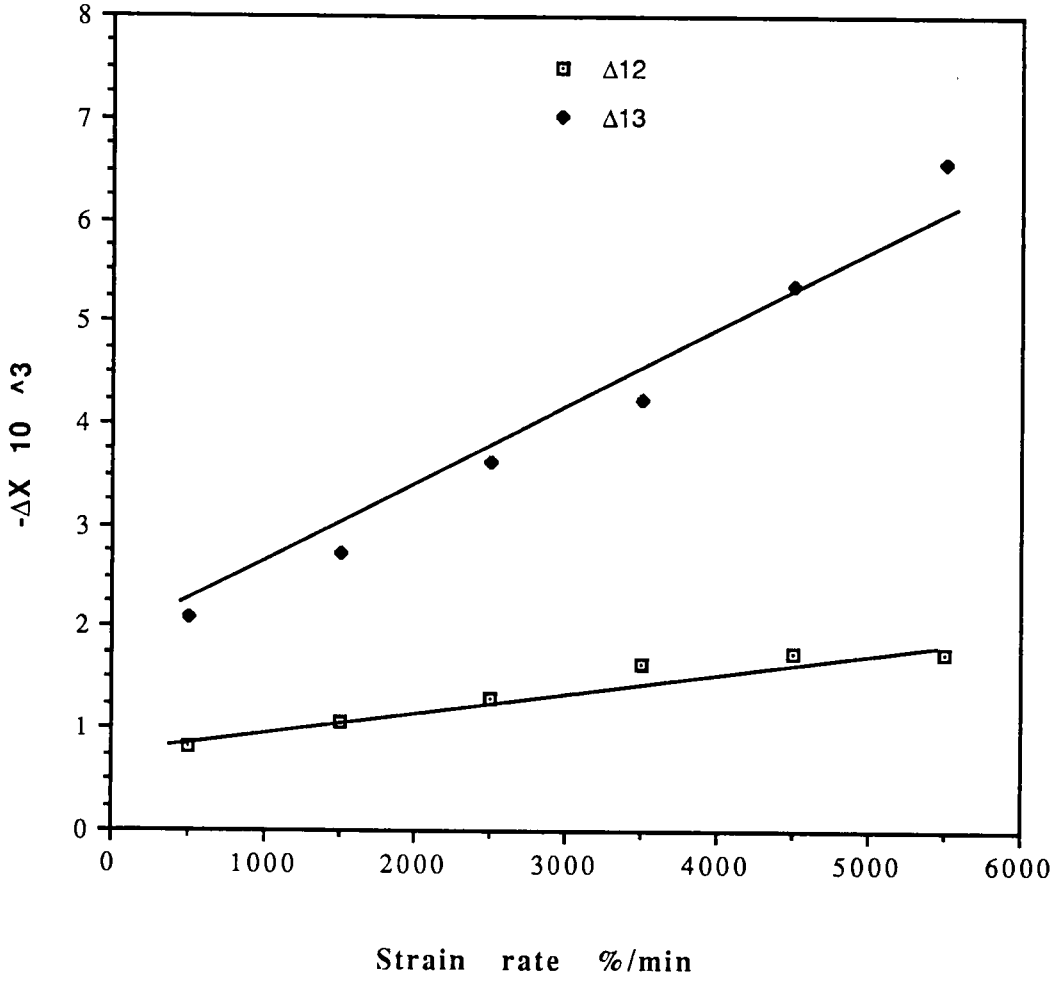


Figure 4.6 Effect of strain rate on a 3000 S/MA film stretched to a 3x2 ratio at 168 C.

increase in the birefringence with an increase in the strain rate.

Based on the above data on the effect of process variables like stretch ratio, temperature and strain rate, we can suggest that molecular orientation during stretching takes place in the following manner: Below the glass transition temperature the polymer chains are rigid and have a random coil conformation. However at and above the glass transition temperature they gain a degree of freedom and become deformable when stress is applied, which in this case is a biaxial stretching operation. The chains undergo some measure of disentanglement, straightening and alignment in the stress field. There are three components to this process: E1, is the instantaneous elastic component caused by valence-angle deformation or bond stretching which is completely recoverable when the stress is removed. E2, is the molecular alignment caused by uncoiling of the chains and which is frozen in as the polymer is cooled. E3 is the viscous flow of the chains. E2 is the desirable component in the process. As the temperature is increased, there is a non recoverable viscous flow caused by the sliding of the chains past one another. With further increase in the temperature, the response time of E3 further decreases with decrease in viscosity, to an extent that it allows E2 to relax more during the stretching process. Thus for a fixed strain rate, the lowest temperature above the Tg will give the greatest orientation.

In order to explain the effect strain rate has on the molecular orientation, the stretching process can be described by the following

equations:

$$\sigma_e = \frac{F}{A} \qquad \ldots 4.2.1$$

Where σ_e is the stress developed in the film due to a force F acting in a direction perpendicular to the 2-3 surface. 'A' is the cross section area of the film (2-3 surface).

The strain rate can be given by the equation

$$\dot{\gamma} = \frac{1}{l_o}\frac{dl}{dt} \qquad \ldots 4.2.2$$

From the above equations, the viscosity during stretching is

$$\eta_e = \frac{\sigma_e}{\dot{\gamma}}$$

$$\sigma_e = \eta_e \dot{\gamma} \qquad \ldots 4.2.3$$

Since the stretching is isothermal, the viscosity during the process is constant

$$\sigma_e \alpha \dot{\gamma} \qquad \ldots 4.2.4$$

As seen from section 2.2.2 the birefringence is related to the stress by the stress optical law

$$\Delta_n \alpha \sigma_e \quad \ldots 4.2.5$$

Combining equations 4.2.4 and 4.2.5 we get

$$\Delta_n \alpha \dot{\gamma}_e \quad \ldots 4.2.6$$

This clearly shows that an increase in the strain rate causes an increase in the orientation when the temperature and stretch ratio is kept constant.

4.2.2 Birefringence of S/MA 2000 (8% MA) Films

Effect of Stretch Ratio

The orientation development in these plaques for a free width uniaxial and equal biaxial films was conducted at a fixed stretch temperature of 155°C and 2000%/min strain rate. As seen in Figure 4.7, the out-of-plane birefringence, $\Delta 23$, for the free width uniaxial films is almost zero indicating a uniaxial stretch or a fiber like symmetry in the orientation. On the other hand, the in-plane birefringence values of the equal biaxial film, as seen in Figure 4.8 is almost zero indicating an equal biaxial nature of the film.

Effect of Stretch Temperature

In order to evaluate the influence of the stretch temperature

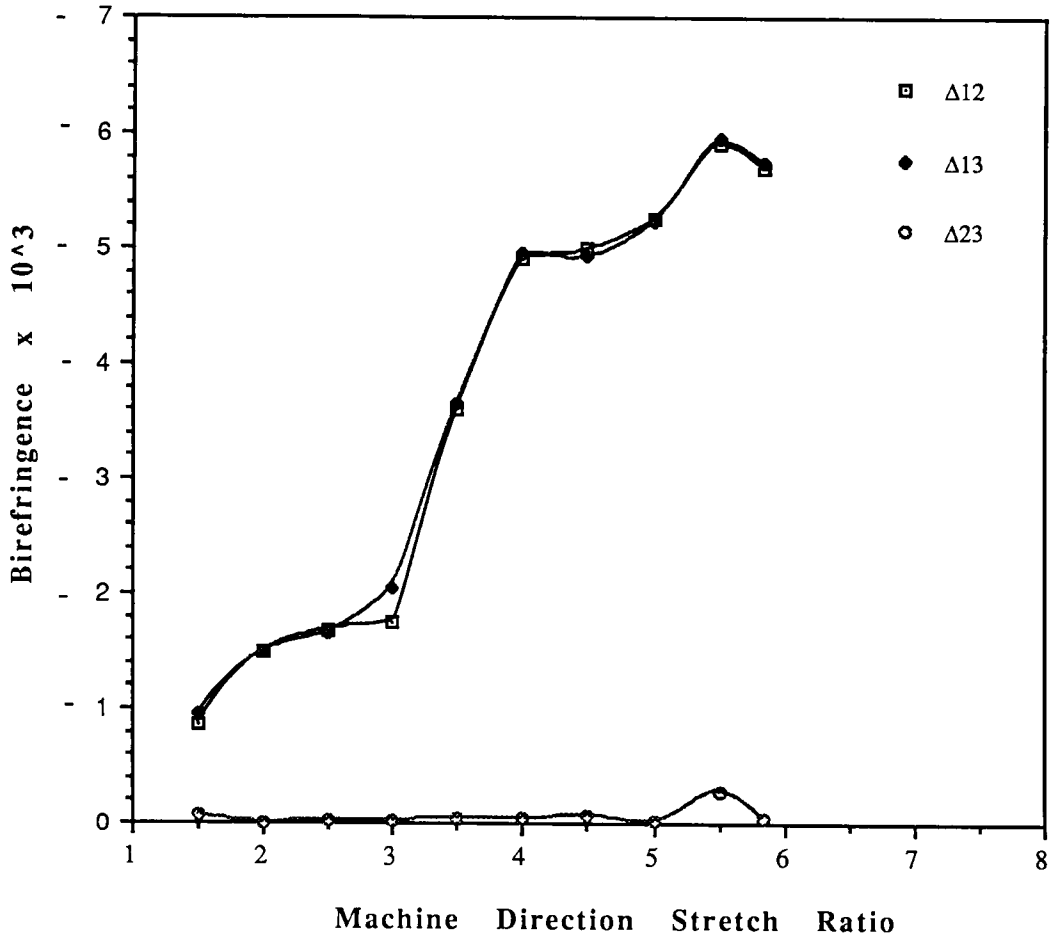


Figure 4.7: Birefringence vs. uniaxial stretch ratio for films from compression molded S/MA 2000 (2000%/min and 155 C)

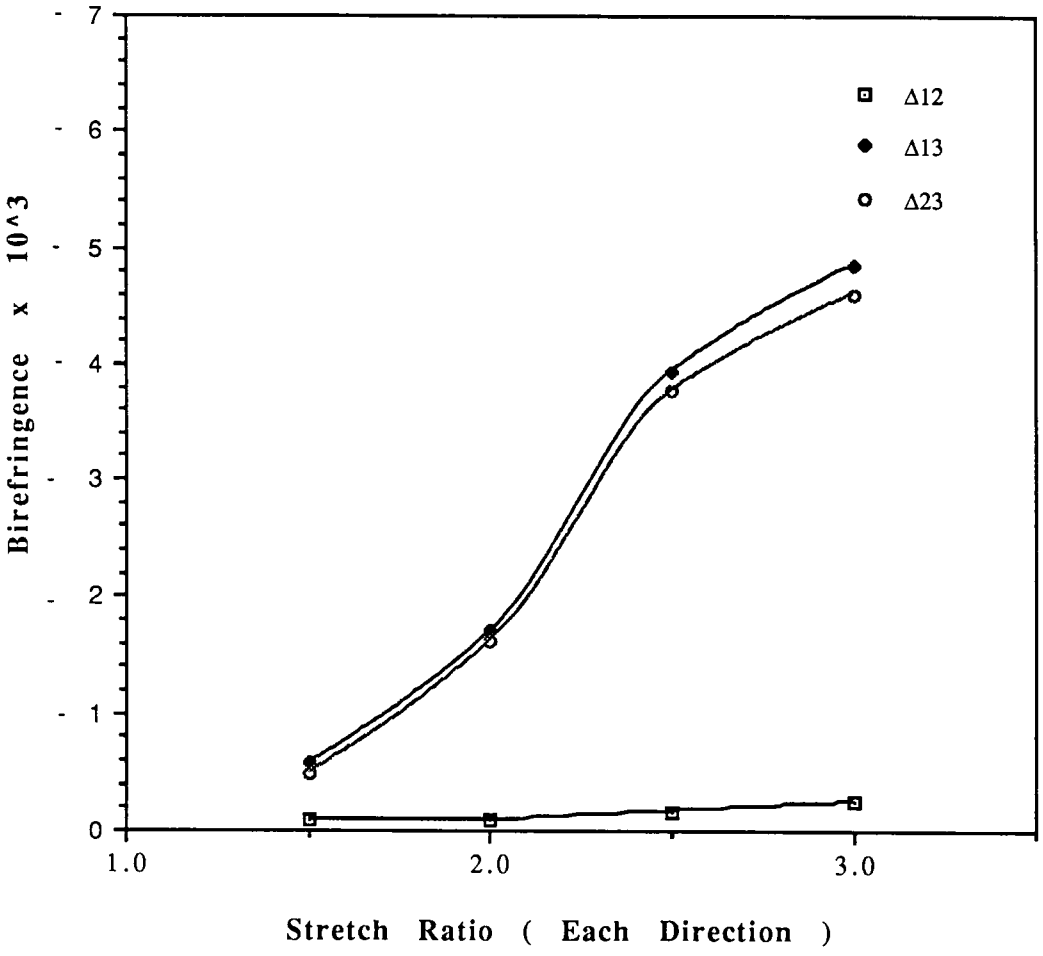


Figure 4.8 Birefringence vs. biaxial stretch ratio for films from compression molded S/MA 2000 (2000%/min and 155 C)

on birefringence, the orientation development for a 2.5 x 2.0 stretch as a function of temperature is shown in Figure 4.9 As with the case of S/MA 3000, the birefringence of S/MA 2000 falls with an increase in the stretch temperature. This decrease in the birefringence occurs over a different temperature range of 155-205°C.

Effect of Strain Rate

Figure 4.10 gives the effect of strain rate for a 3 x 2 stretch ratio. As expected there is an increase in the molecular orientation with an increase in the strain rate.

4.2.3 Birefringence of Polystyrene 8G (0% MA) Films

In the preceding discussion we have seen that the presence of maleic anhydride in the mainchain of polystyrene (S/MA) not only raises the processing temperature for film stretching but also limits a wide range of attainable biaxial stretch ratios. Polystyrene on the other hand has the lowest processing temperature compared to S/MA 3000 and S/MA 2000 and also allows high stretch ratios to be attained.

Effect of Stretch Ratio

Polystyrene (Dylene 8G) was stretched to several stretch ratios ranging from uniaxial to biaxial at 140°C and a strain rate of 2000 %/min. Figure 4.11 shows the increase in the in-plane birefringence,

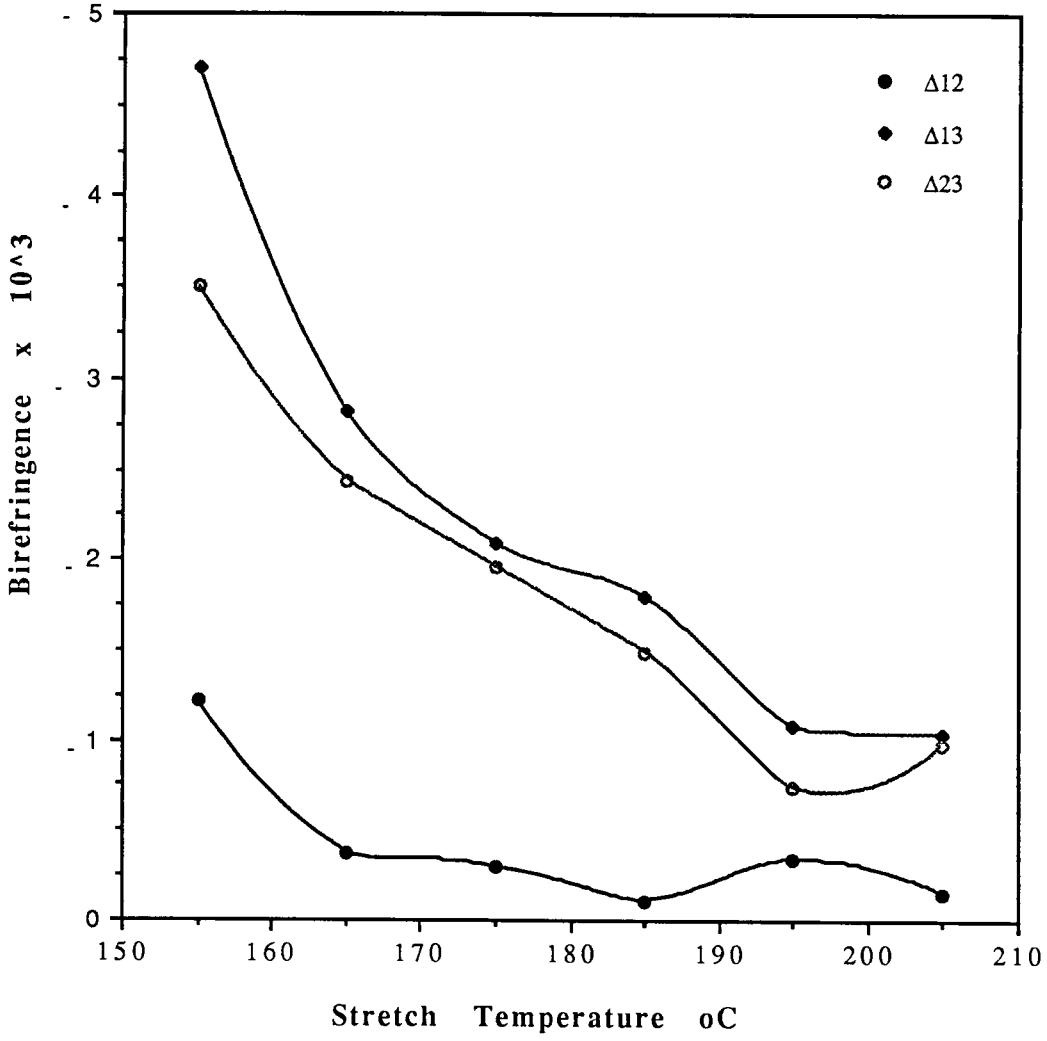


Figure 4.9 Effect of Stretch temperature on orientation for films made from compression molded S/MA 2000. (2.5MD x 2.0TD Stretch Ratio, 2000%/min)

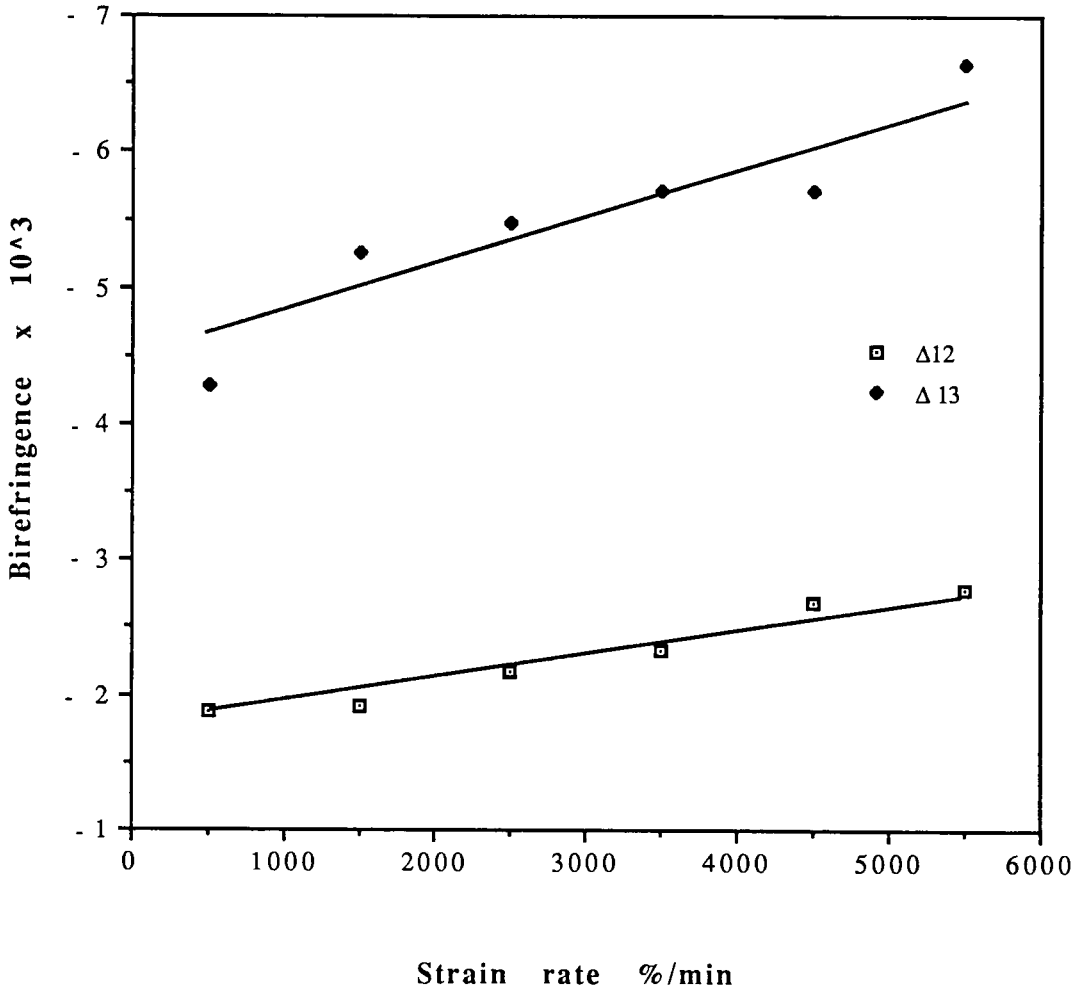


Figure 4.10: Strain rate effect for S/MA 2000 stretched to a 3x2 ratio at 155 C

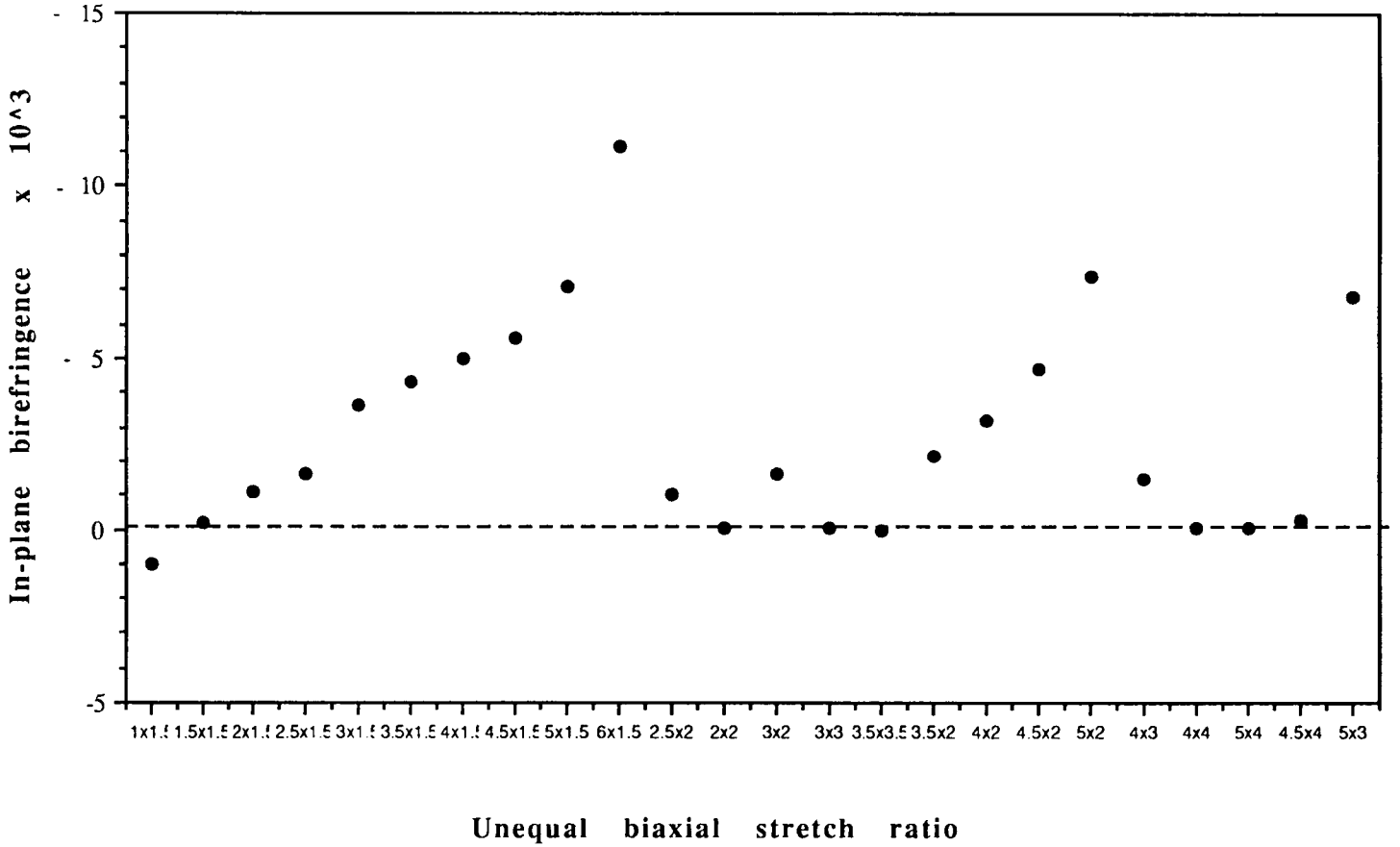


Figure 4.11 In-plane birefringence for PS for several biaxial stretch ratios. (140 C and 2000 %/min)

$\Delta 12$, with an increase in the stretch ratio while Figure 4.12 shows that the out-of-plane birefringence, $\Delta 13$, increases with increase in stretch ratio. The data for equal biaxial stretch of PS are shown separately in Figure 4.13.

Effect of Stretch Temperature

The orientation representation for a 2.5 x 2.0 stretch ratio as a function of temperature is shown in Figure 4.14. As expected, we see a decrease in the birefringence with increase in the stretch temperature. Comparing the data for 3000FG and 2000FG we see that Dylene possesses the lowest range of processing temperatures (140-190°C).

Effect of Strain Rate

As seen for the case of S/MA 3000 and S/MA 2000, an increase in the strain rate increases the orientation induced in the sample in a linear fashion. Figure 4.15 gives the development of birefringence as a function of strain rate.

4.2.4 Comparison of Orientation Developed in the Three Resins

In order to compare the orientations developed in these three materials, the birefringence values must be converted to orientation functions values by dividing by the intrinsic birefringences.

A comparison of the molecular orientation developed by the

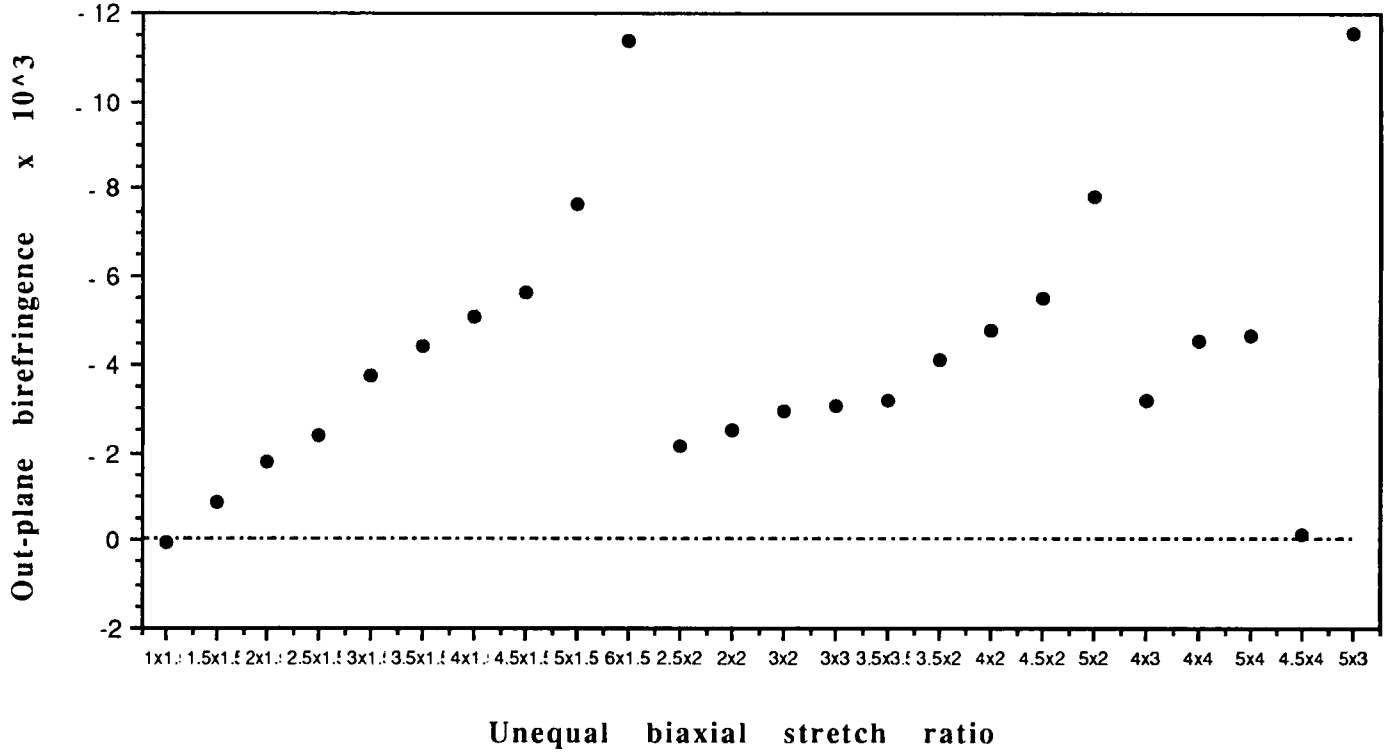


Figure 4.12 Out of plane birefringence for PS for several biaxial stretch ratios. (140 C and 2000%/min)

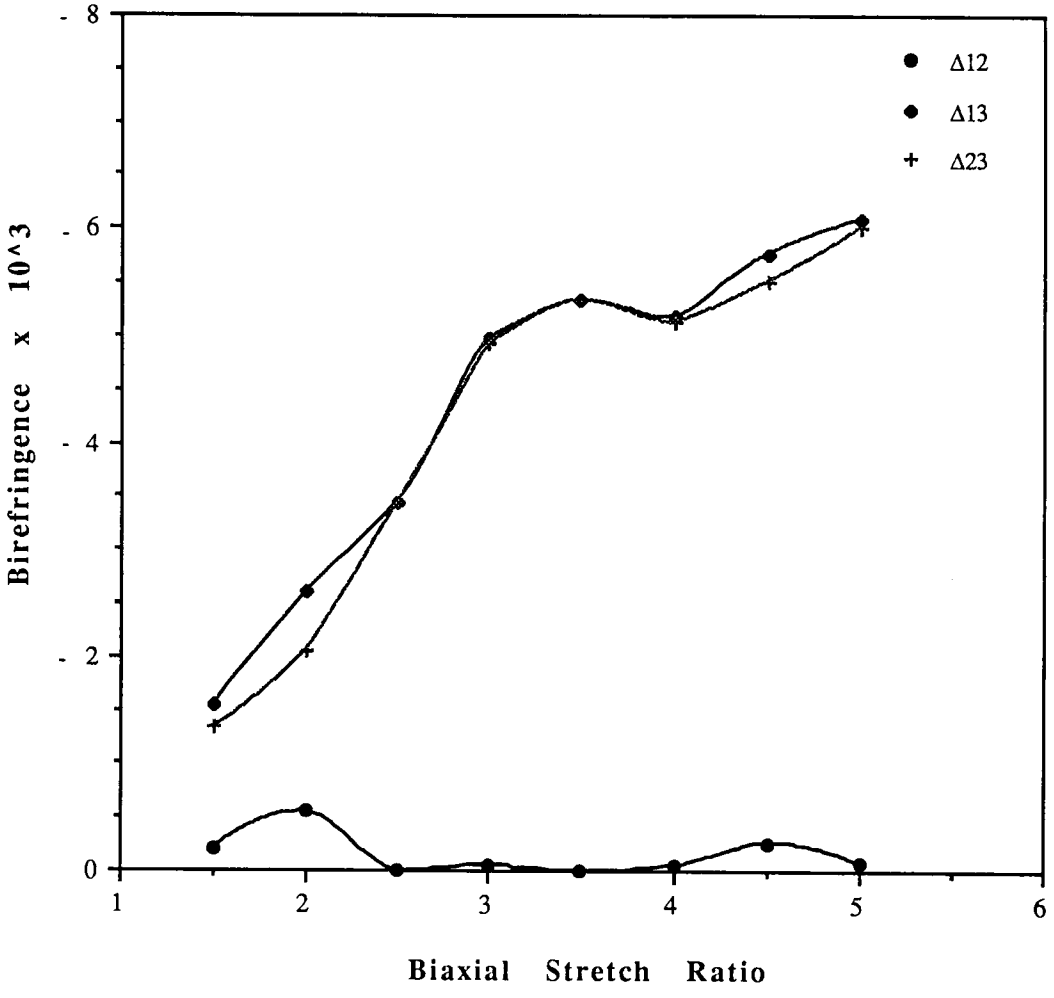


Figure 4.13 Birefringence data for equal biaxial stretch of polystyrene films made from compression molded plaques (2000%/min, 140 C)

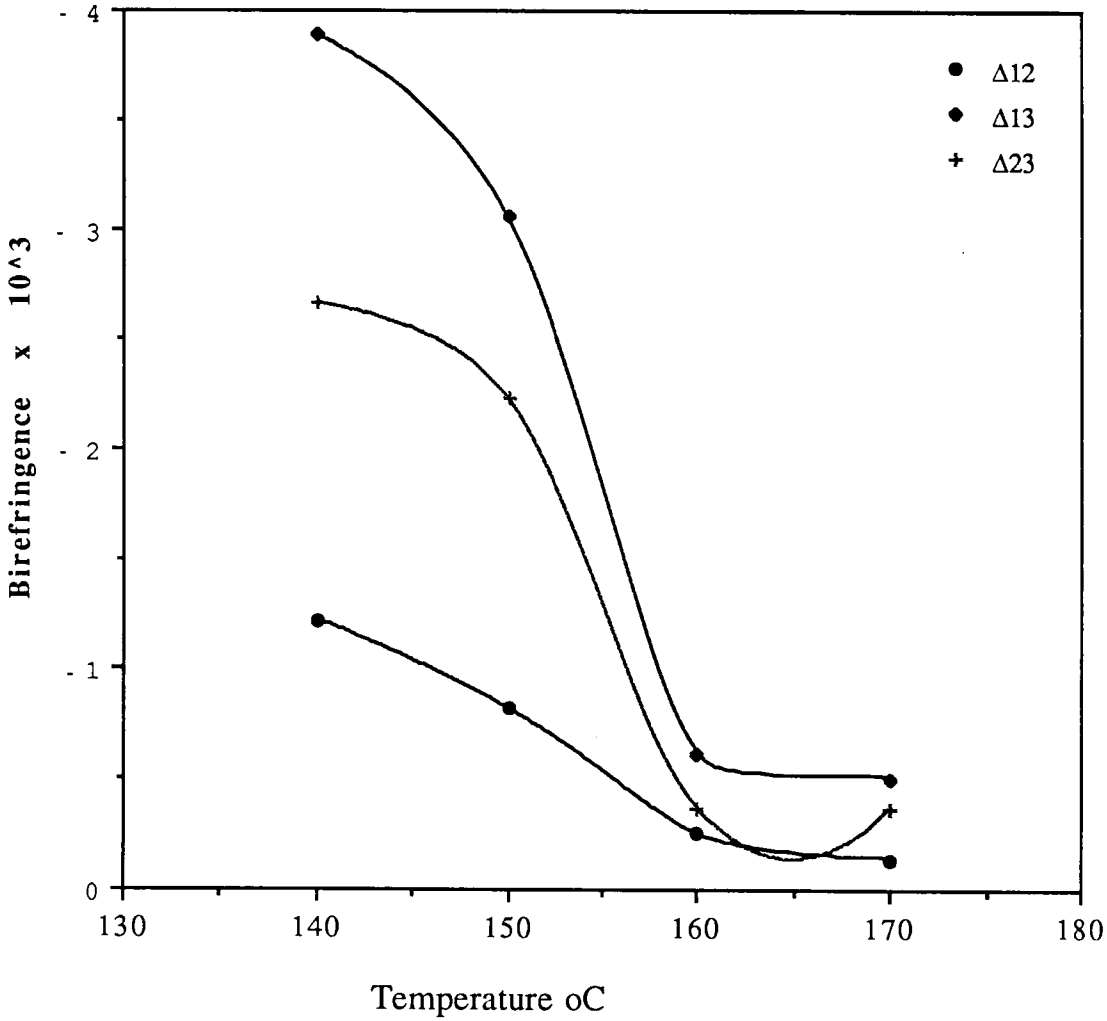


Figure 4.14: Effect of stretch temperature on orientation for films made from compression molded PS. (2.5 MD X 2.0 TD)

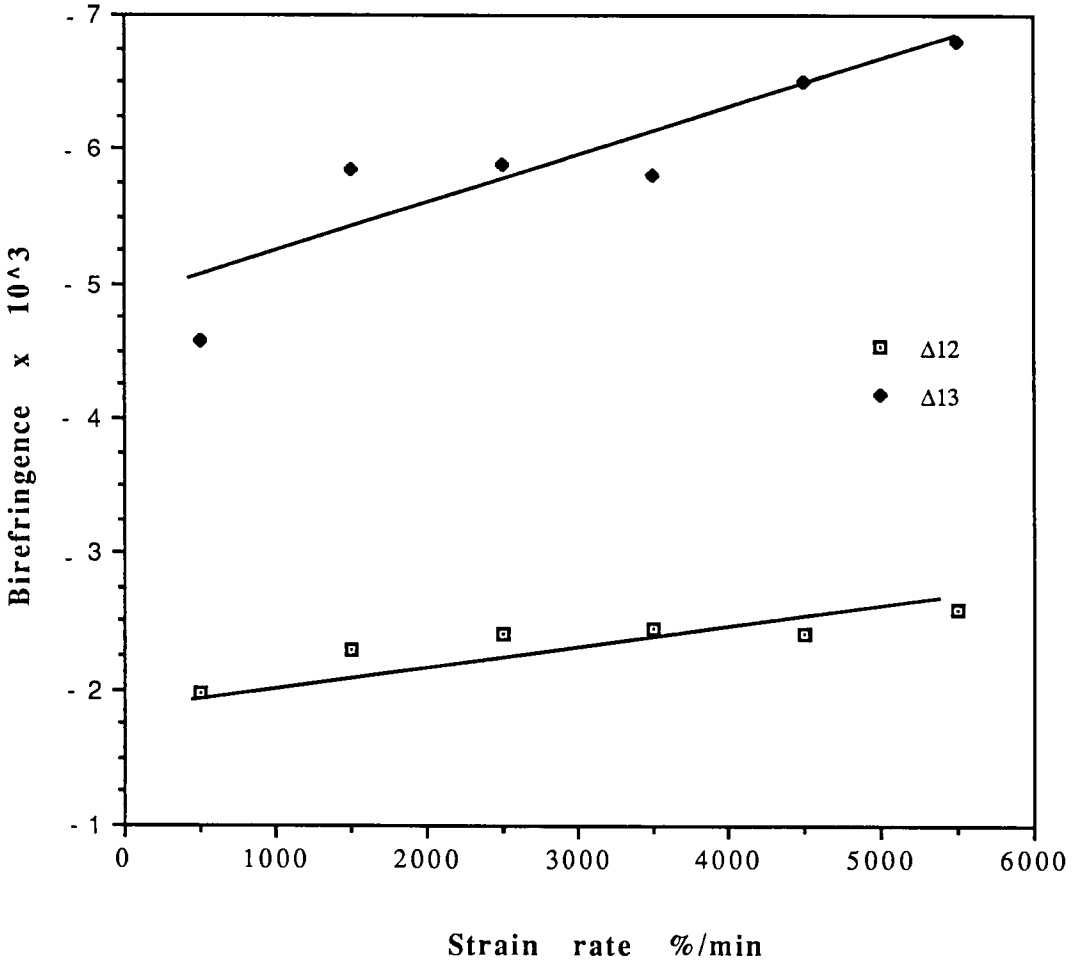


Figure 4.15 Effect of birefringence on strain rate for films stretched from 26 mils plaques of PS to a 3x2 stretch ratio,140 C

2.5 x 2.0 stretch in the three materials as a function of temperature is shown in Figure 4.16 which shows a plot of f_1^B versus temperature. The range of molecular orientations that were developed in these materials were similar, but development of a given molecular orientation required processing the different materials at very different temperatures. For example, the development of a molecular orientation of 0.01 required processing the polystyrene at only about 150°C, Dylark 2000 FG at about 162°C and Dylark 3000 FG at about 172°C. These differences are reasonably consistent with the differences in the glass transition temperatures reported for these materials.

The range of stretch ratios that could be taken without failure varied with stretch temperature and from one material to another. We attempted to establish the optimum temperature for stretching based on maximum stretch ratio achievable without sacrificing too much molecular orientation or encountering too many sample failures. The temperatures selected were 140°C for polystyrene, 155°C for Dylark 2000 FG, and 170°C for Dylark 3000 FG. The maximum consistently achievable biaxial stretch ratios at these temperatures were 4.5 x 4.5 for Dylark 3000 FG , 3 X 3 for Dylark 2000 FG and 5 x 5 for polystyrene.

In Figure 4.17 f_1^B is shown plotted versus f_2^B for the biaxially stretched films of all compositions. As expected, the data for all the stretch ratios lie very close to the line corresponding to equal biaxial orientation where $f_1^B = f_2^B$, indicating that alignment of the chains

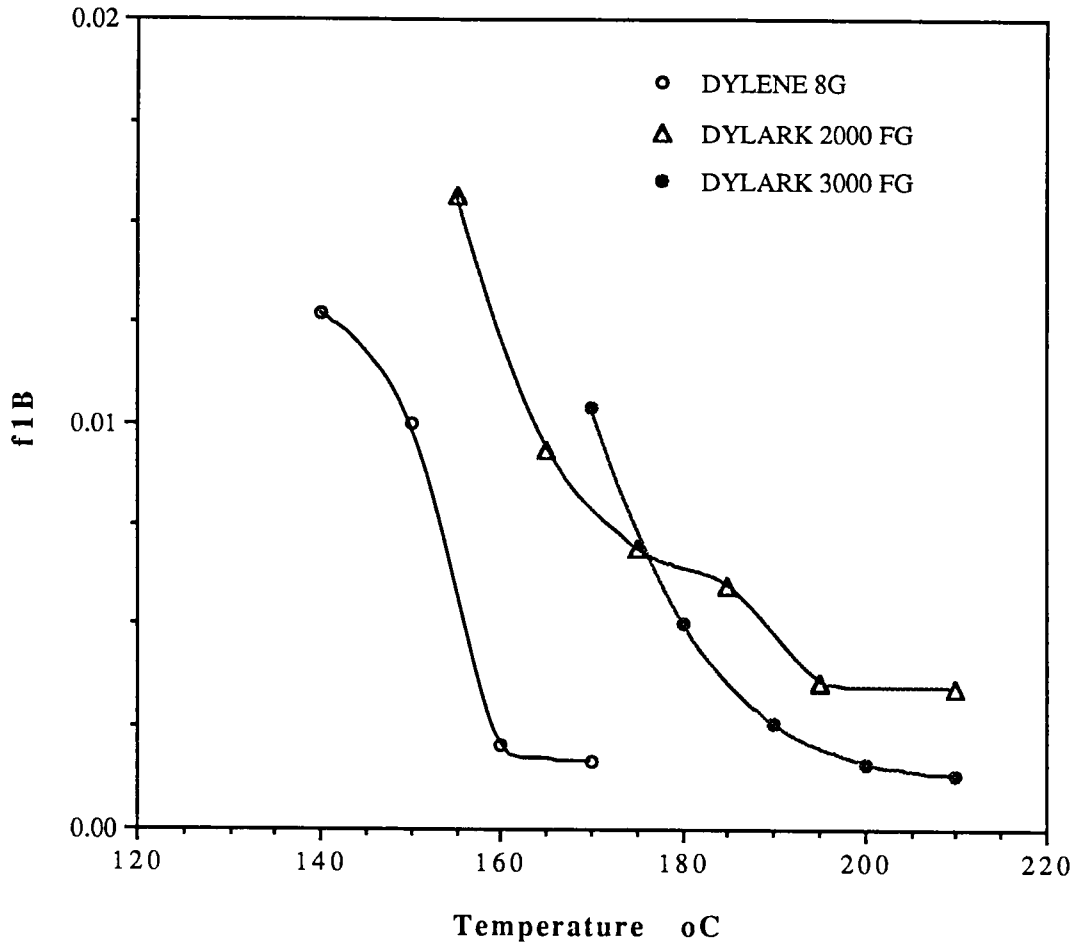


Figure 4.16 Effect of stretch temperature on the orientation of films made from compression molded polystyrene and S/MA copolymers (2.5MDx2.0TD, 2000%/min)

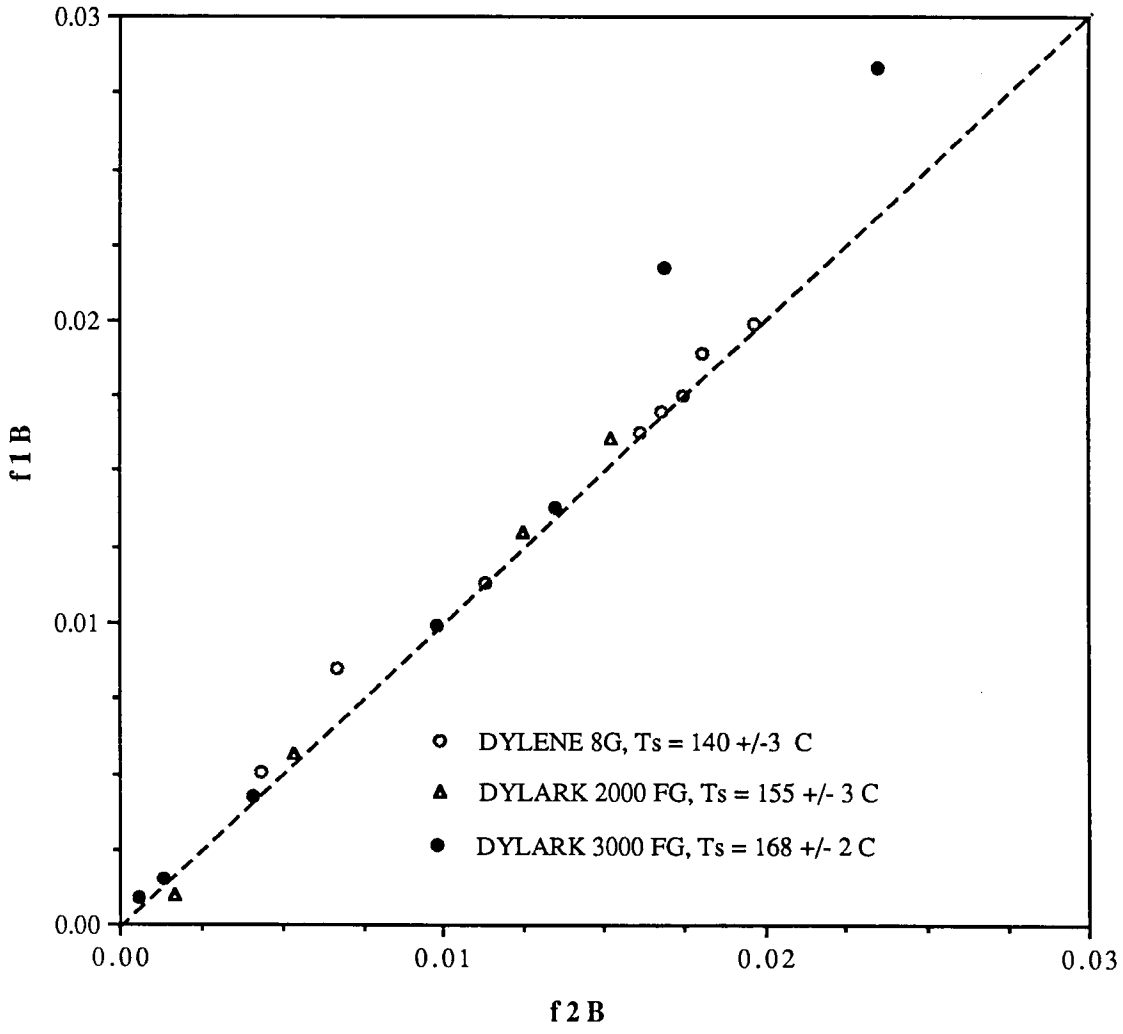


Figure 4.17 Orientation diagram for biaxially stretched films of PS and S/MA copolymers for a strain rate of 2000%/min and the indicated stretch temperatures, Ts.

is the same with respect to both the MD and TD directions. The orientation factors shift away from the origin along the 45° diagonal with an increase in the stretch ratio. Again, the same approximate range of orientation factors is developed in each of the three materials, but with different stretching temperatures for each material.

Molecular Orientation for the Three Resins at a Common Stretch Temperature

In view of the increase in the glass transition temperature of S/MA copolymers with an increase in the maleic anhydride content, the experiments hitherto, dealt with separate processing temperatures depending upon the polymer in question. From a practical view point for film processing, it is of interest to evaluate the relative levels of orientation in the three grades, when processed under equivalent conditions.

In order to attempt such a comparison, S/MA 2000, S/MA 3000 and Dylene 8G were stretched to a 4 MD X 2.5 TD ratio at 2000 %/min for a common stretch temperature. A stretch temperature of 145°C was sufficient for stretching polystyrene but marginally enough for 2000 S/MA. At this temperature S/MA 3000 did not stretch at all. A second temperature (165°C) was so high for stretching polystyrene that the hot air from the blowers ripped the plaque even before stretching could be effected. However, at this temperature both the S/MA 2000 and 3000 grades could be

stretched (the latter with some difficulty). Thus 145°C was chosen as the common stretch temperature for PS and S/MA 2000 while 165°C was used as a common temperature for S/MA 2000 and S/MA 3000.

A comparison of the MD and TD orientation factors using the White-Spruiell orientation factors was made and is presented in Figure 4.18. Comparing PS and S/MA 2000 at 145°C, it is seen that the 8% MA copolymer of styrene(S/MA 2000) had about 58 % higher MD orientation factors than PS (0%MA). At a temperature of 165°C an increase to 14% MA did not give such a rapid increase as from 0% to 8% MA at 145°C. The increase in the orientation level in 3000 S/MA (14% MA) in comparison to 2000 S/MA (8% MA) was about 15%.

4.3 MECHANICAL PROPERTIES OF FILMS PREPARED FROM COMPRESSION MOLDED PLAQUES

4.3.1 S/MA 3000 (14%MA)

The tensile strength vs. the stretch ratio for equal biaxial films seen in Figure 4.19 shows a steady increase in the tensile strengths with increase in the biaxial stretch ratio. The elongation to break, Figure 4.20 shows a maximum of 8.06% at 2x2 stretch ratio and decreases with further increase in the stretch ratio. All the samples have failed in a brittle manner.

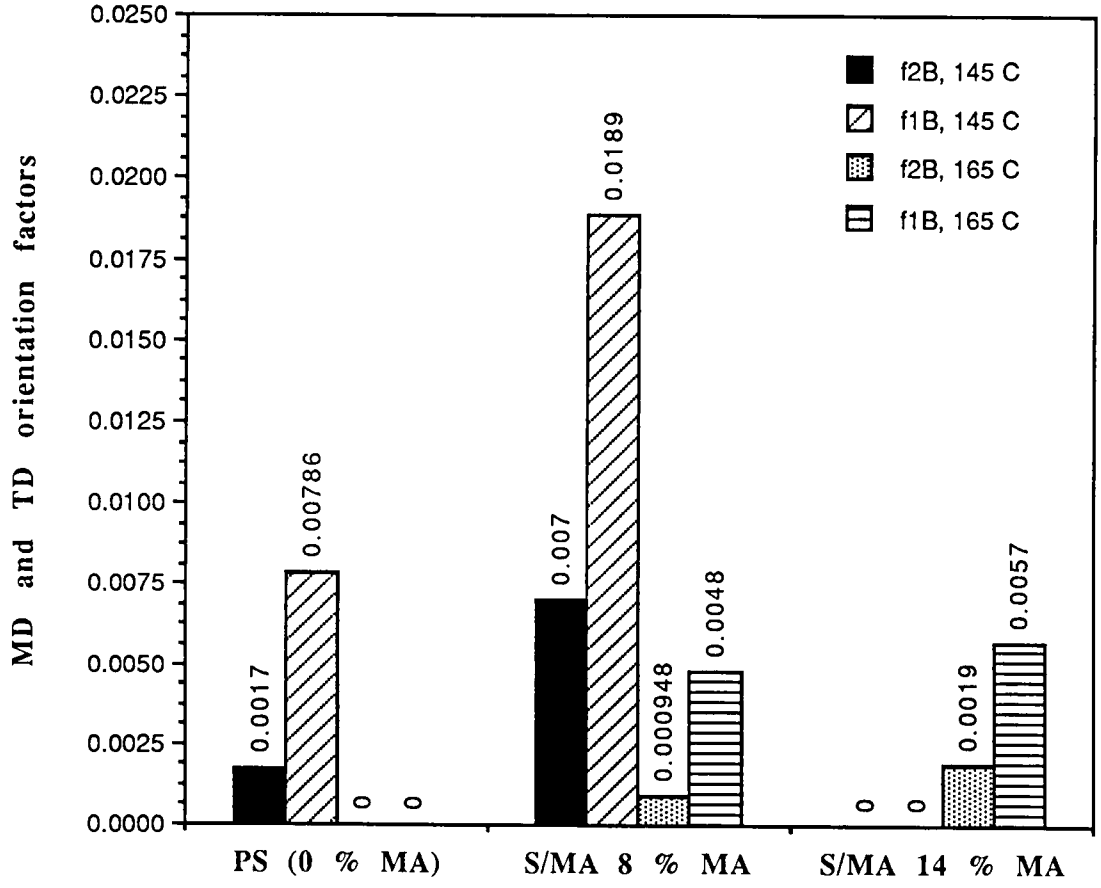


Figure 4.18 Orientation factors for PS and S/MA stretched to a ratio of 4 MDx 2.5 TD at 2000%/min.

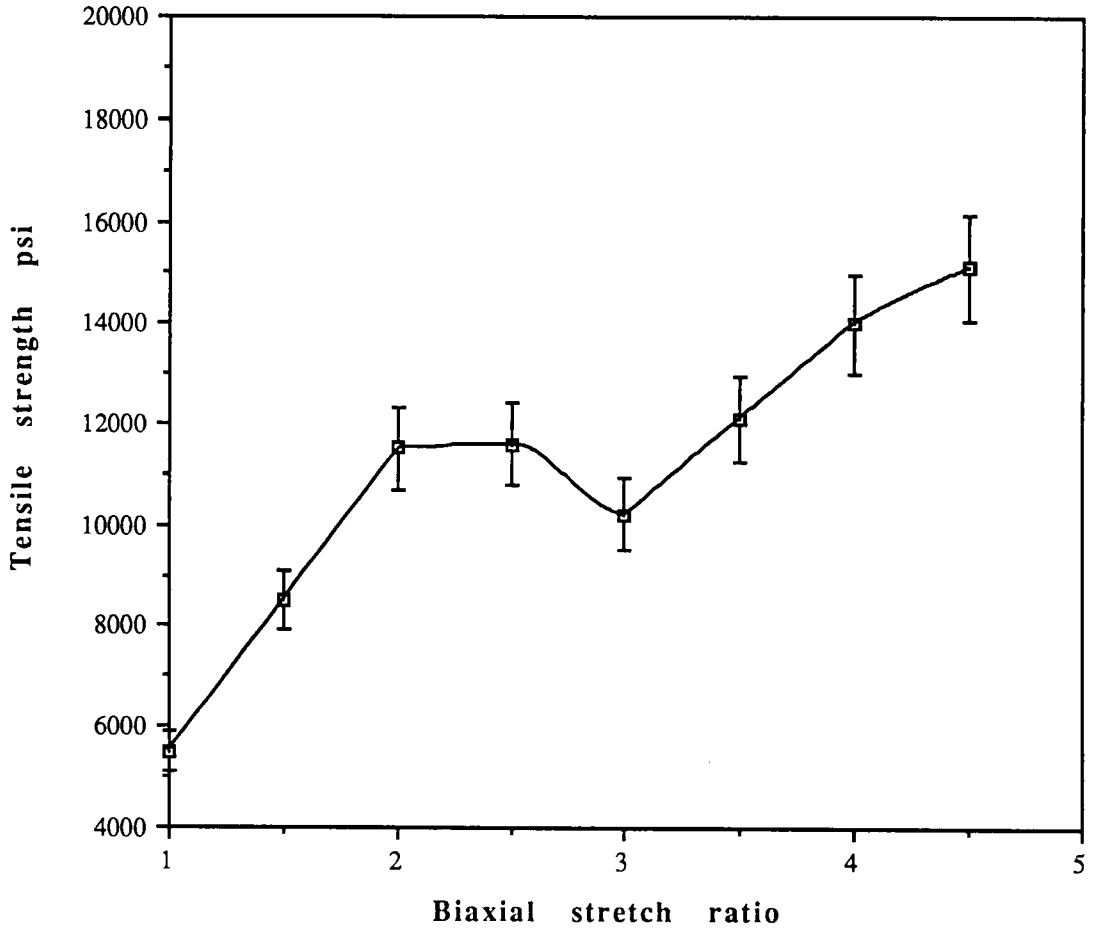


Figure 4.19 Tensile strength for compression molded S/MA 3000 equal biaxial stretch at 2000 %/min.

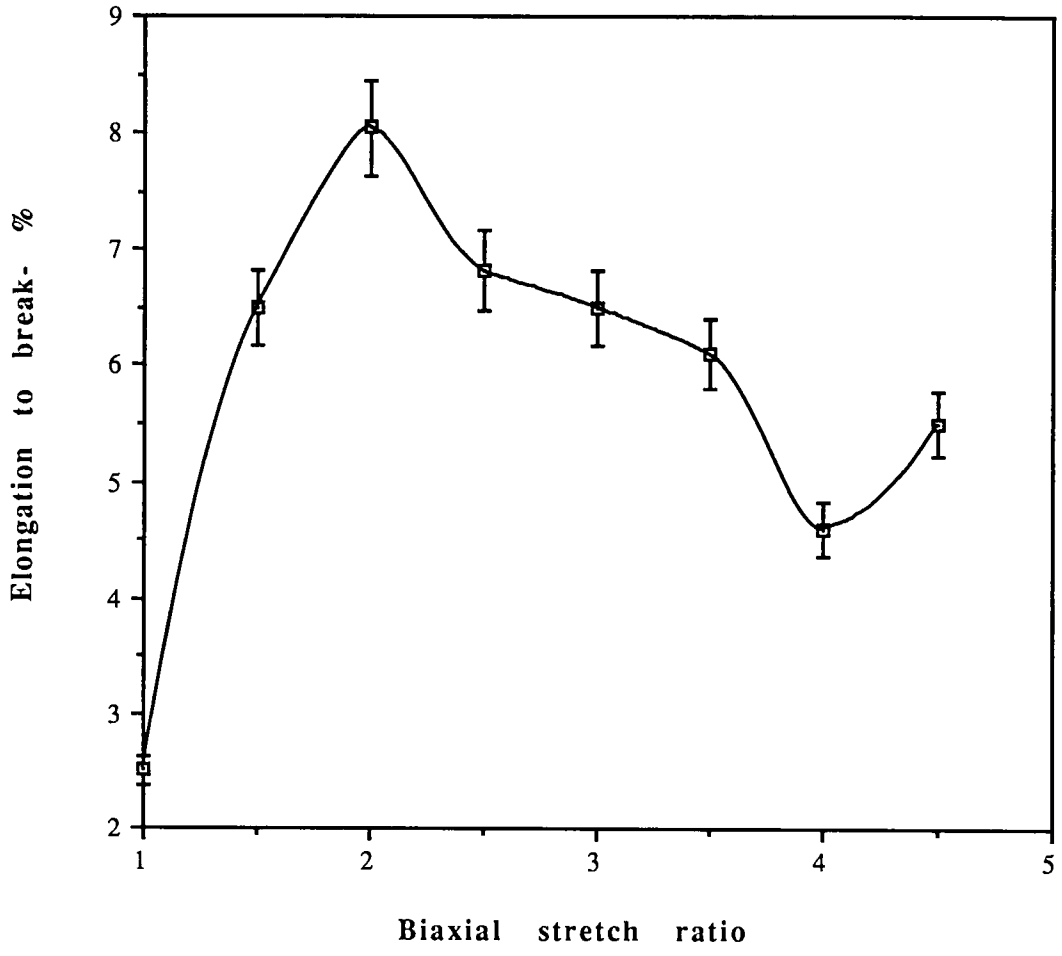


Figure 4.20 Elongation to break for compression molded S/MA 3000 equal biaxial stretch at 2000 %/min

4.3.2 S/MA 2000 (8% MA)

4.21 and 4.22 plot the data on the tensile strength and elongation to break as a function of biaxial stretch ratio. In this case the tensile strength and the elongation to break increase with increases up to a stretch ratio of 2.5 after which it nearly levels off. The samples studied here also failed in a brittle fashion.

Figure 4.23 shows the stress at break for samples with stretch ratio 2.5 x 2.0 for the range of temperatures between 155°C and 205°C. The samples are the same as those shown in Figure 4.9. The stress at break is lower along the TD than in the MD. This can be easily explained by the fact that for a fixed temperature, a higher stretch ratio along the MD gives rise to a greater orientation of the chains. In general both the MD and TD property somewhat decrease with an increase in the stretch temperature. Figure 4.24 shows the percentage elongation to break vs. temperature for the same set of films. The failure of all the samples, irrespective of the stretch temperature, can be best described as brittle.

4.3.3 Polystyrene 8G (0%MA)

The films of Polystyrene were examined for their mechanical behavior in tension. For the biaxial films the results were independent of the choice of test direction. Unequal biaxial films, were tested along the MD (direction with the higher stretch ratio).

Figure 4.25 shows that the stress at break for films with a fixed stretch ratio of 1.5 along the TD increases initially with an increase in

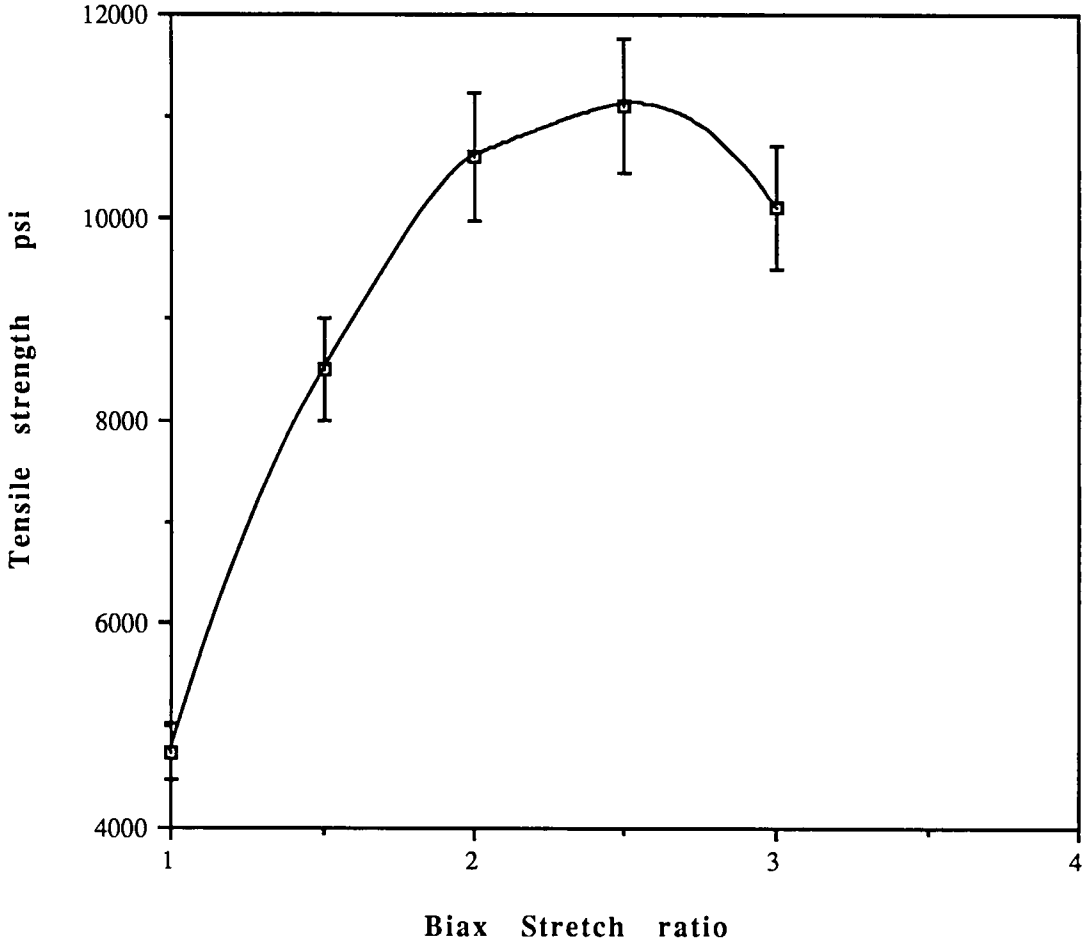


Figure 4.21 Tensile strength for compression molded S/MA 2000 equal biaxial stretch at 2000 %/min

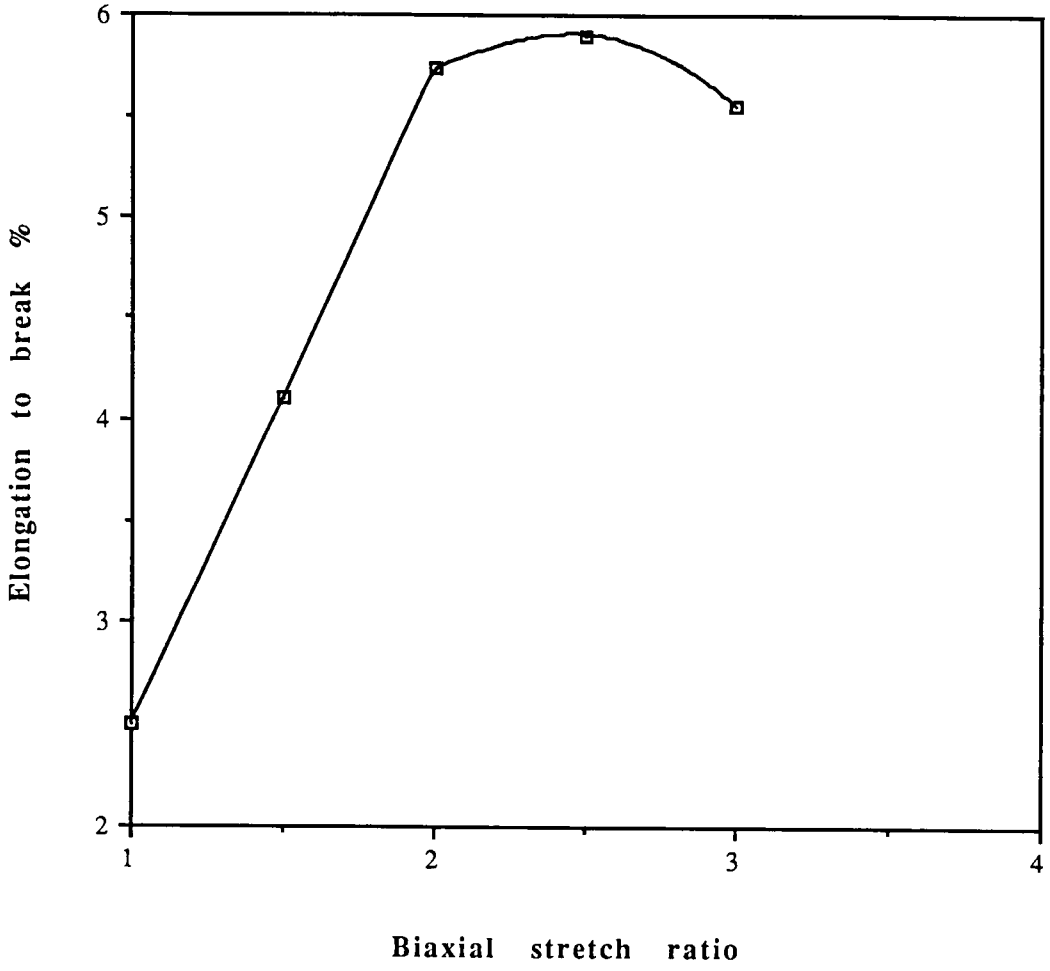


Figure 4.22 Elongation to break for compression molded S/MA 2000 equal biaxial stretch at 2000 %/min

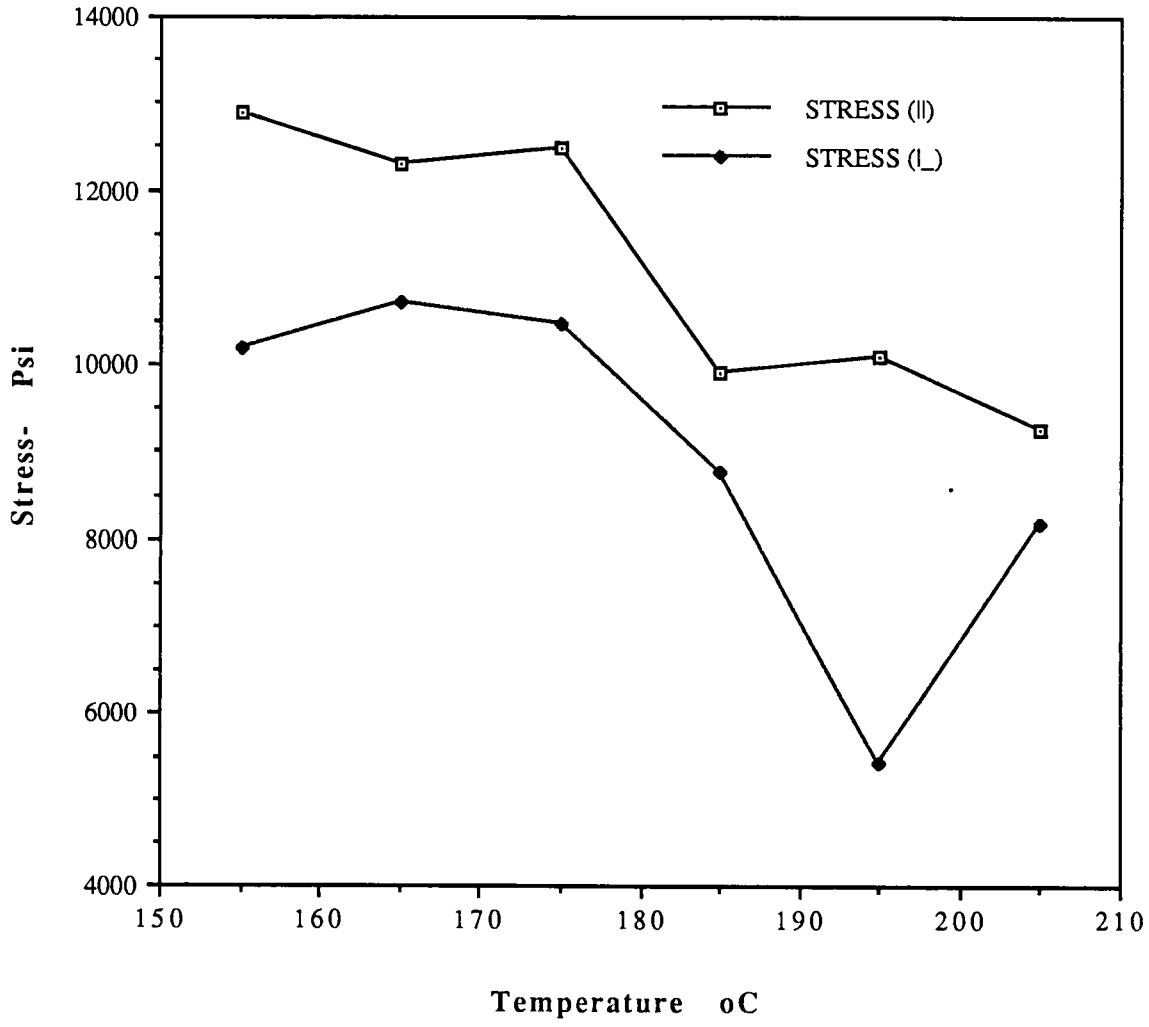


Figure 4.23 Effect of temperature on the stress at break for compression molded S/MA 2000 and 2.5MD x 2.0 TD stretch ratio.

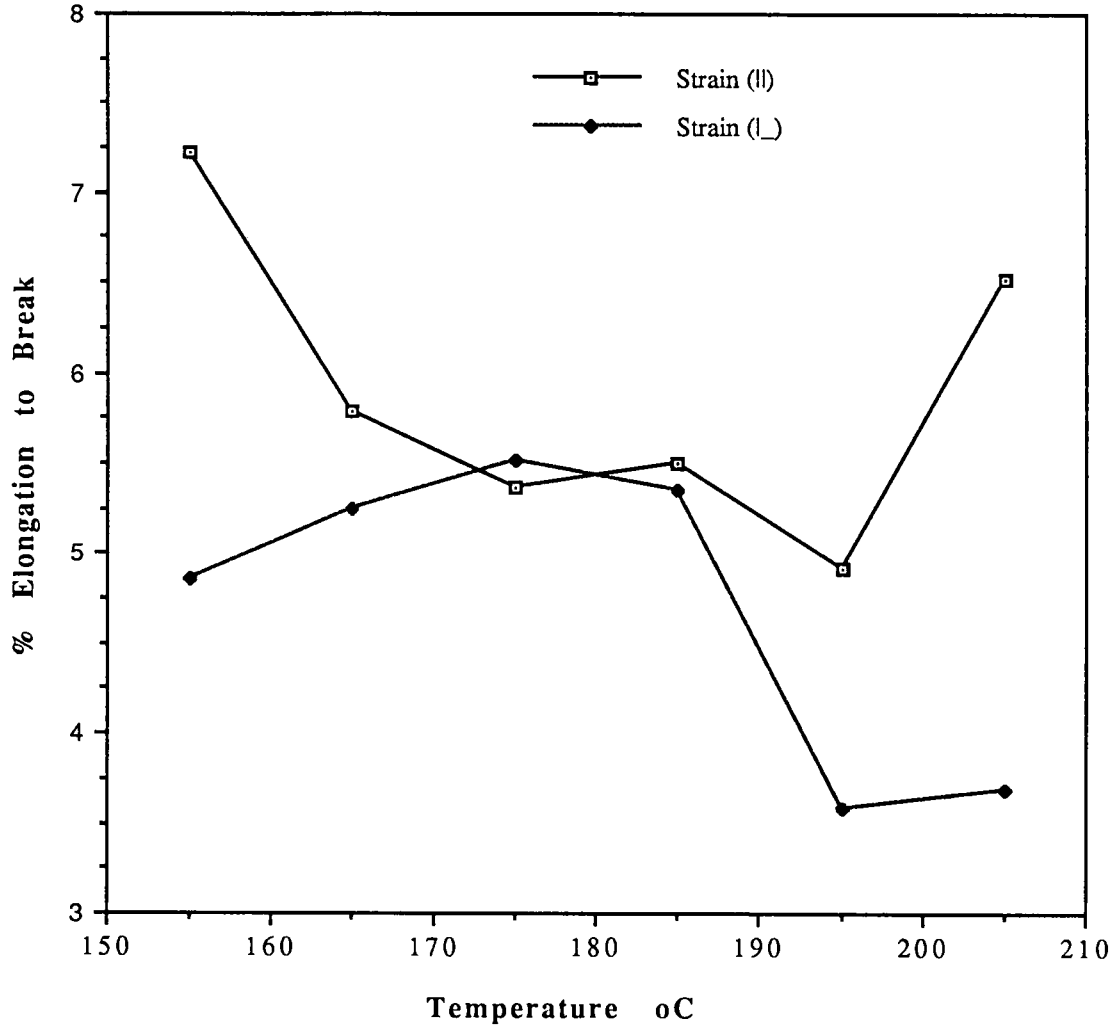


Figure 4.24 Effect of temperature on the strain at break along and transverse to the machine direction for compression molded S/MA 2000 and 2.5 MD x 2.0 TD stretch Ratio.

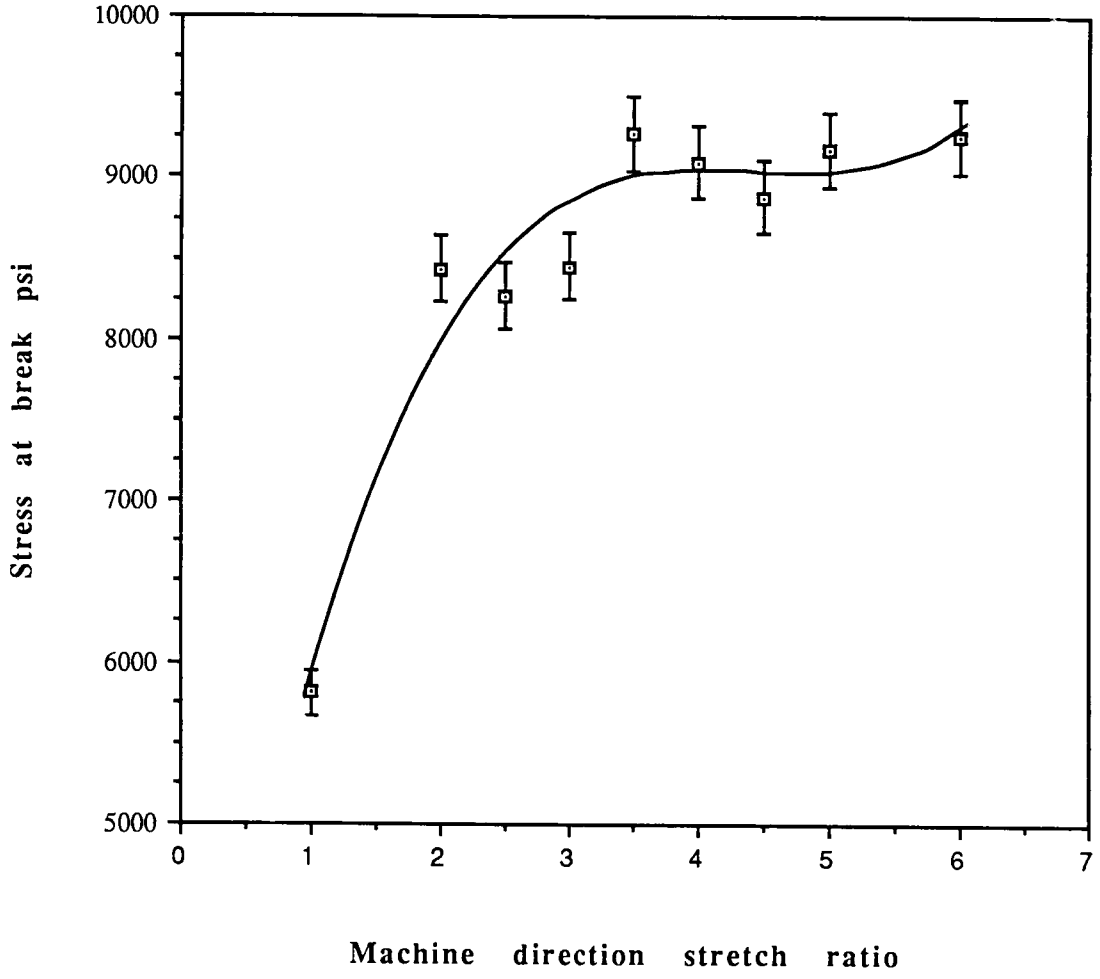


Figure 4.25 Stress at break for films of PS with a fixed stretch ratio of 1.5 along the TD and tested along the MD (26 mils thk, 140 C and2000%/min)

the machine direction stretch ratio, but almost levels off after a 3.5 stretch ratio along the MD. The elongation to break values of these films shown in Figure 4.26 exhibits a low and nearly constant value till a MD ratio of 3.5 after which there is a considerable increase until a MD stretch ratio of 4.5. Further increase in the stretch ratio gives decreasing values of elongation. This marked increase in elongation in the neighborhood of 4.0 stretch ratio has been observed in earlier studies of polystyrene (57). It is presumably related to a critical level of molecular orientation needed to induce ductility.

Figures 4.27 and 4.28 show that an increase in the TD stretch ratio to 2.0 gave similar levels of stress to break and elongation irrespective of the MD stretch ratio. Figure 4.29 illustrate the change from brittle to ductile failure with increase in stretch ratio. Such transitions from brittle to ductile failure were not encountered with films from S/MA.

The tensile strengths of some of the Dylene 8G films have been plotted in the orientation diagram in Figure 4.30. The data show an increase in the stress at break with increase of molecular orientation for low orientations followed by a leveling off at higher orientations. The machine direction stress at break does not appear to be very dependent on the nature of the molecular orientation once the plateau level is reached. These trends are similar to those observed by Choi et al.(57) for other polystyrenes, and the behavior is also similar to the results for S/MA films discussed earlier.

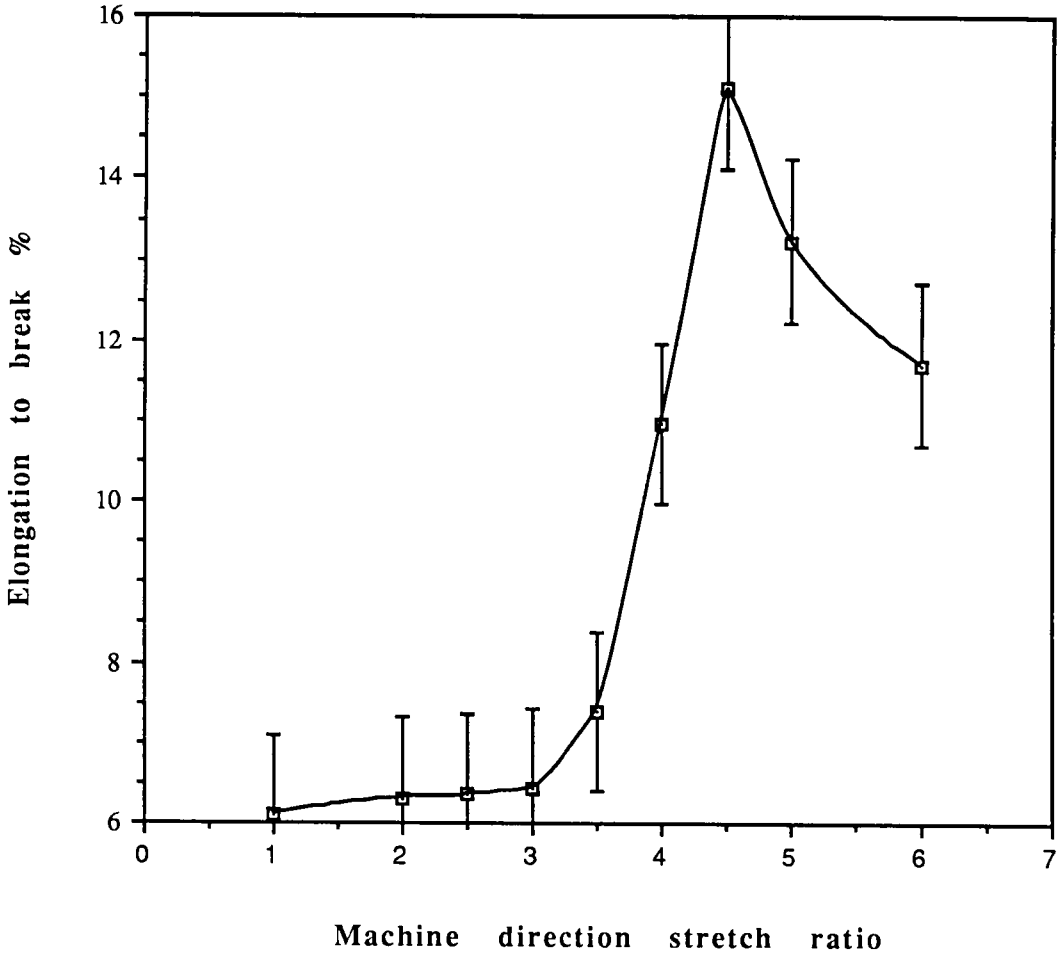


Figure 4.26 Elongation to break for films of PS with a fixed stretch ratio of 1.5 along the TD and tested along the MD (26 mils thk, 140 C and 2000%/min)

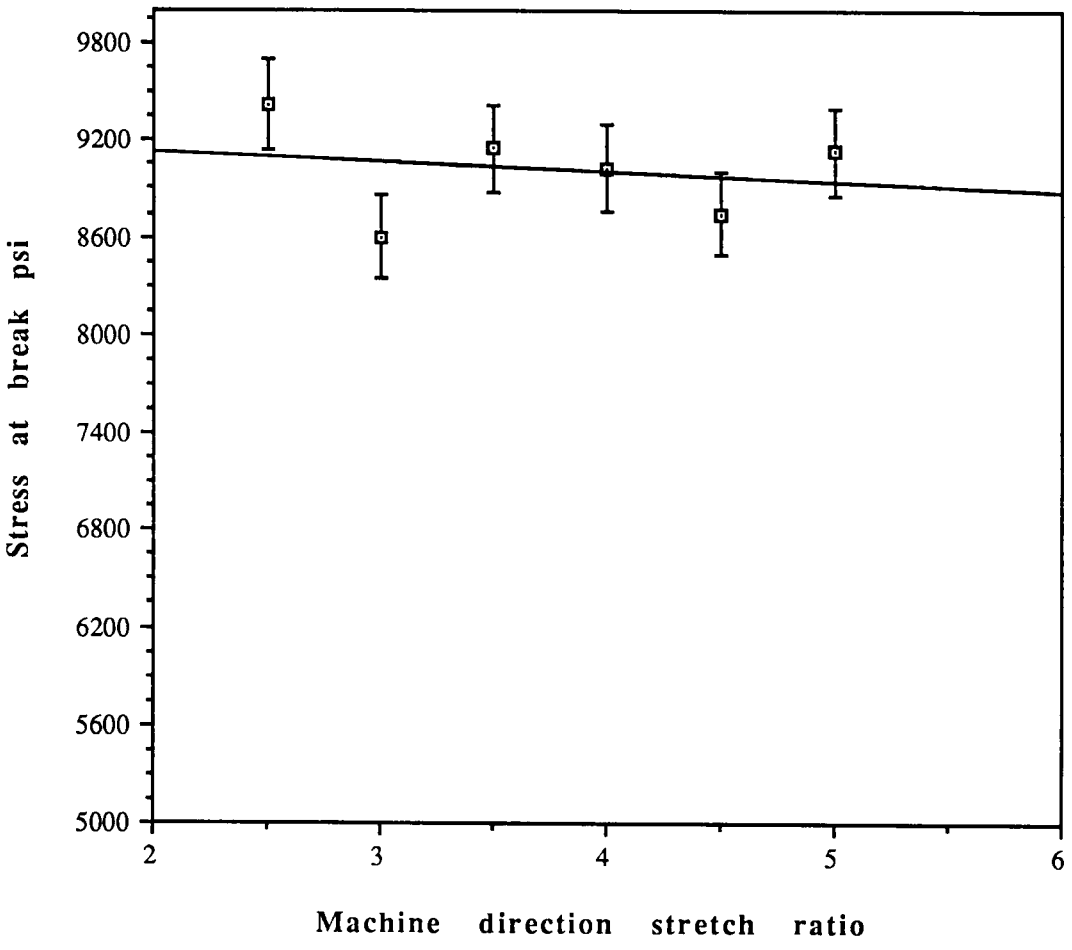


Figure 4.27 Stress at break for films of PS with a fixed stretch ratio of 2.0 along the TD and tested along the MD (26 mils thk, 140 C and 2000 %/min)

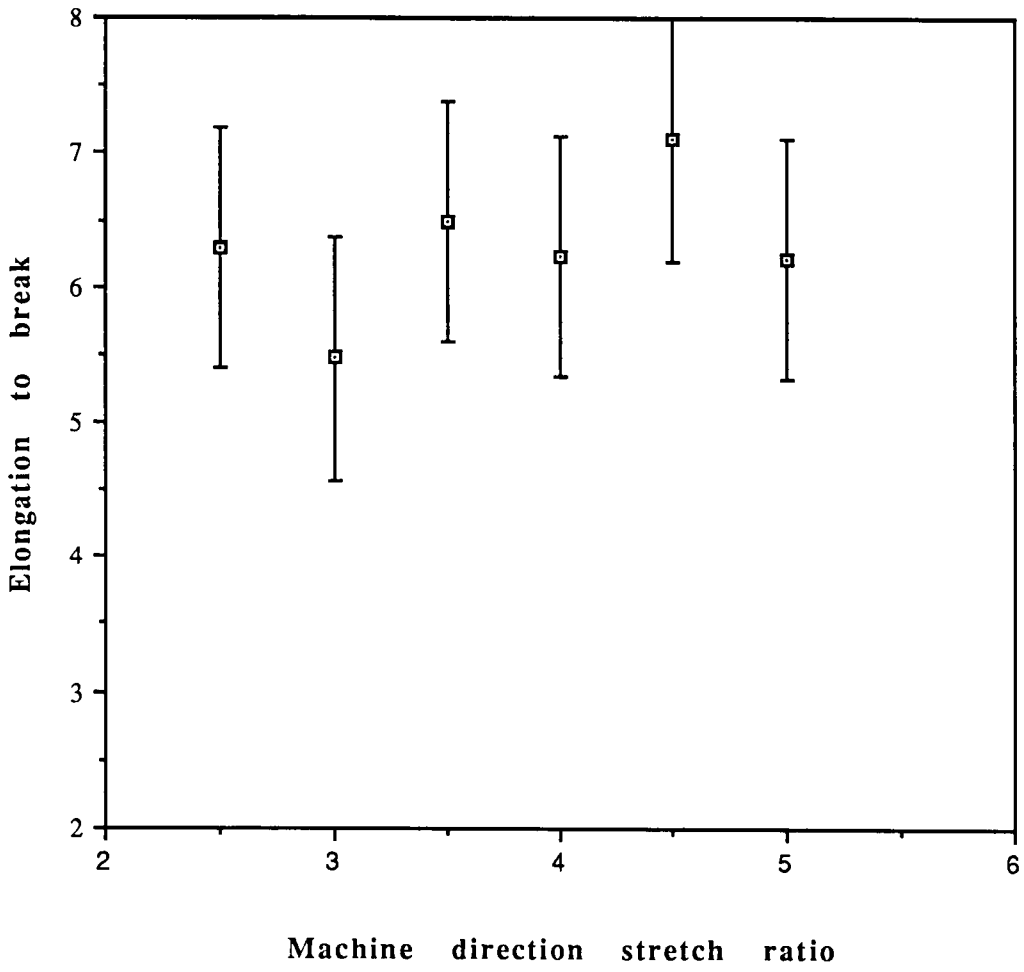


Figure 4.28 Elongation to break for films of PS with a fixed stretch ratio of 2.0 along the TD and tested alongthe MD (26 mils thk, 140 C and 2000%/min)

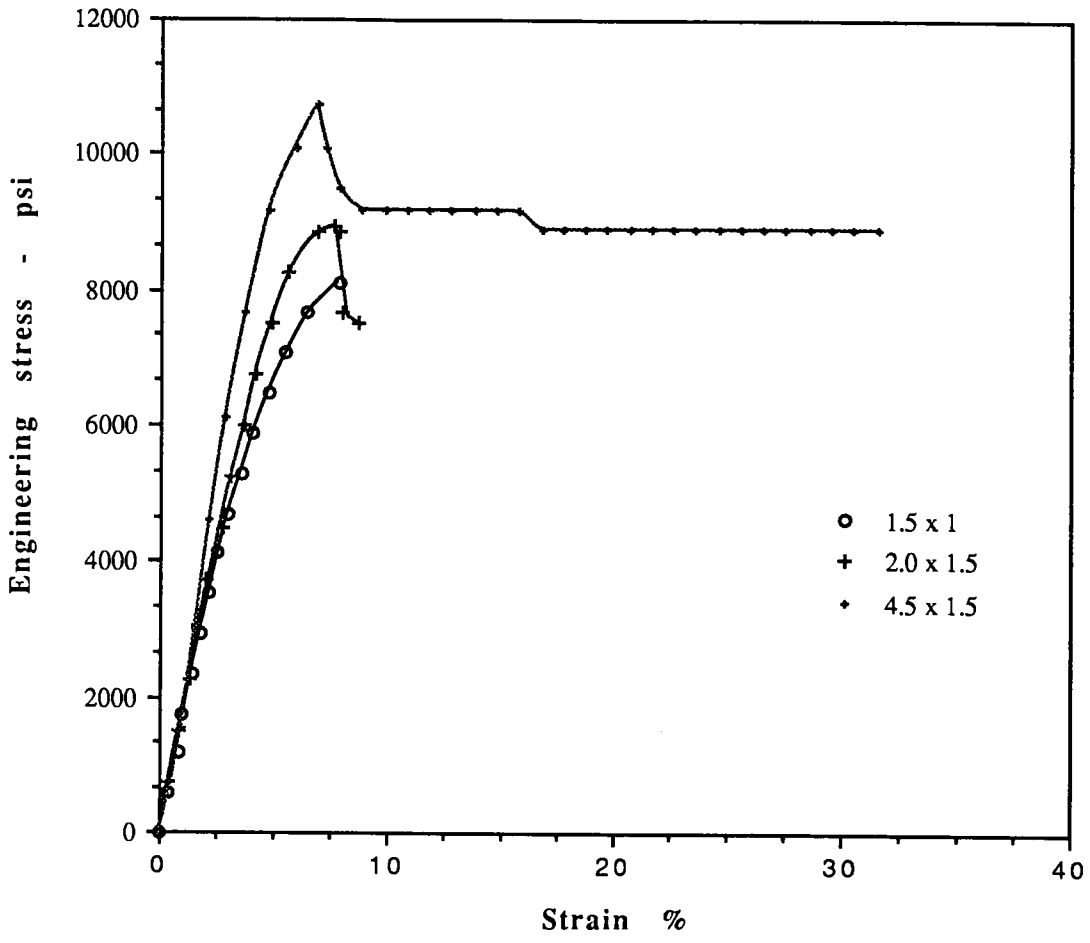


Figure 4.29: Stress-strain curves for PS showing change from brittle to ductile failure with increase in stretch ratio.
(140 C, 2000%/min and 21 mils thk)

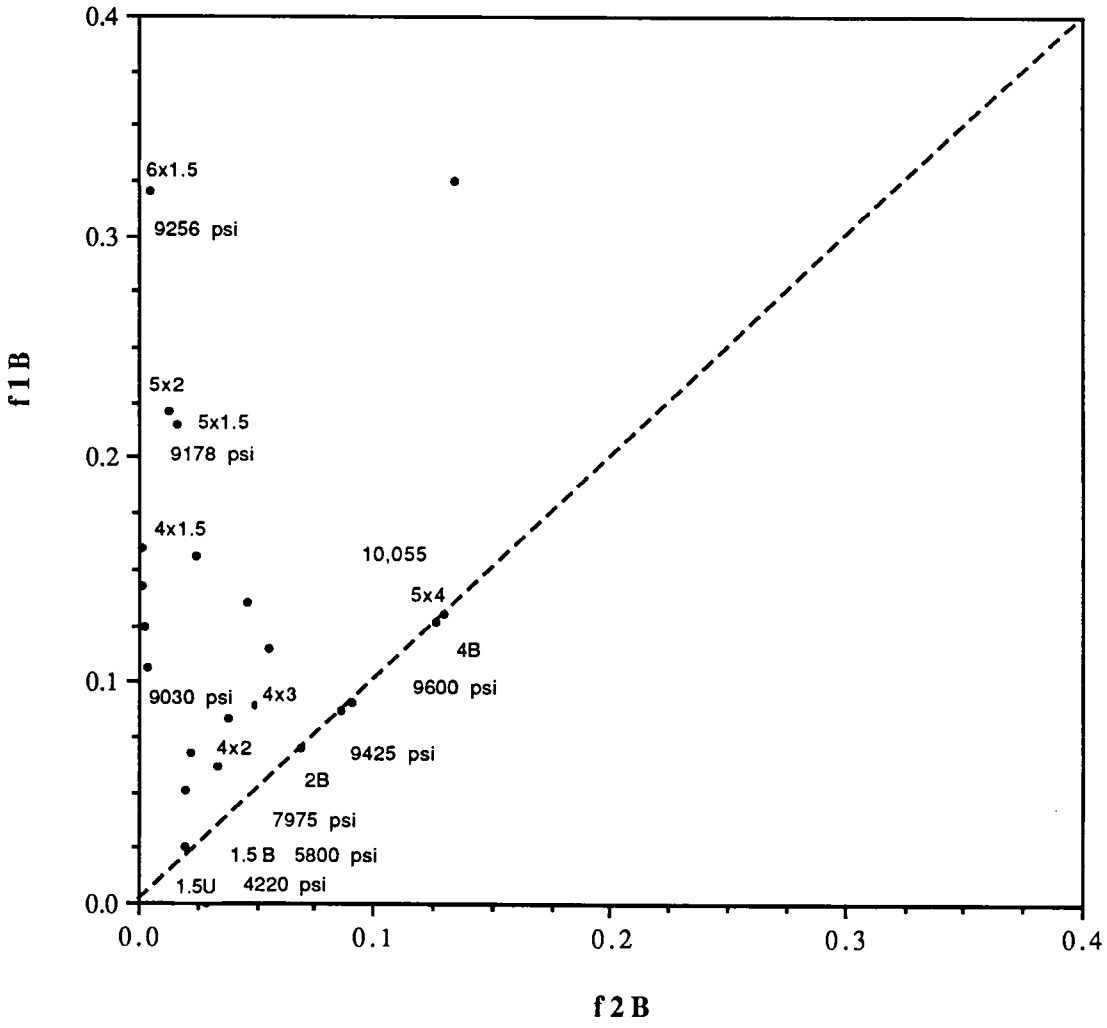


Figure 4.30 Orientation factors for PS showing stress at break for several biaxial stretch ratios. (26 mils, 140 C and 2000 %/min)

4.3.4 Comparison of the Three Resins

The measured tensile strength is plotted versus the equal biaxial stretch ratio for the three materials in Figure 4.31. All materials show an improvement in the tensile strength with increase in the stretch ratio due to the increased molecular orientation relative to the direction of testing. For a given stretch ratio the tensile strength increases with the maleic anhydride content for the chosen stretching conditions. The data for grade Dylark 3000 FG shows a particularly strong dependence on the stretch ratio with high values of tensile strength occurring for high stretch ratios and, consequently, high molecular orientations. Both the polystyrene and Dylark 2000 FG appear to develop a maximum in the tensile strength versus stretch ratio curve. For the range studied S/MA 3000 recorded the highest tensile strength of 15,000 psi while S/MA 2000 and PS gave peak values of 11,000 psi and 9000 psi in the tensile strength, respectively.

For this set of samples the data show that the elongation to break, seen in Figure 4.32 lies in the modest range between 4 and 11%. There are no strong trends observed within the range of materials or film preparation conditions examined.

4.4 EFFECT OF INITIAL PLAQUE THICKNESS ON THE ORIENTATION DEVELOPMENT IN FILMS OF POLYSTYRENE

In the discussion so far we have seen the development of

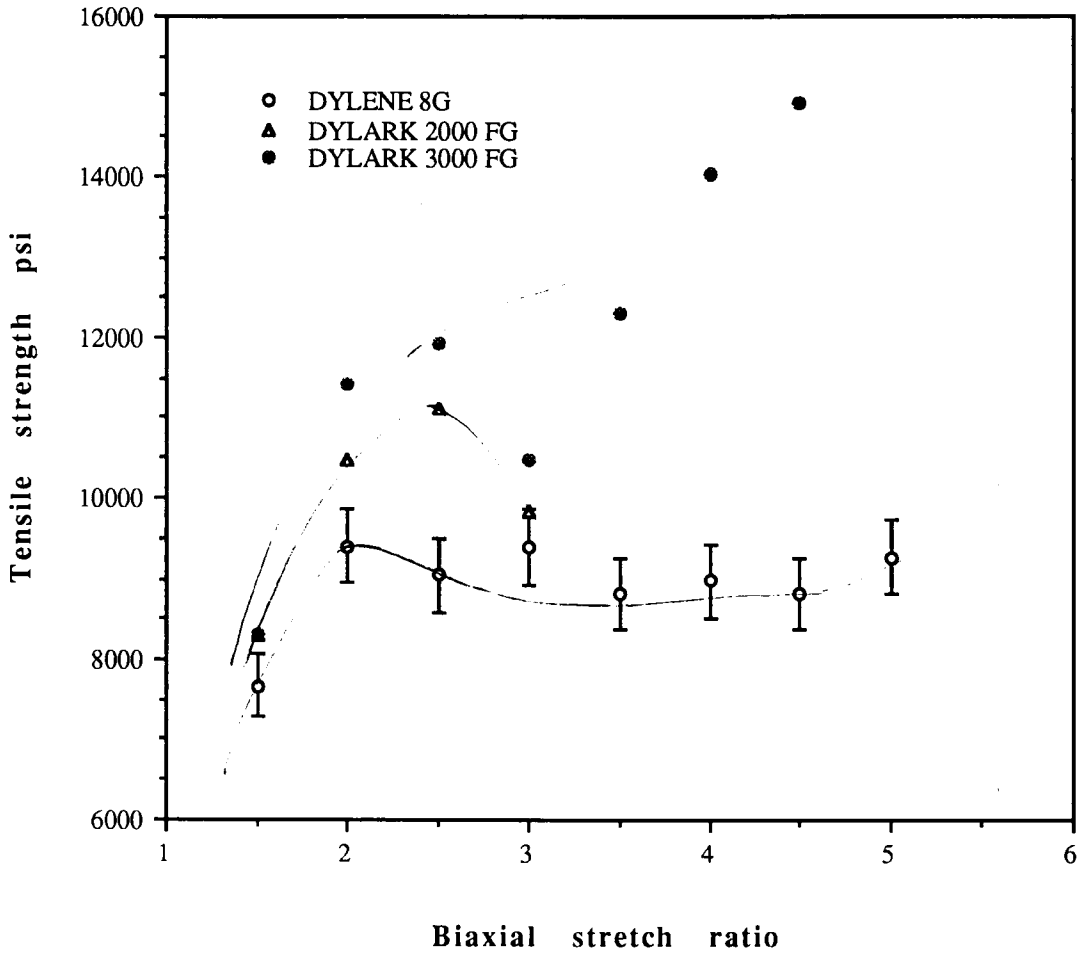
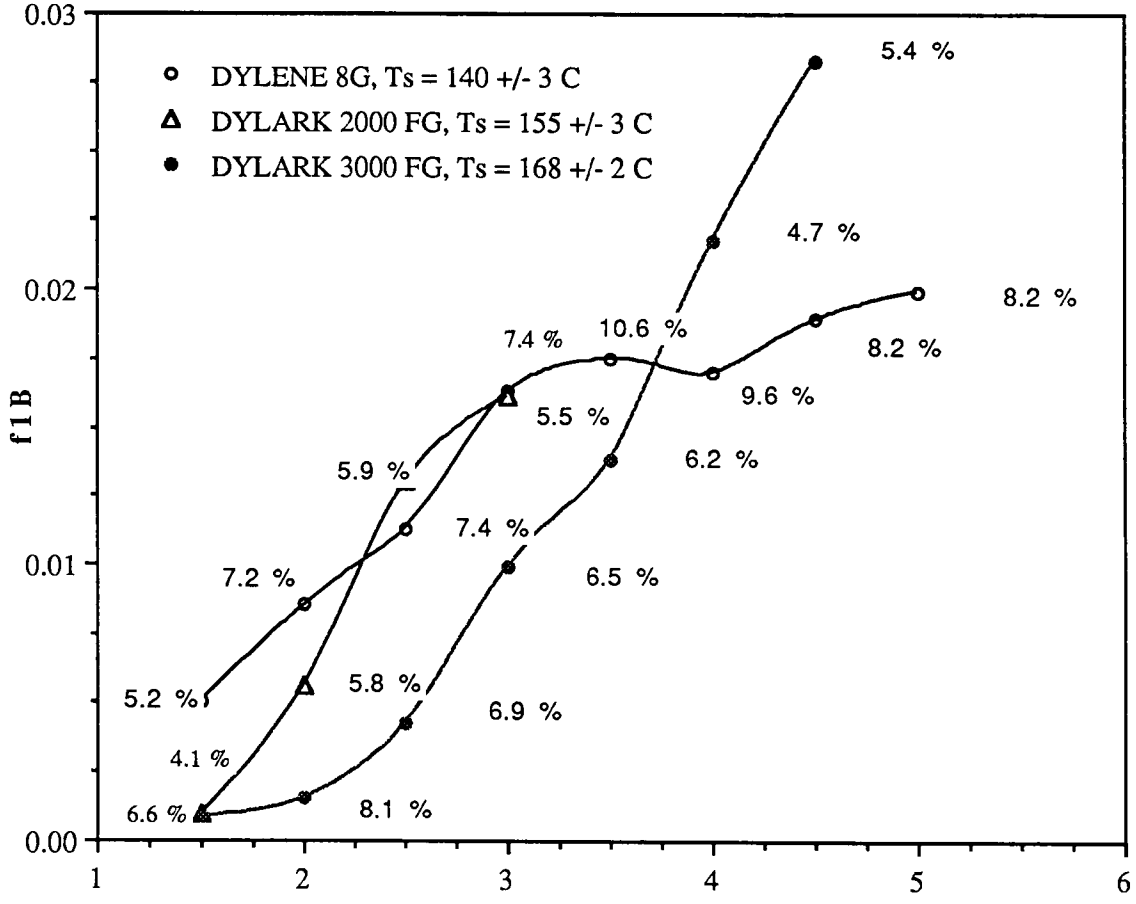


Figure 4.31 Tensile strengths for S/MA and PS samples that were compression molded and stretched biaxially at 2000 %/min and tested along the MD



Biaxial Stretch Ratio

Figure 4.32 Orientation factors vs. equal biaxial stretch ratio at 2000 %/min showing percentage elongation to break for PS and S/MA tested along the MD

molecular orientation under various process conditions. In all these experiments we have made use of 26 mil thick plaques. In order to determine if the initial thicknesses had any effect on the final properties of the film we attempted similar experiments with two other initial thickness of polystyrene plaques. In all, three thicknesses of these compression molded plaques(26 mil, 21 mil and 14 mil) were employed to study differences in the final properties of films of different thicknesses produced under identical processing conditions.

Birefringence

Figures 4.33 and 4.34 give the in-plane and out-of-plane birefringences for films stretched with a fixed ratio of 1.5 along the TD and step increases in the MD stretch ratio. The films prepared from 21 mil plaques show slightly higher birefringence values than films made from 14 and 26 mils thick plaques (especially for the out-of-plane birefringence). The films from 14 mil thick plaques could not be stretched to ratios greater than 3.5 along the MD. The reasons for the somewhat higher birefringence of the films produced from 21 mil plaques is not very clear, though it seems to be reproducible.

Mechanical Properties

Figure 4.35 shows that the stress at break is consistently higher for samples made from 21 mil initial thickness plaques while

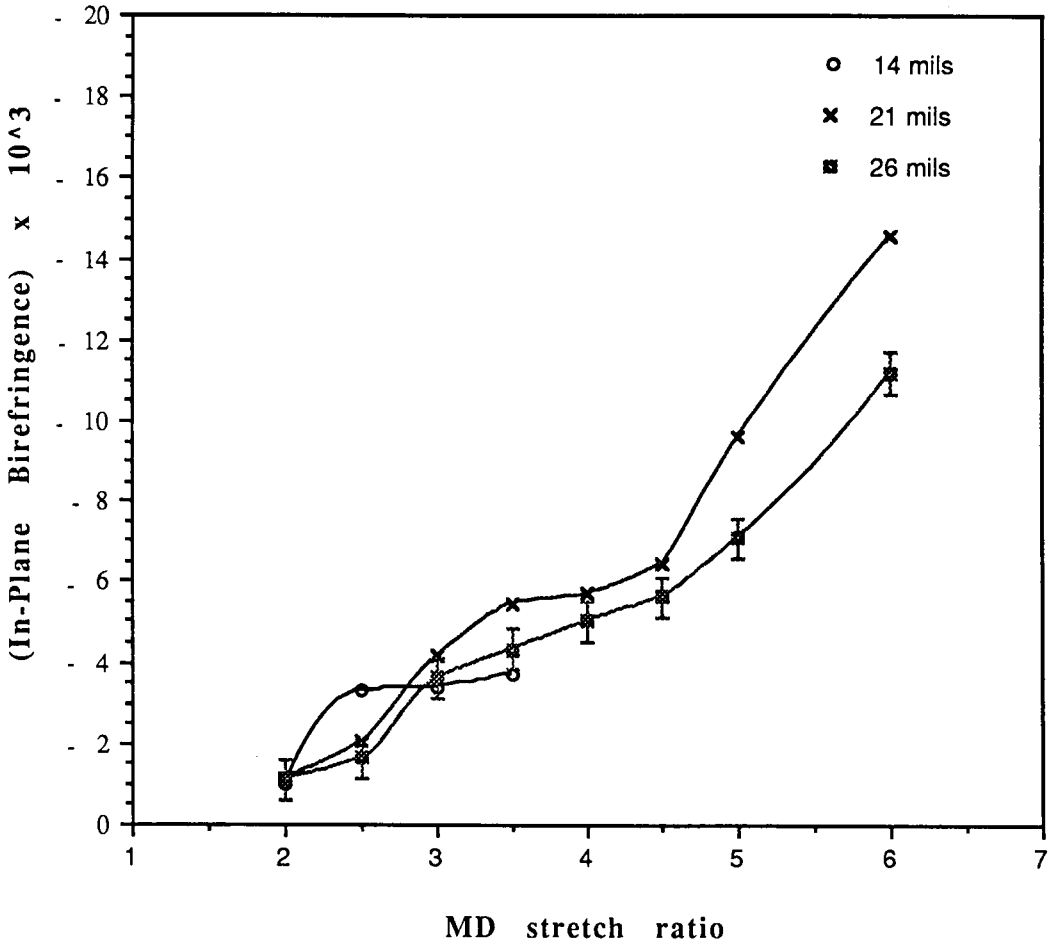


Figure 4.33 Effect of plaque thickness on the in-plane birefringence for films of PS stretched with a fixed ratio of 1.5 along the TD. (140 C and 2000%/min)

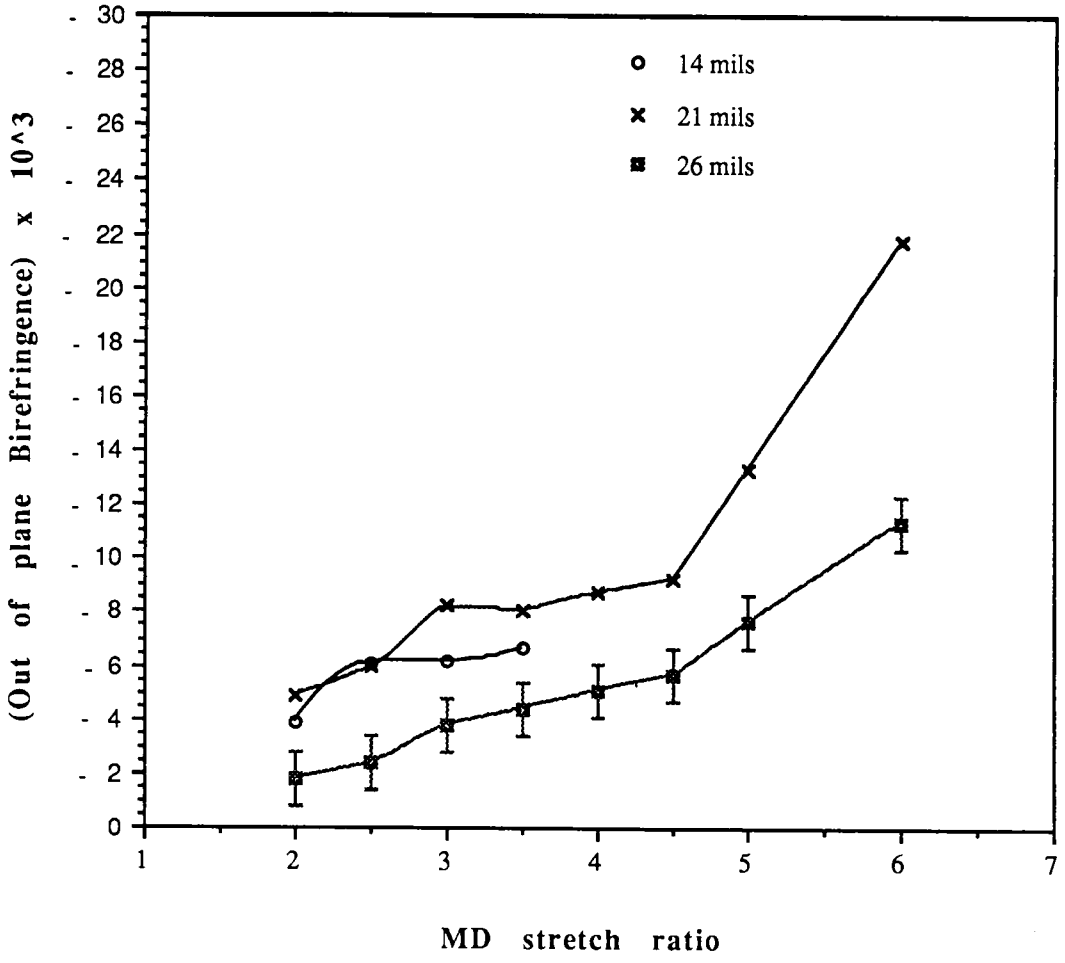


Figure 4.34 Effect on the out of plane birefringence with change in plaque thickness for films of PS stretched with a fixed ratio of 1.5 along the TD. (140 C and 2000%/min)

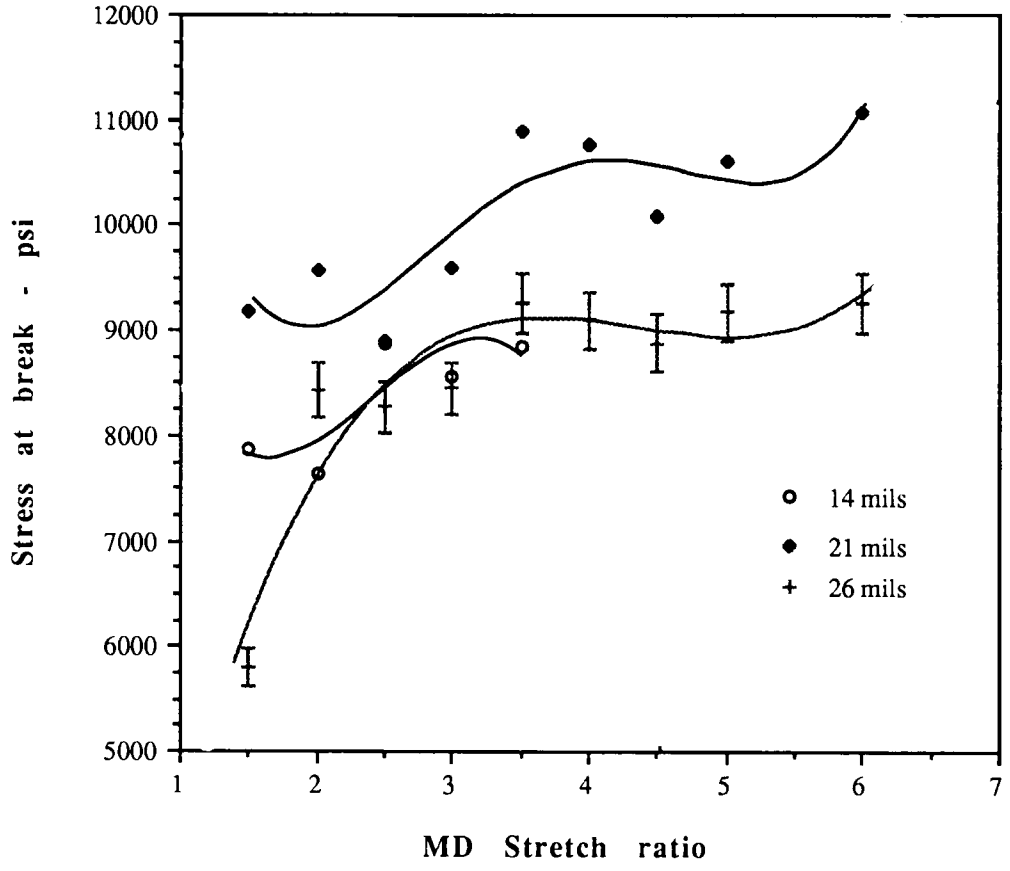


Figure 4.35 Effect of stress at break with change in the initial sample thickness for films of PS stretched with a fixed ratio of 1.5 along the TD. (140 C and 2000%/min)

samples from 26 mil plaques recorded values that were about 15% lower. Figure 4.36 shows the elongation to break values following a similar trend as the stress to break. For both cases, films prepared from 14 mil plaques give tensile stress and elongation values that lie between films prepared from 21 mil and 26 mil thick plaques. The values shown for the 26 mil samples are the same as those shown in Figure 4.25.

The values of the stress at break and elongation at break have been plotted vs. the out-of-plane birefringence to get an idea if the change in the mechanical properties is due to molecular orientation or due to some inherent effect of the thickness of the film. Fig. 4.37 shows that the stress at break increases with increase in the out of plane birefringence indicating that increasing molecular orientation is contributing to the increase in the stress at break. However, there also appears to be a significant difference between samples of different thickness and similar birefringence. For the case of elongation to break seen in Figure 4.38, both 21 mil and 26 mil samples show similar trends in elongation with out-of-plane birefringence, but films from 21 mil plaques record higher values of both birefringence and elongation to break. The brittle to ductile transition for the films prepared from 26 mil and 21 mil plaques was observed to be in the neighbourhood of 4.5 x 1.5 stretch ratio. For a ratio of 4.5 x 1.5, both the in-plane and the out-of plane birefringence for these samples are almost equal. This is especially true for the MD orientation factor with a value of 0.0197 for both

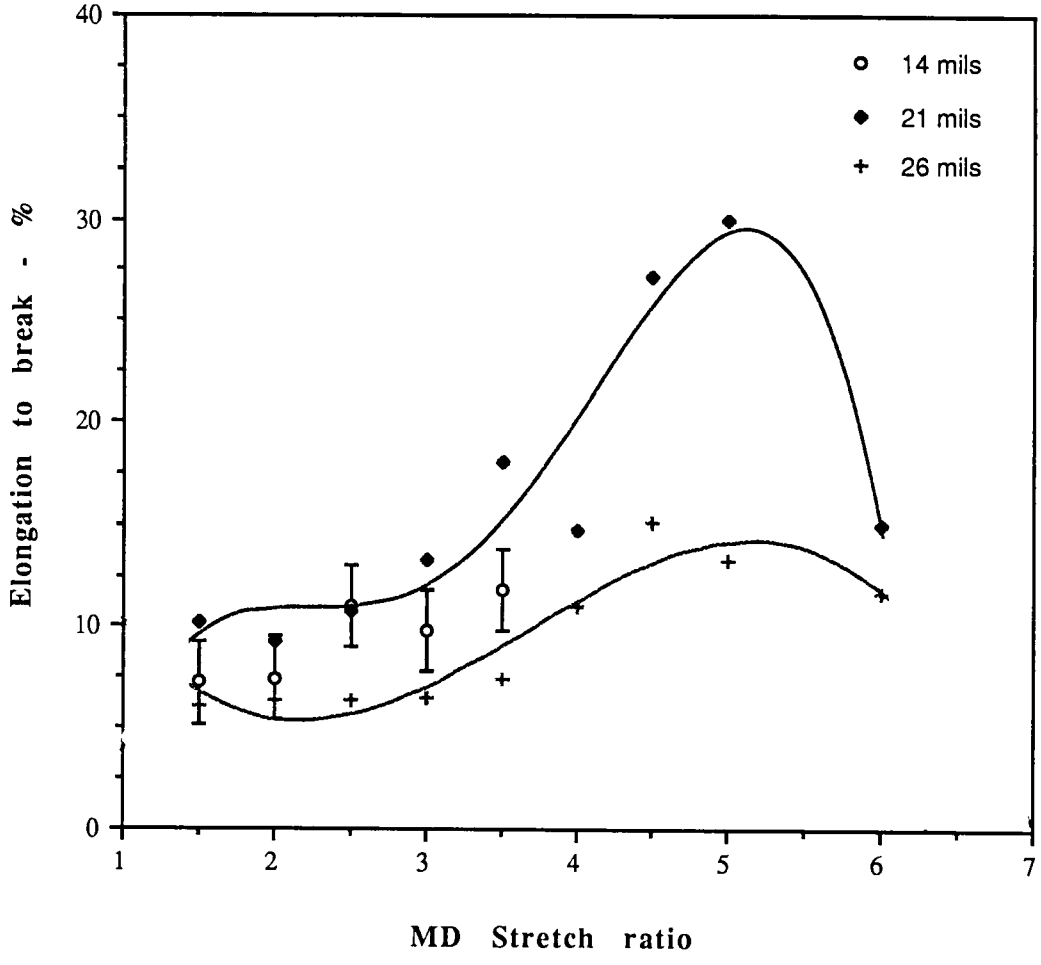


Figure 4.36 Effect on elongation to break with change in the initial sample thickness for films of PS stretched with a fixed ratio of 1.5 along the TD. (140 C and 2000%/min)

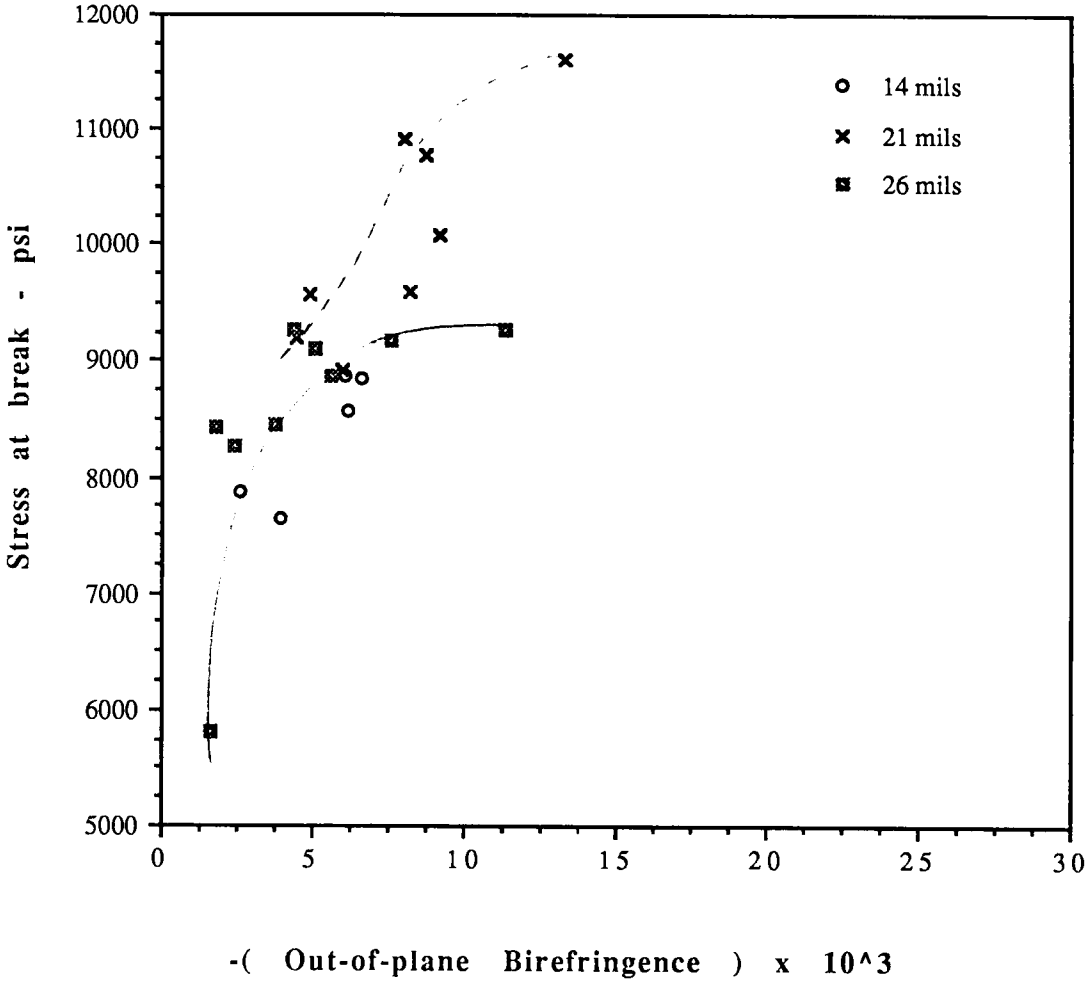


Figure 4.37 Stress at break vs. birefringence for films made from different plaque thicknesses of PS.(2000%/min, 140 C)

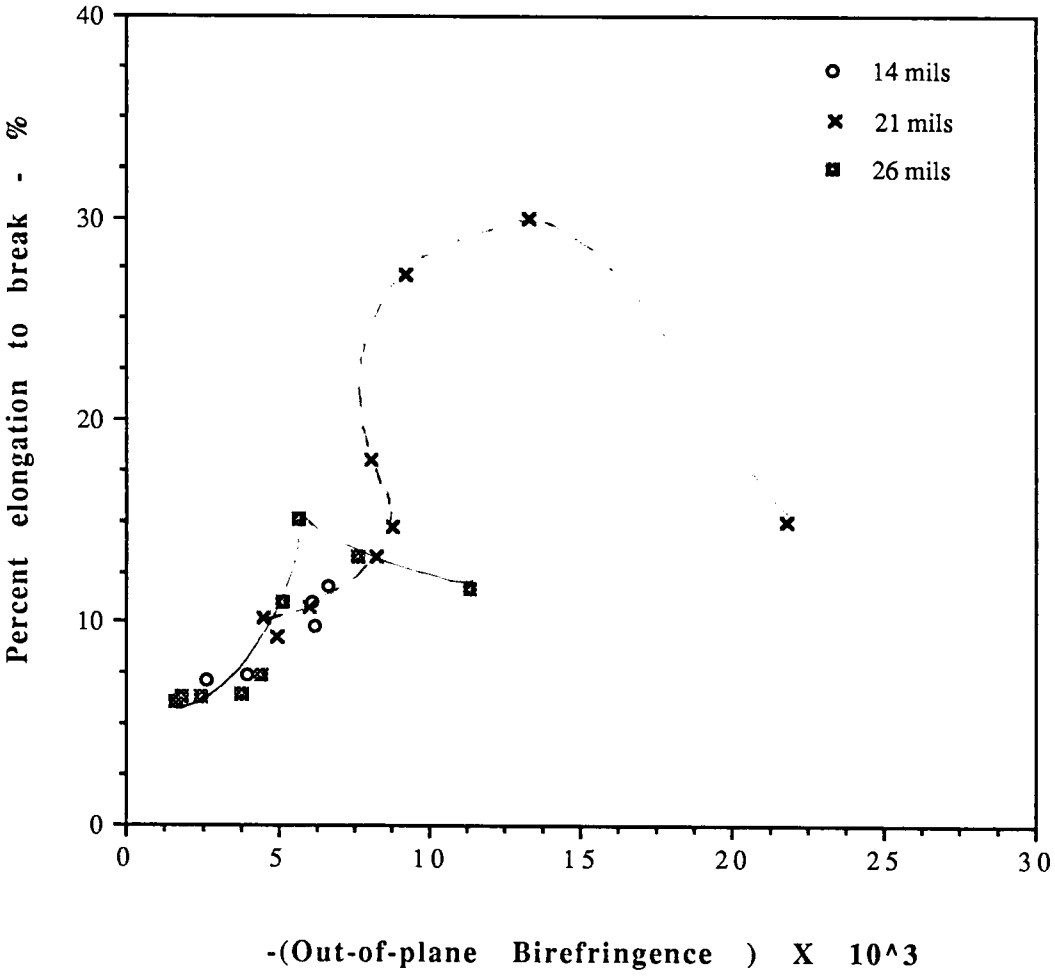


Figure 4.38 Percent elongation vs birefringence for films made from different plaque thicknesses of PS. (2000%/min, 140 C)

thicknesses. However, the elongation to break values in Figure 4.36 shows that there is a substantial increase in the ductility for films stretched from plaques with a thickness of 21 mils. It can be safely said that molecular orientation plays a major role in determining the mechanical behavior of polystyrene films, but the effect of thickness cannot be ruled out as the increase in ductility is related to the critical thickness in the initial plaque.

Comparison of data obtained from films prepared from 14 mil plaques was not possible as the thickness was too low to obtain a range of stretch ratios that were possible with the other two plaque thicknesses.

4.5 SHRINKAGE BEHAVIOR OF S/MA AND PS FILMS

The molecular orientation induced due to stretching is frozen into the glassy state to preserve the orientation. This orientation is similar to applying a frozen stress in the material that will relax when there is sufficient thermal energy for chain mobility.

For a given polymer, the extent of reversion is directly proportional to the degree of orientation prior to shrinkage and temperature and time of exposure to shrink. Ekio Ito etal.(58) have reported a 100 % reversal of PS when kept at the shrink temperatures for long periods.

Shrinkage at a Fixed Temperature

In order to measure the shrinkage the three grades were allowed to shrink freely without restraints for 8 min. at their respective stretch temperatures. All the data presented are for equal biaxial films with both the MD and TD shrink being measured and the average of 5 such values reported here. Figures 4.39 through 4.41 gives the data recorded on S/MA 3000 , S/MA 2000 and PS , respectively. The numbers on the curves indicate the machine direction orientation factors prior to shrinkage.

An increase in the stretch ratio increases the molecular anisotropy along the chosen reference direction and produces a higher residual stress that tends to relax on heating. Visual observation showed that most of the shrinkage for all the three grades was complete within one minute in the oven, at the indicated temperatures. All three grades show that there is an increase in the shrinkage of the material with an increase in the MD orientation factor prior to shrink.

Recovery as a Function of Temperature

S/MA 3000, S/MA 2000, and PS stretched to a 3 x 3 stretch ratio at 168°C, 155°C and 140°C, respectively were tested for their recovery as a function of temperature. Figure 4.42 shows that there is a shift in the minimum temperature required to induce recovery with an increase in the maleic anhydride content. For example a 20% recovery in PS needed about 100°C, 120°C in S/MA 2000 and 140°C

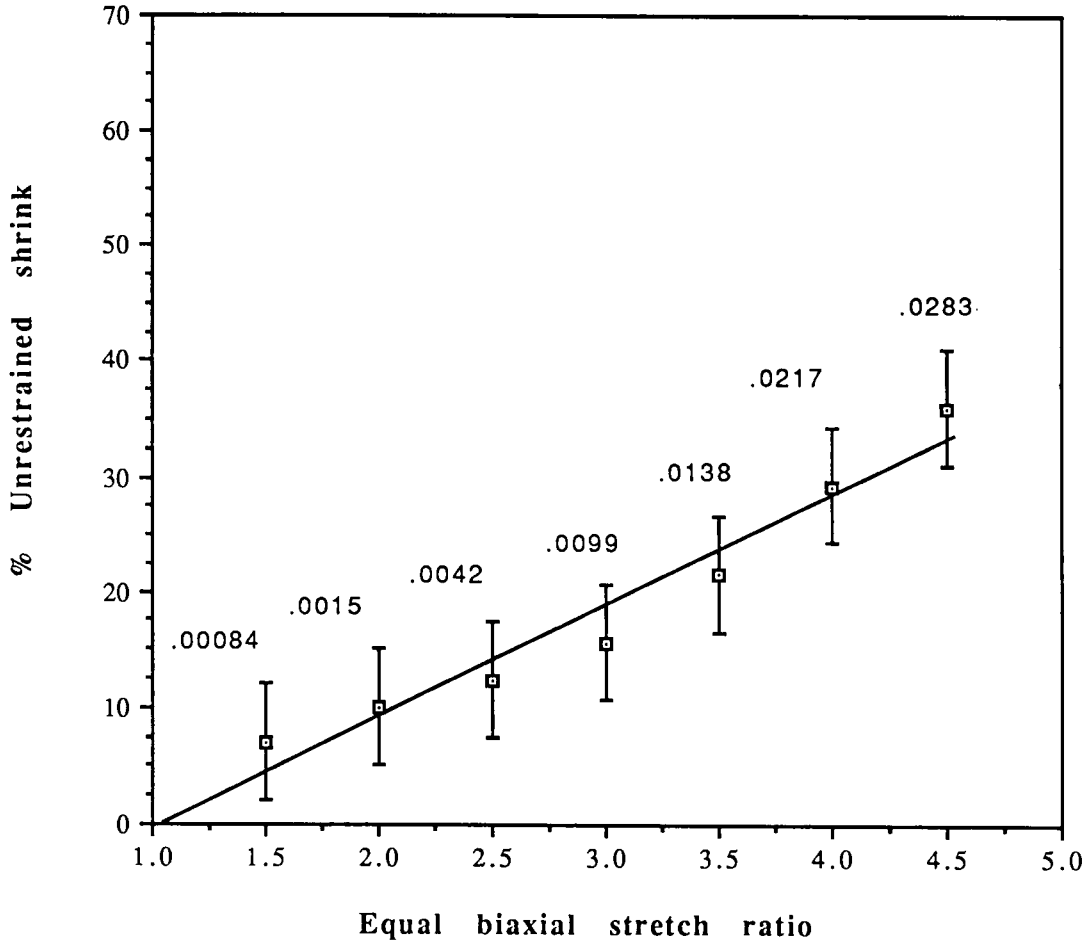


Figure 4.39 Unrestrained shrinkage of S/MA 3000 as a function of stretch ratio showing MD orientation factors (165 C for 8 min.)

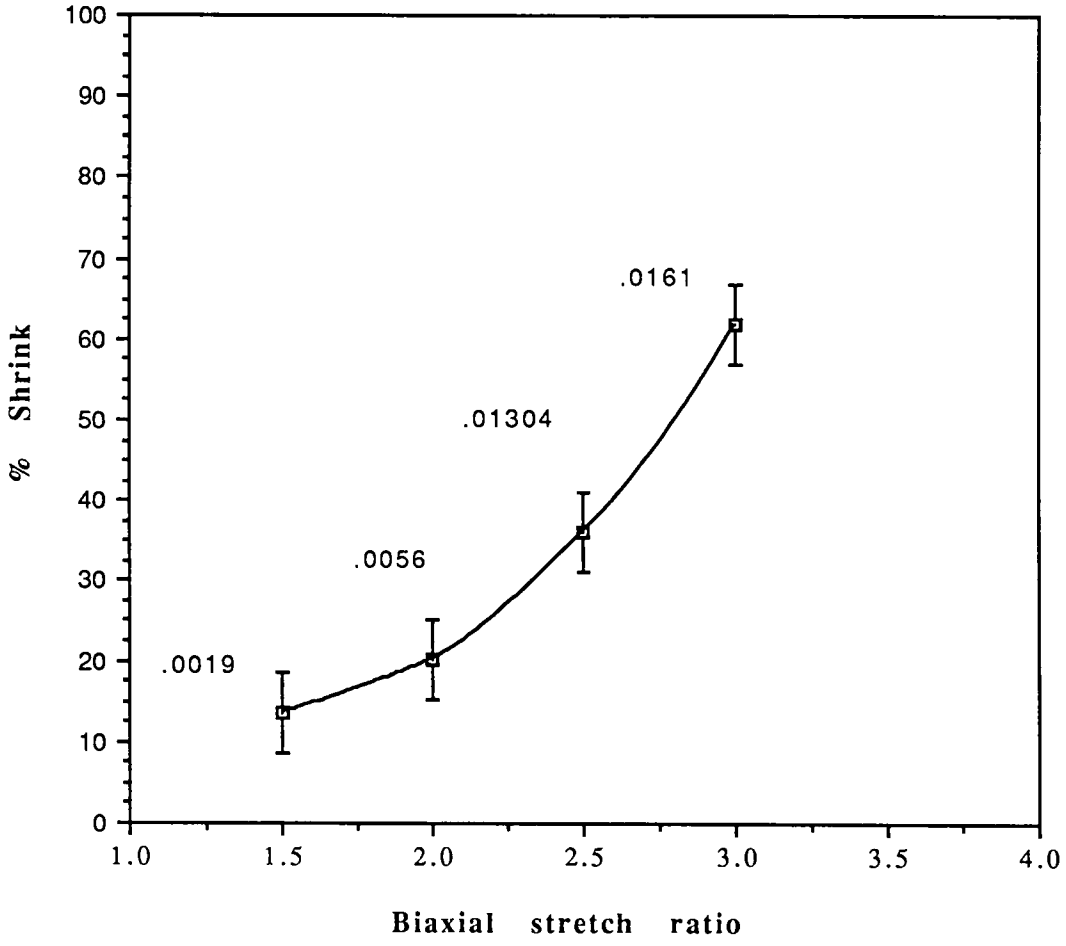


Figure 4.40 Unrestrained shrinkage of S/MA 2000 as a function of stretch ratio showing MD orientation factors. (155 C for 8 min.)

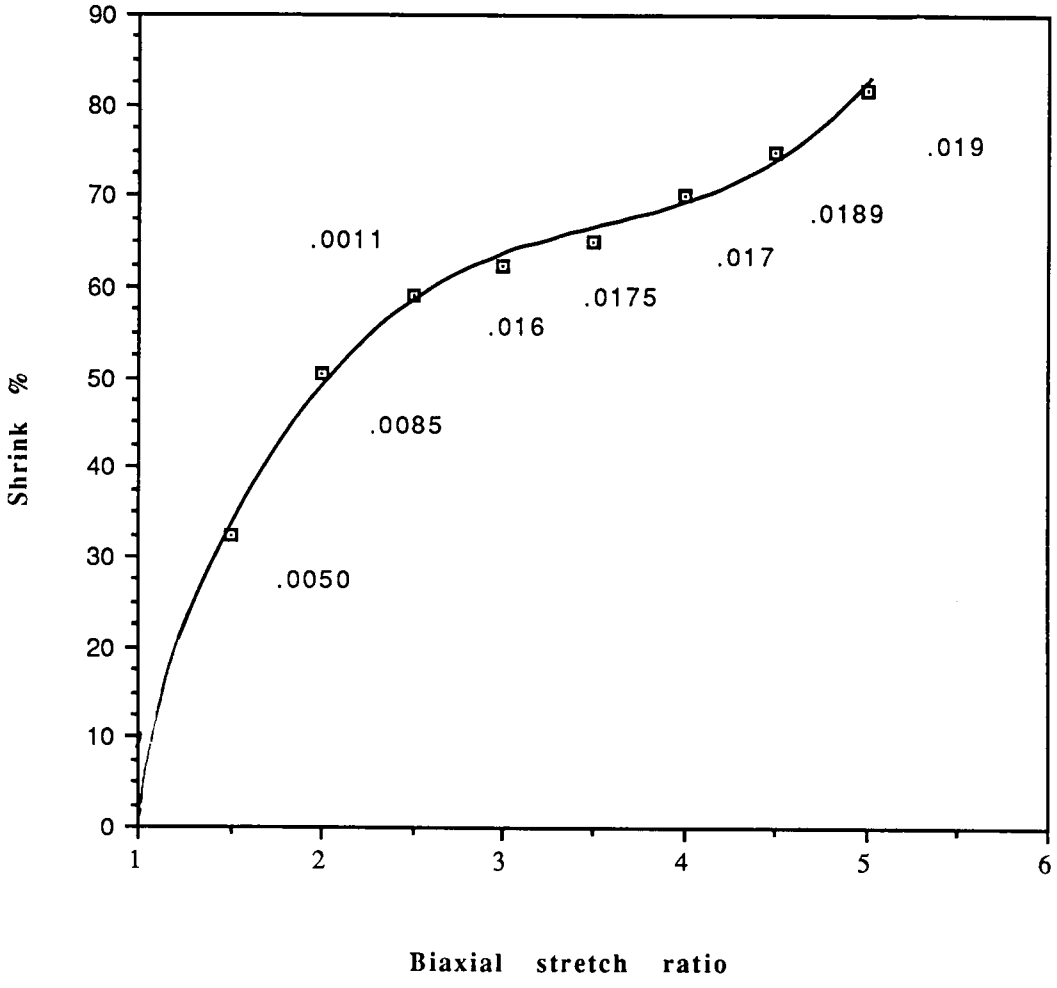


Figure 4.41 Unrestrained shrinkage of PS as a function of stretch ratio showing MD orientation factors. (140 C and 8 min.)

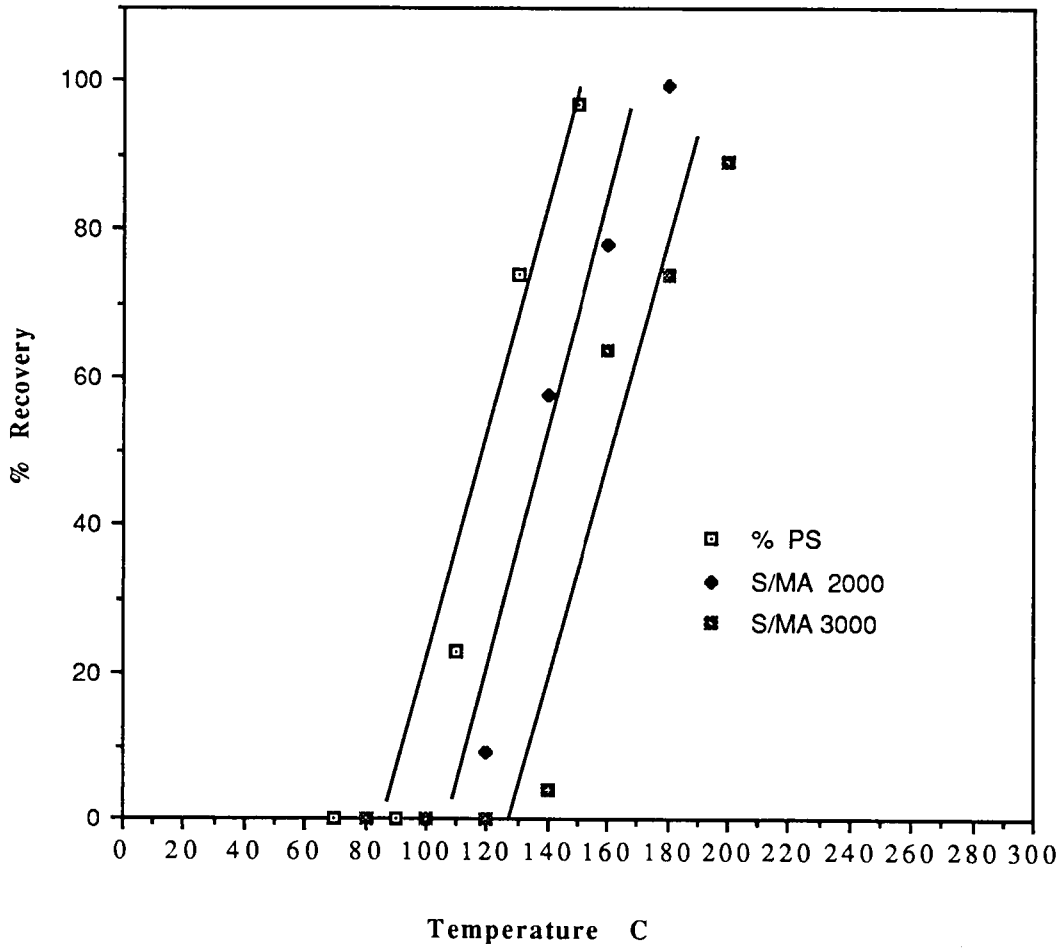


Figure 4.42: Recovery as a function of temperature for 3x3 films of PS and S/MA

in S/MA 3000. It is felt that the shift in temperature required to induce shrinkage is largely associated with the chemical composition and the effect of composition on chain mobility at the glass transition. In order to confirm this explanation, the glass transition temperature of each polymer in question was subtracted from the shrink temperatures shown in Figure 4.42. This was done in order to remove the effect of Tg if any. The results plotted in Figure 4.43 clearly show that the three curves for the three polymers come closer to each other. Thus the shift in the temperatures needed to induce shrink in the three polymers is largely associated with the glass transition temperature of the composition. It is felt that all the data points for such a plot would lie on one straight line if the initial orientation prior to shrink in the three materials were equal. In the present data shown, all the three films have the same stretch ratio of 3 x 3 prepared under their optimum process conditions. As seen the final orientation developed after stretch are not identical. The orientation factors in the materials prior to shrinkage and subsequent to stretch, in decreasing order was Dylene 8G > S/MA 2000 > S/MA 3000.

The activation energy for these processes calculated from Figure 4.44 yields a value of about 4 kcal/mole. Ferry (59) has reported a value of 12 kcal for the activation energy for the viscous flow of polystyrene. The figure we have arrived at, is only an approximate value as the data was collected with the limited aim of estimating the shrink in the three polymers.

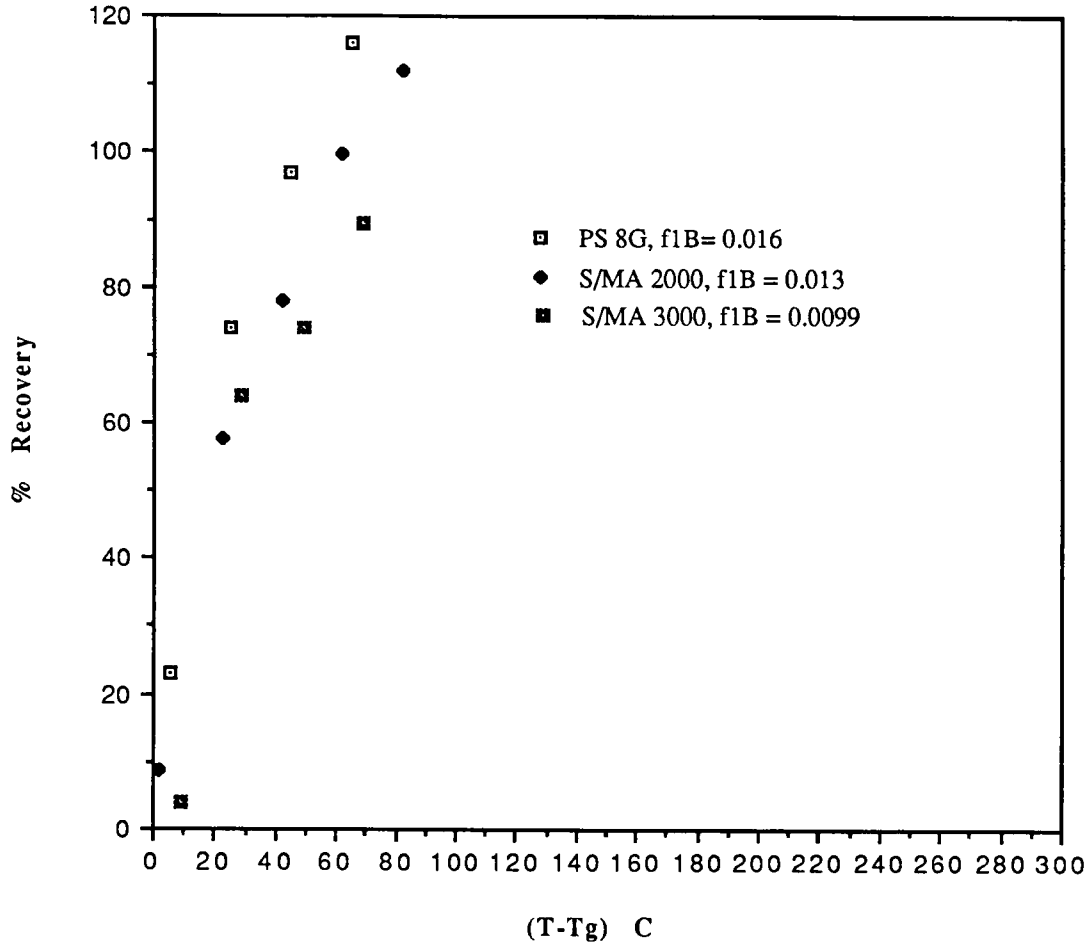


Figure 4.43: Percent recovery as a function of (T-Tg). (T being the shrink temperature) for 3x3 films of PS and S/MA copolymers

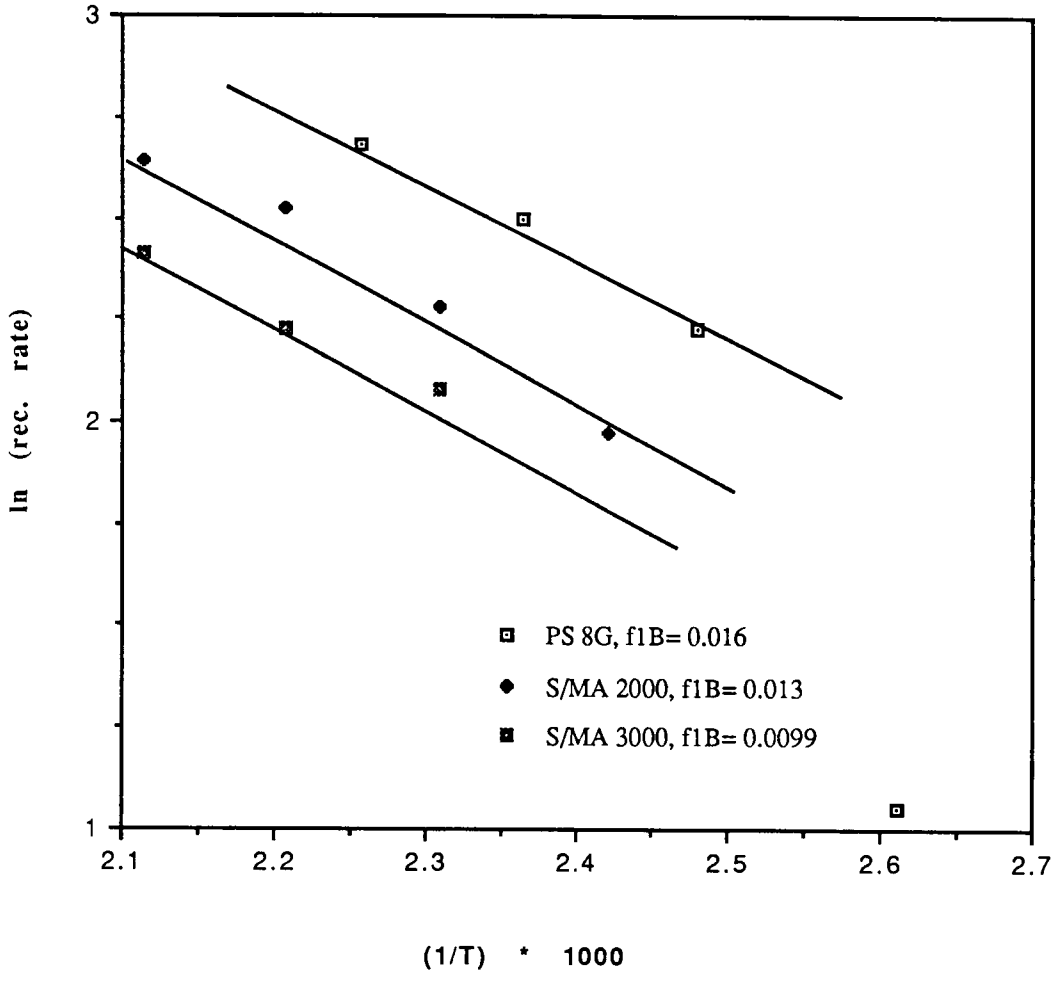


Figure 4.44: Arrhenius type plots for PS and S/MA copolymers

4.6 STRETCHING TO FILMS FROM EXTRUDED SHEETS

As described in chapter 2, continuous manufacture of films in commercial processes employ extruded sheets for biaxial stretching. The next logical step in our study was to see how well the data obtained from films prepared from compression molded plaques relates to the data from films prepared from extruded sheets.

When similar experiments to follow the orientation development with stretch ratio on films made from extruded sheets were conducted, the birefringence data as a function of stretch ratio showed marked variations, or data scatter. Such deviation from the smooth monotonic increase in the birefringence values with increase in stretch ratio, were not found in the results for samples stretched from compression molded plaques. This suggested that the cause of the variations was associated with the initial extruded samples rather than the stretching process itself. We had previously assumed that the in-plane birefringence of the extruded samples was uniform over the sheet area. In order to investigate the possibility that this assumption was in error, extruded sheets were cut into small square pieces. Each piece was assigned identification coordinates with respect to directions along the extrusion direction and across the width of extrusion (Figure 4.45). These areas were then examined for in-plane birefringence.

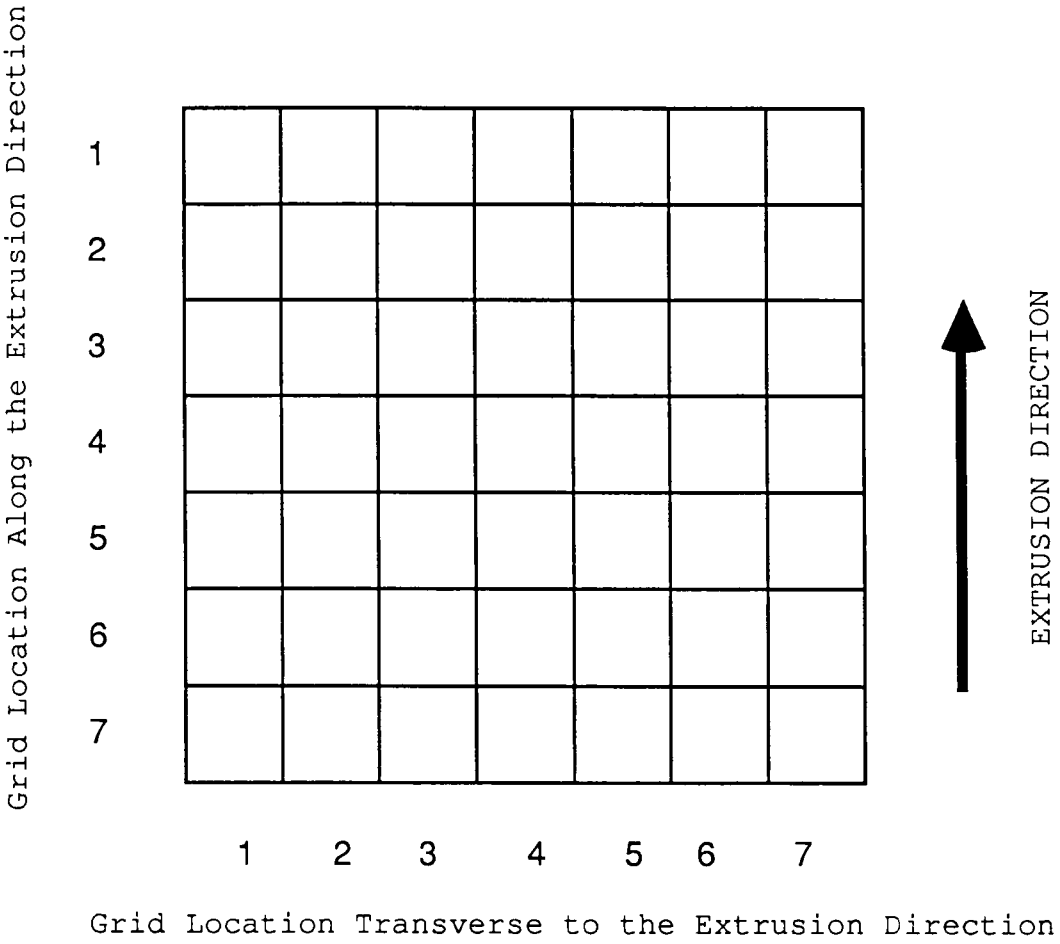


Figure 4.45 Grid depiction for identification of extruded samples of S/MA coplolymers

S/MA 3000

It was found that there was an appreciable variation in the levels of in-plane birefringence in the extruded sheets. For example, there was a difference of 33% between the high and low values for the case of Dylark 3000 FG LLHP-1E samples as shown in Figure 4.46. The variation along the direction of extrusion was not very significant compared to that across the width of the sheet. The in-plane birefringence distribution profile resembled a parabola which was probably related to the stress distribution while the polymer was in a melt state before being frozen into the glassy state. The center of the sheet had the maximum birefringence while the areas along the borders had much lower in-plane birefringence. This provided an opportunity to study the development of birefringence in stretched films as a function of the magnitude of the in-plane birefringence of the as-extruded sheet. Samples for stretching were cut from the S/MA 3000 FG LHHP-1e extrusion and divided into "high" and "low" initial orientation samples. These two groups of samples were then stretched to different stretch ratios at a stretch rate of 3000%/min and a stretch temperature of 170°C. Other stretching conditions remained the same as in earlier experiments of S/MA 3000. Birefringence data for the low initial orientation samples are shown in Figure 4.47 while the birefringence data for the "high" initial orientation samples are shown in Figure 4.48. The 1 direction is the same as the extrusion direction and the 2 direction is perpendicular

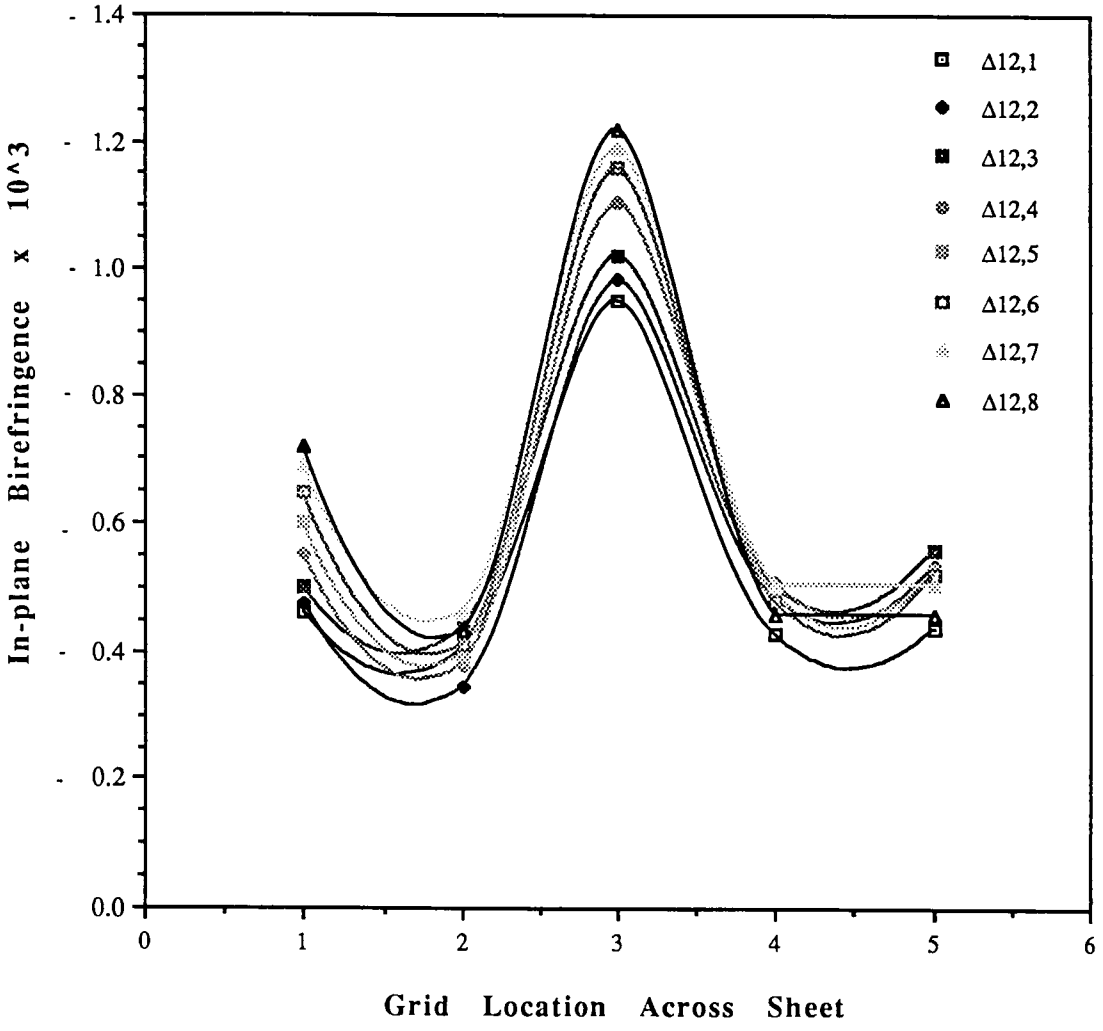


Figure 4.46 Variation in In-plane birefringence across the width of extrusion of S/MA 3000 lhhp-1e. Different curvesrepresent variations with grid location along the extrusion direction.

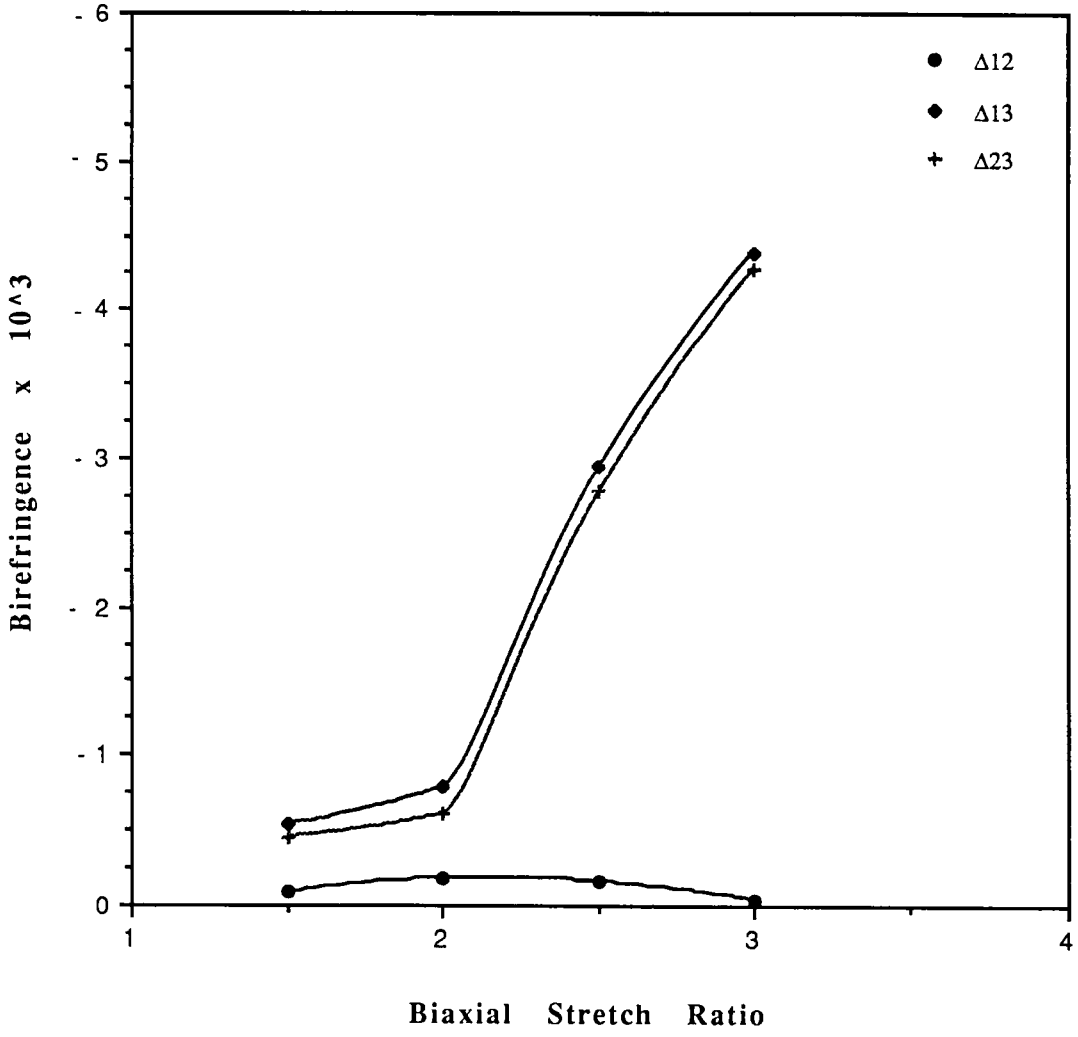


Figure 4.47: Low initial orientation areas of S/MA 3000 LLHP-1e extruded sheet biaxially stretched at 3000%/min and 170 oC.

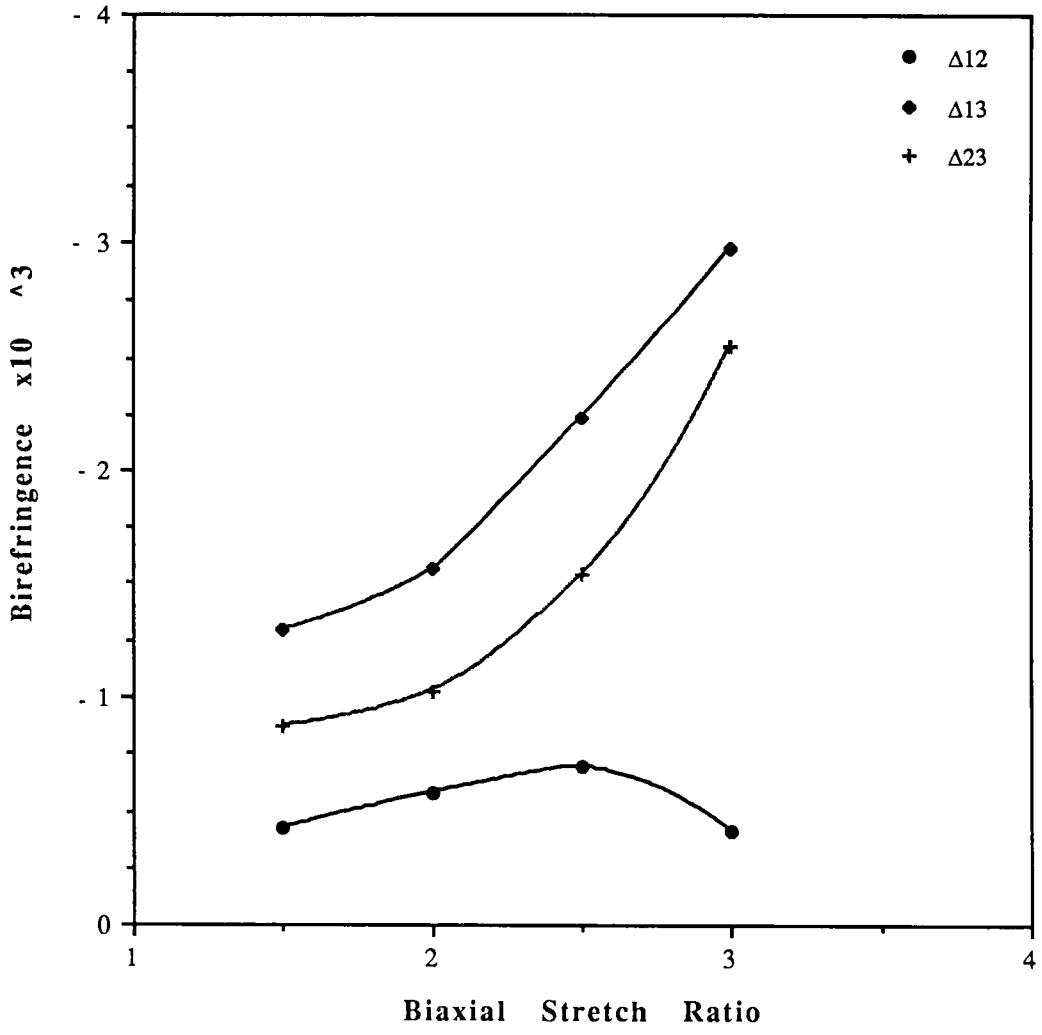


Figure 4.48: High Initial Orientation Areas of S/MA 3000 LLHP-1E extruded and biaxially stretched at 3000%/min and 170 C.

to the extrusion direction, but in the plane of the extrudate sheet or stretched film for all cases reported here. The data in the figures do not show the apparent data scatter (sudden jumps in the birefringence) that were observed in the results in which the initial sample orientations were not monitored. The data in Figure 4.47 for low initial orientation samples are very similar to the data for the compression molded (unoriented) samples shown in Figure 4.4. The data in Figure 4.48 show similar trends obtained from films from extruded specimens where the initial sample orientation is not monitored, but without the data scatter. Thus the cause of the scatter was largely the variability of the initial orientation in the extrudate samples.

Comparing the data in Figure 4.48 to that in Figure 4.47 shows the very substantial effect of the higher initial orientation in the samples used to obtain Figure 4.48. Figure 4.48 shows a higher Δ_{12} birefringence than Figure 4.47, in agreement with the effect expected due to the higher Δ_{12} of the extrudate samples used for Figure 4.48.

It is clear that biaxially stretched films from compression molded plaques of S/MA have more uniform and reproducible properties than those made by their extruded counterparts. The birefringence of films from extruded samples that have been investigated here is not high but seems to have a noticeable effect compared to films from unoriented compression molded plaques.
Figure 4.49 shows a comparison of the orientation resulting from a biaxial stretch of low initial orientation and high initial orientation

areas of the S/MA 3000 FG LLHP-1e extrudate sample. While the samples with low initial orientation develop equal biaxial orientation upon stretching, the samples with high initial orientation do not. The nature of the shift in orientation in the final stretched sample due to the presence of the "high" initial orientation is easily ascertained from examination of Figure 4.49.

S/MA 2000

Figures 4.50 through 4.54 show the distribution of the in-plane birefringence for extruded sheets of the S/MA 2000 grade prepared using differing extrusion conditions. It is again clear that each set of extrusion conditions results in a different birefringence distribution for the as-extruded sheet. Both the magnitude and distribution of in-plane birefringence varied considerably with extrusion conditions. Figure 4.55 was obtained from samples cut from the low orientation areas of the Run 5 Trial 10 extruded sheet (initial biregfringence about -0.2×10^{-3}). Figure 4.56 shows data from samples cut from the high orientation areas of Run 9 Trial 12 (initial birefringence about -1.9×10^{-3}). The effects of molecular orientation are also obvious in these data. Areas of sheet cut from low initial orientation gave birefringence data that were similar to data from compression molded plaques where the in-plane values of the birefringence were very close to zero. Plaques cut from high initial orientation areas gave a non zero value in the in-plane birefringence that was only slightly lower than the starting non-zero value of the in-plane

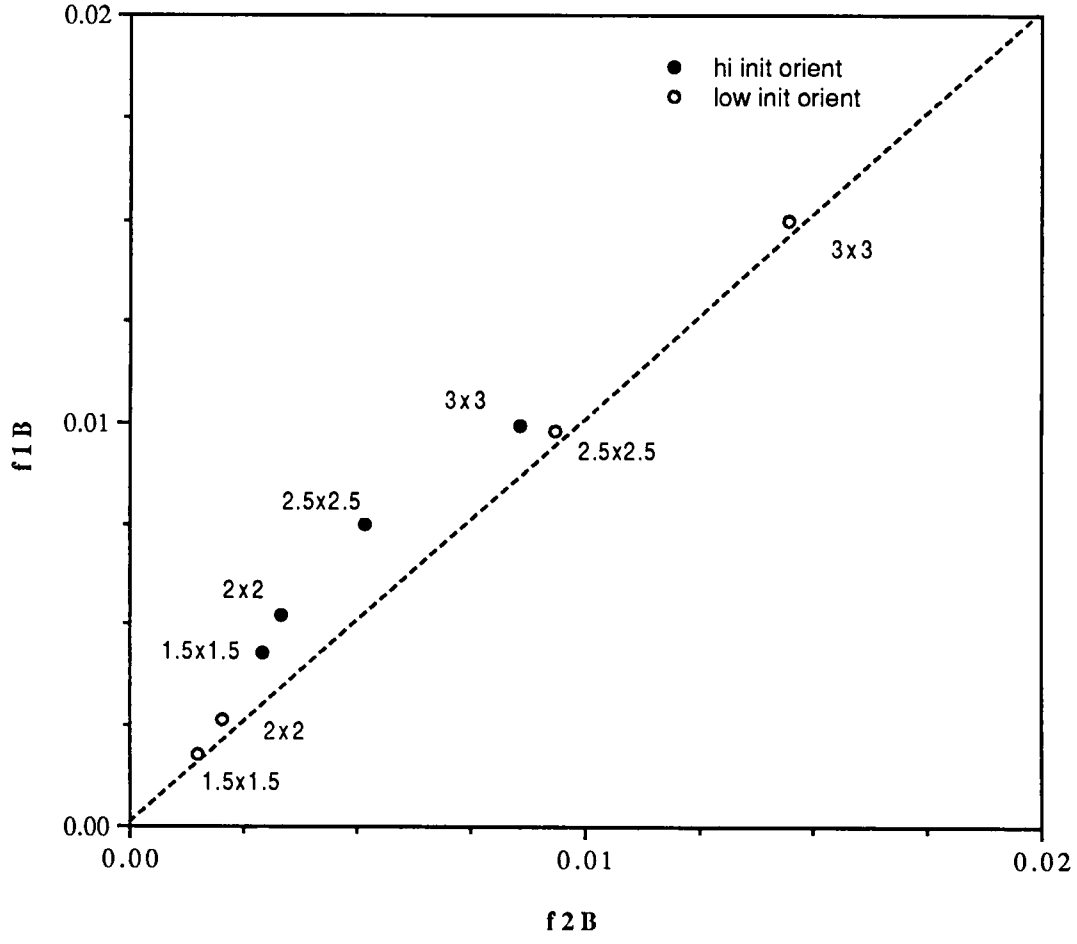


Figure 4.49: Orientation factors of biaxially stretched films from high and low initial oriented areas of S/MA 3000, (3000%/min, 168 +/- 2 C)

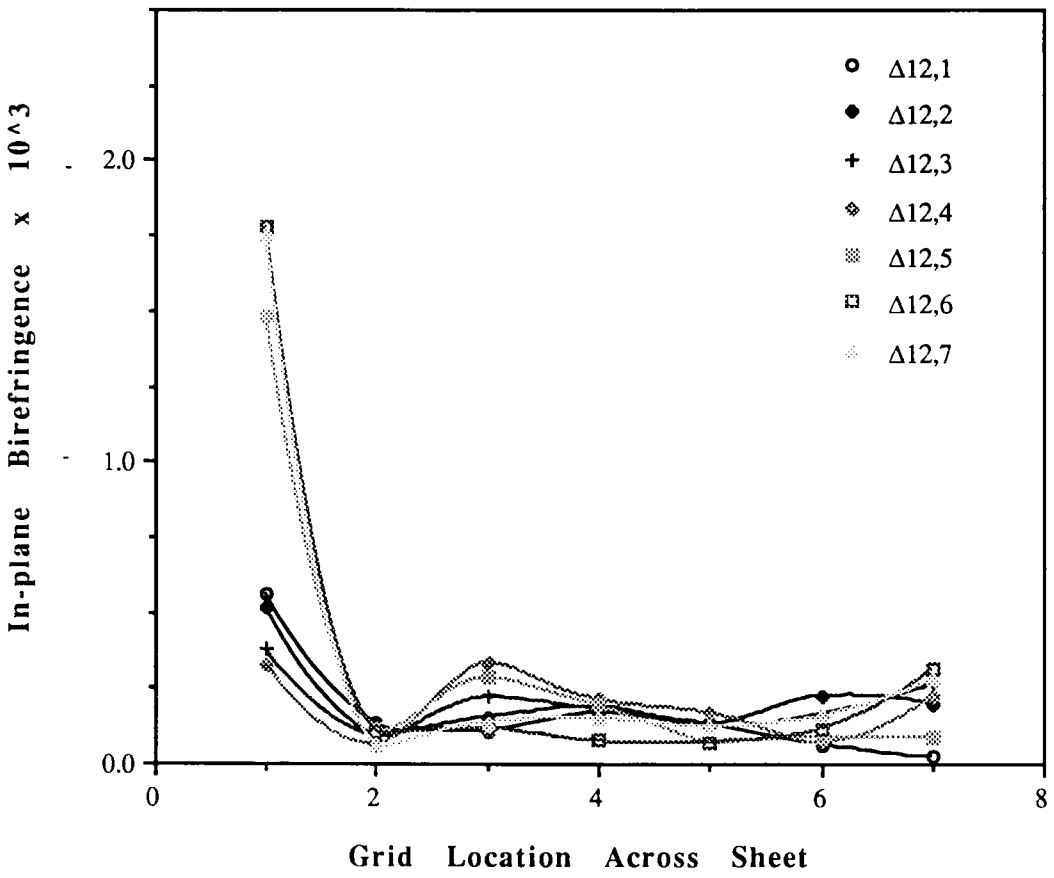


Figure 4.50 In-plane birefringence variation across the width of extrusion for S/MA 2000 run 5 trial 10. Different curves represent variations with grid location along the extrusion direction.

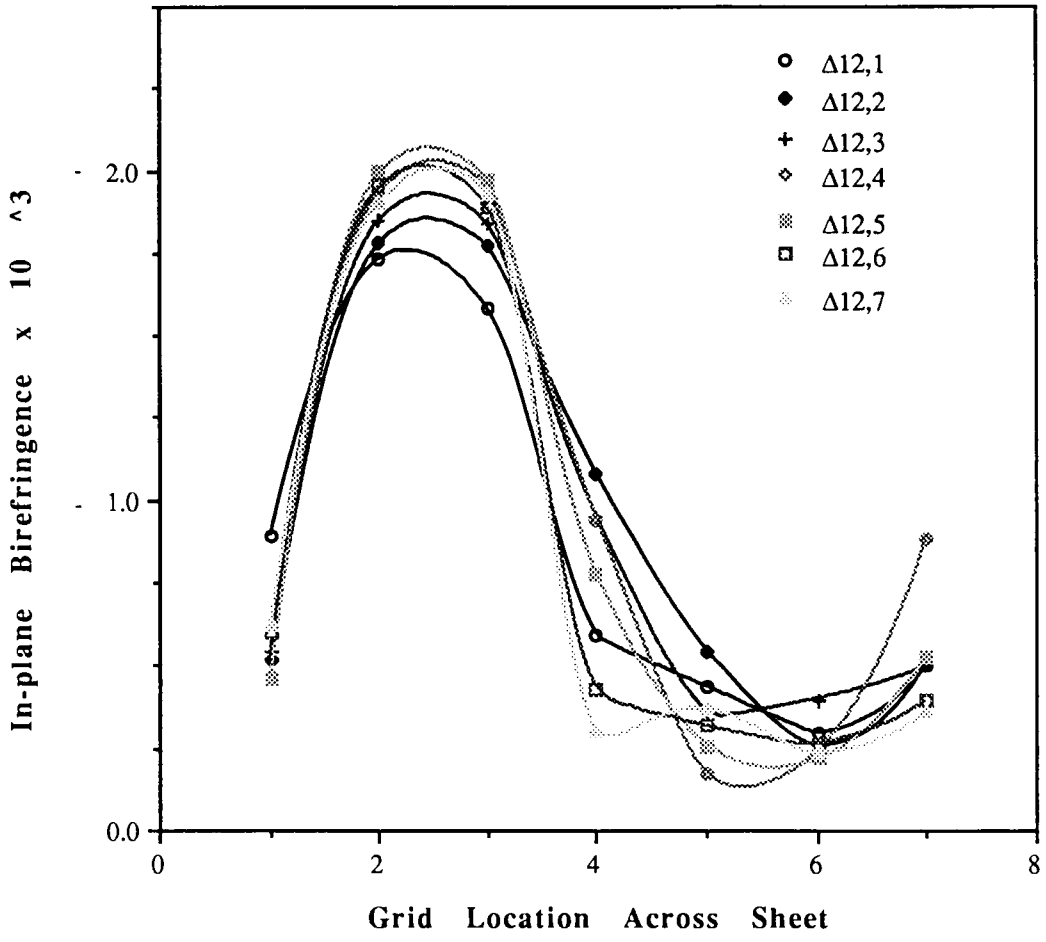


Figure 4.51: In-plane birefringence variation across the width of extrusion of S/MA 2000 fgx run 9 trial 12. Different curves represent variations with grid location along the extrusion direction.

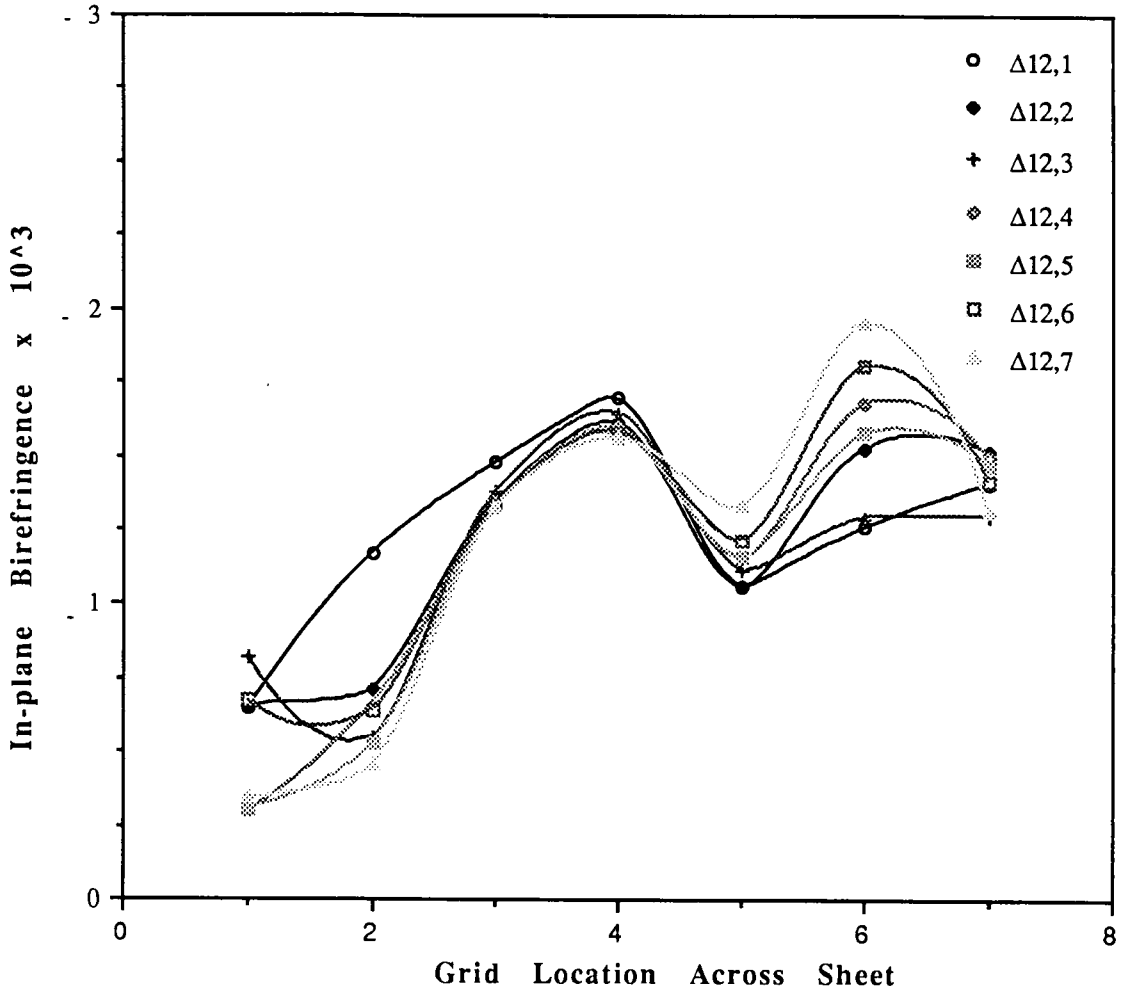


Figure 4.52: Variation in In-plane birefringence across the width of extrusion of S/MA 2000 hhp21-b. Different curves represent variations with grid location along the extrusion direction.

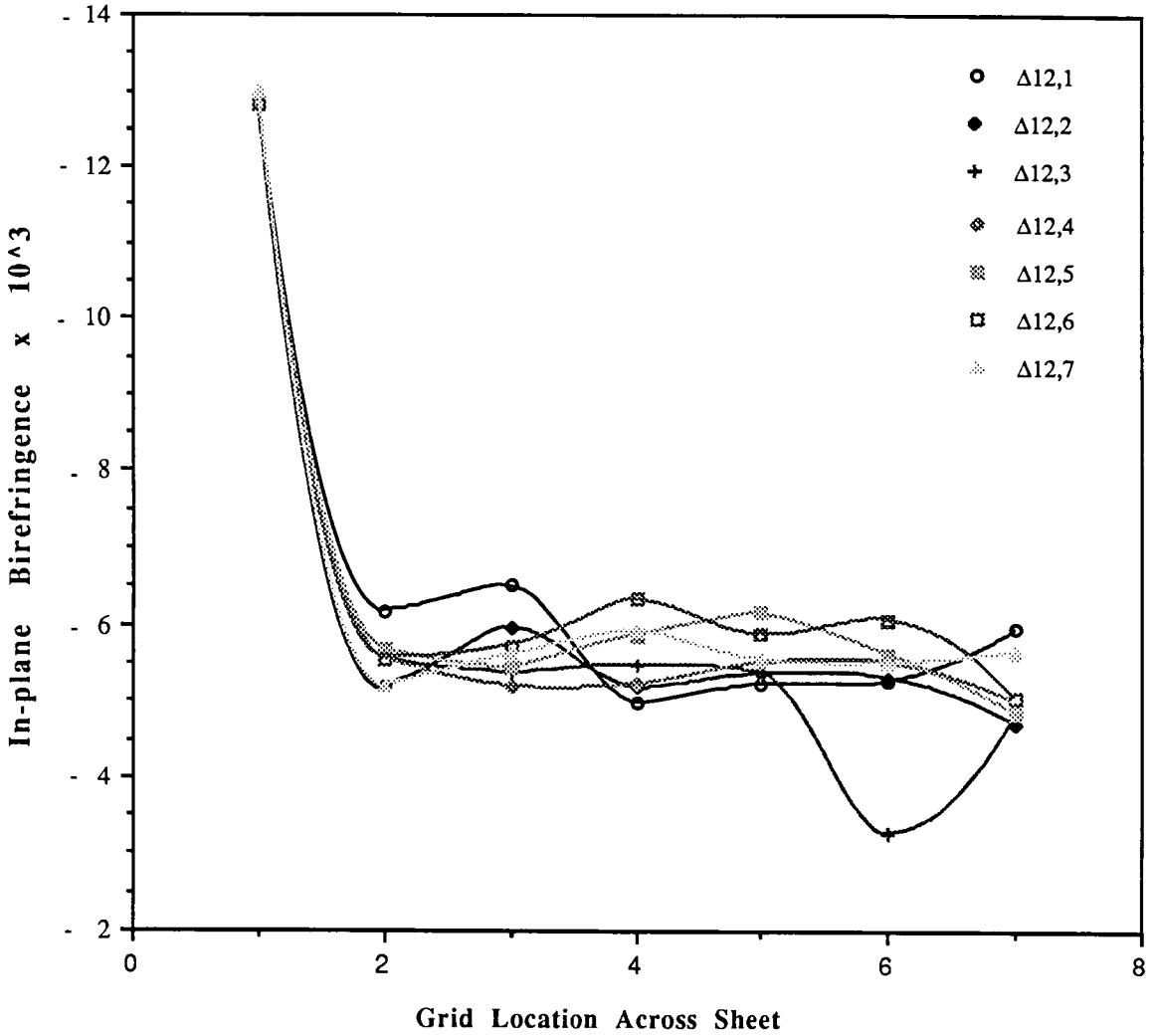


Figure 4.53: Variation in In-plane birefringence across the width of extrusion for S/MA 2000 hhp21-a. Different curves represent variations with grid location along the extrusion direction.

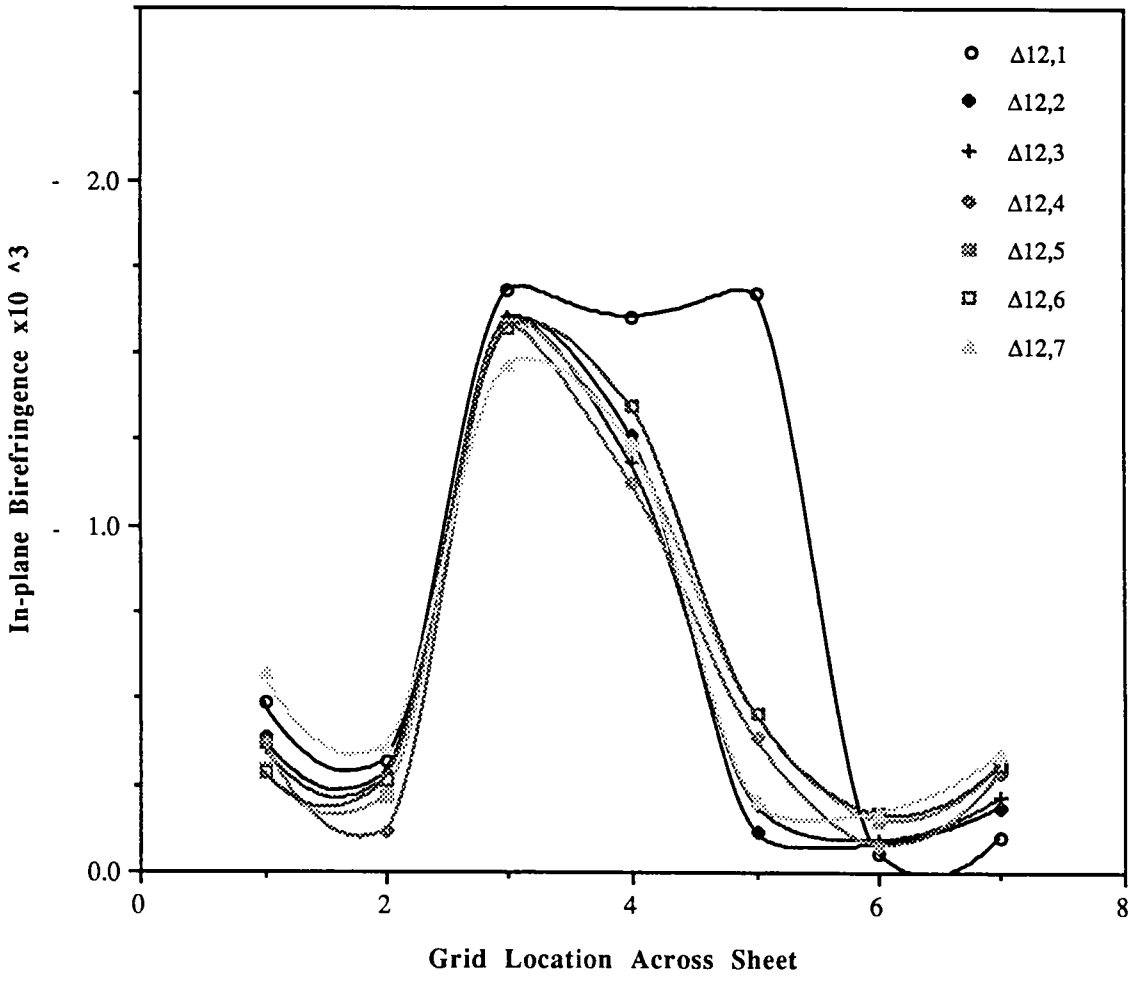


Figure 4.54: In-plane birefringence variation across the width of extrusion of S/MA 2000 run 11 trial 9. Different curves represent variations with grid location along the extrusion direction.

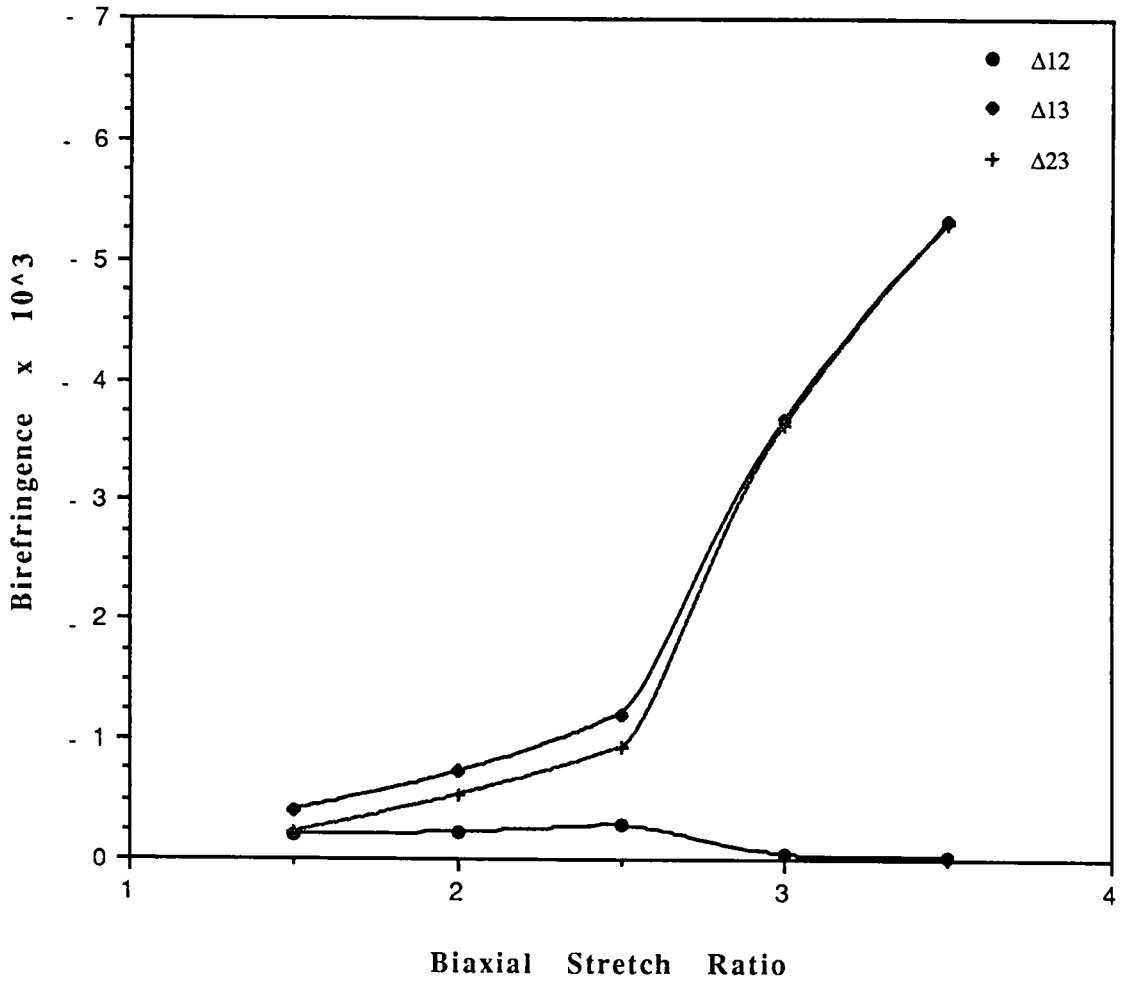


Figure 4.55: Birefringence vs. biaxial stretch ratio for low initial orientation areas of extruded S/MA 2000 (Run 5 Trial 10) sheet biaxially stretched at 3000%/min

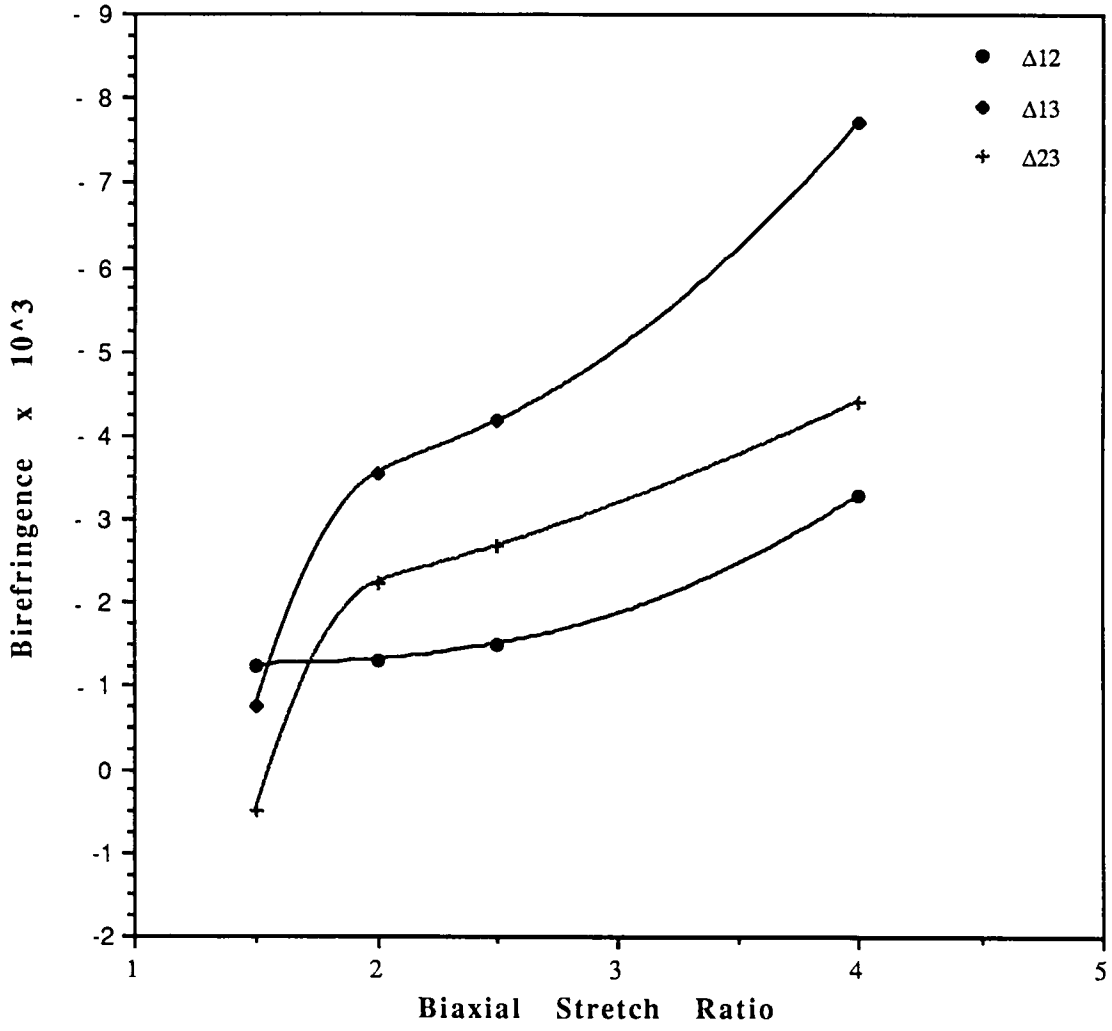


Figure 4.56 Birefringence vs. biaxial stretch ratio for high initial orientation areas of extruded S/MA 2000(Run 9 Trial 12)sheet biaxially stretched at 3000%/min

birefringence. Thus the residual orientation does not relax out fully during the heat-up prior to the stretching process.

With the expectation that residual orientation did not relax out during the stretching process, experiments on 2000 S/MA hhp-21a were carried out with sheets cut from areas with an initial $\Delta 12$ value of about -7.67×10^{-3}. This was done with the intention to produce films with a very high level of orientation. The main assumption being that the residual orientation will add to the orientation induced due to stretching. Several attempts to stretch at identical conditions (3000 %/min and 155°C) failed with the film ripping along the MD repeatedly. An increase in the temperature to 165°C keeping all the other conditions the same, yielded films that could be easily stretched up to equal biaxial stretch ratios of 3.5. The birefringence data of these films are shown in Figure 4.57. These results resemble the data from compression molded plaques. This suggested that the higher stretch temperature had resulted in orientation relaxation prior to stretching.

This led us to investigate the relaxation of residual orientation in the sheet as a function of the stretch temperature when held in clamps of the T.M. Long stretcher for 45 seconds. Figure 4.58 shows that at 155°C there is about 33% relaxation in the as extruded sheet giving a start value in $\Delta 12$ at -5.1×10^{-3} for the stretch process. This value being probably still high, it was not possible to stretch films at all. At 160°C there was about 84% relaxation in the residual orientation due to extrusion while at 165°C there was complete

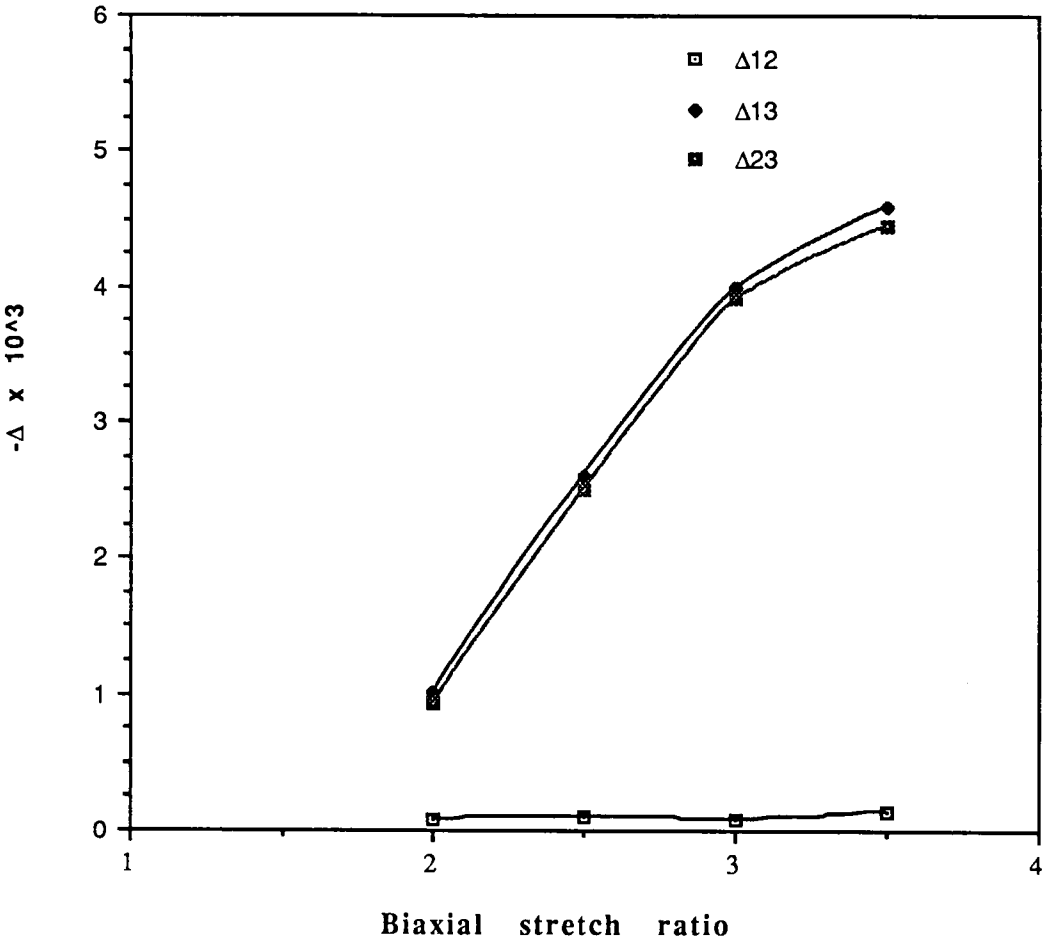


Figure 4.57 Birefringence vs. stretch ratio for extruded 2000 S/MA- llhp-1a at 165 C and 3000 %/min

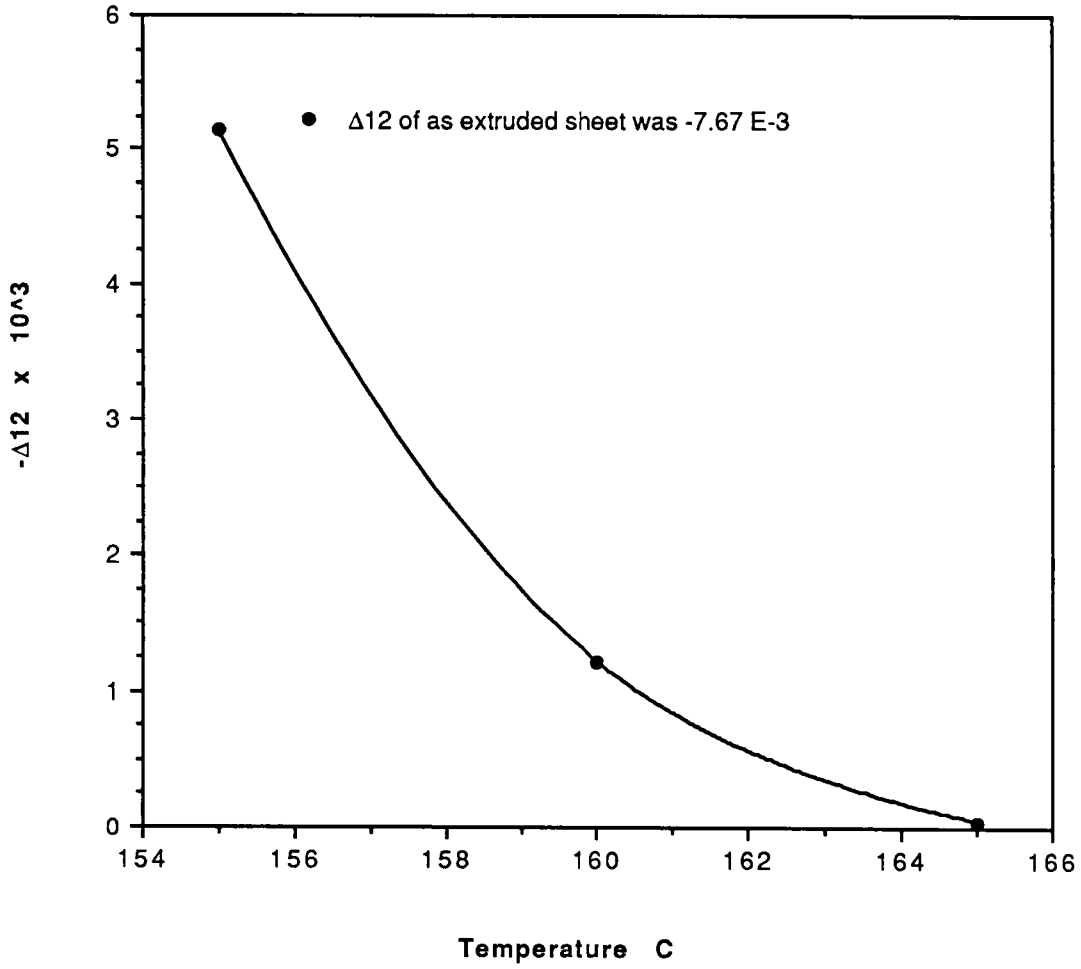


Figure 4.58 Effect of stretch temperature on relaxation of residual orientation of extruded sheet llhp-21a -S/MA 2000

recovery to random in-plane distribution of the chains. The sheets no longer behaved like extruded specimens and could be stretched easily.

With the above data in mind we can say that the key variables in stretching from extruded sheets are the magnitude of residual orientation induced due to the extrusion process and the stretch temperature. If the sheet prior to stretching has a very high level of residual orientation then it is likely that it may not stretch at all and if it does stretch, it may not have reproducible properties. Increase in the stretch temperature, the magnitude of which will depend from case to case will eliminate the effects of extrusion by relaxation to yield films with uniform properties over the area of the film. Too high a relaxation and stretch temperature will result in decreased levels of orientation. Thus for most optimum levels of orientation and success during stretching, the lowest temperature must be determined at which there is a relaxation of any high levels of residual orientation. It would probably be feasible to relax the initial orientation at one temperature and stretch at another, lower temperature in order to produce desired molecular orientation and production levels. However, this produces additional complications in the processing schedule.

CHAPTER 5

SUMMARY AND CONCLUSIONS

1. There is clearly a distinct difference in the processing temperatures of polystyrene and S/MA copolymers. Increase in the level of maleic anhydride increases the processing temperature needed for stretching into films. Approximate optimum stretching temperatures for the three materials studied here were 140°C for polystyrene (Dylene 8G), 155°C for the 8 % MA copolymer (Dylark 2000) and 170°C for the 14 % MA copolymer (Dylark 3000).

2. For each material the magnitude of molecular orientation developed by stretching is very sensitive to the stretch temperature. It is best to use as low temperatures as possible to develop maximum molecular orientation.

The above temperatures were chosen after many attempts to stretch in a range of temperatures. However one will have to employ higher temperatures when higher stretch ratios are needed. The resulting decrease in orientation with an increase in the stretch temperature can possibly be reduced by employing the highest strain rate possible. From a practical view point, considering both magnitude of orientation and the stretching success ratio, a temperature of 130°C, 155°C and 165°C for PS, S/MA 2000 and

S/MA 3000 respectively would probably be optimum for manufacturing processes employing 2.5 x 2.5 stretch ratios.

3. S/MA copolymer films prepared under approximately optimum stretching conditions have significantly greater tensile strengths than polystyrene. For the grades investigated the tensile strengths decreased in the following order: Dylark 3000 FG > Dylark 2000 Fg > Dylene 8G.

5. There was no major difference in the elongation to break with change in stretch ratios for S/MA 3000 and S/MA 2000. All values of elongation recorded were between 4 and 10%. Polystyrene however did show a change from brittle to ductile failure with increase in stretch ratio and a maximum of 33 % for a 4.5 MD X 1.5 TD ratio was recorded.

6. Polystyrene films prepared from plaques of 21 mils starting thickness gave superior properties to films prepared from 26 or 14 mils thick samples. It can be safely said that molecular orientation plays an important role in determining the behavior of polystyrene films, but it is not entirely clear what role, if any, sample thickness plays.

7. The amount of shrink or recovery in the film was proportional to the molecular orientation induced due to the

stretching process and followed a similar trend as the birefringence as a function of stretch ratio.

8. The shift in temperatures required to induce shrinkage in the three grades is more dependent on the chemical composition of the polymers and the glass transition temperatures than the level of orientation.

9. Residual orientation present in extruded sheet can have a marked effect on the orientation of stretched samples prepared from them. The initial orientation can change both the nature and magnitude of the orientation developed during stretching. Further, the initial orientation in extruded sheet is frequently nonuniform across the sheet, and the nature and magnitude of initial orientation varies considerably with the extrusion conditions. This suggests that it would be best to either induce as low orientation level as possible during extrusion or heat at one temperature and stretch at another lower temperature, if stretched materials are to have uniform and reproducible levels of orientation.

REFERENCES

REFERENCES

1. ASTM D 882-83, 451, (1988).
2 Modern Plastics, Vol. 69,1, (1992).
3 Francis, P.S., A.D.Wambach, Engg. Matls. Handbook, Vol. 2, 217 (1988).
4 Seymor, R. B., C.E. Carrater, Jr.,"Polymer Chemistry an Introduction" Marcel Dekker, Inc., N.Y.(1981).
5 Concise Encl. Pol.Sci.Eng. 1115, (1990).
6 Moore, E.R., Ind. Eng. Chem. Prod. Res. Dev., 25, 315-321 (1986).
7 Studt, E. and U. Meyer, U.S.Patent 2,074,285 (1937).
8 Modern Plastics Encyclopedia, Biaxial Orientation, Alan J Stoppard, 382, (1991).
9 Whiteside, R., Modern Plastics Enc., 332, (1991).
10 Desper, R.,CRC Crit. Rev.M.Sci, 2, 501 (1973).
11 Brewster, D., Phil. Trans. R. Soc,106, 156 (1816).
12 Matsumoto T. and D.C. Bogue J. Poly. Sci., A2 15 1663,(1977).
13 Han, C.D. and L.H. Drexler, J.App.Poly.Sci.17, 2329, (1973).
14 Wales, J.L.S., Rheol.Acta 8, 38 (1969).
15 Oda,K, J.L.White, E.S.Clark, Poly.Eng.Sci,18,53 (1978).
16 Choi, K.J., Thesis, University of Tennessee (1990)
17 Choi, K. J., J.L.White, J.E. Spruiell,J. App.Poly. Sci.25, 2777
18 Deitz,W., J.L.White, E.S.Clark, Poly. Eng. Sci.18,273 (1978).
19 Janeschitz-Krieg 1,H., Rheol.Acta, 16, 327 (1977).
20 Carothers,W.H., J.W.Hill, J.Am.Chem.Soc.,54, 1579, (1932).

21 Sisson,W.A., G.L. Clark, Ind. Eng. Chem., Anal.Ed., 5, 296 (1933).

22 Heffelfinger,C.J., R.L.Burton, J.Poly.Sci., 47, 289, (1960).

23 Hermanns,P.H., P.Platzek, Koll.Zeit., 88, 68 (1939).

24 Stein, R.S., J.Poly.Sci., 31, 327, (1958).

25 White,J.L., J.E.Spruiell, Poly. Eng. Sci., 21, 859, (1981).

26 Nomura, S., H. Kwai, I. Kimura, M. Kagiyayama, J. Poly. Sci. A2, 8, 383 (1970).

27 Alexander, L.E., "X-Ray Diffraction Methods in Poly. Sci"., R.E.

28 Enc. Pol. Sci. and Tech., Orientation, vol 9, M-P, 635, (1968)

29 Samuels, R. J., J. Poly. Sci., A-3, 1741, (1965).

30 Schmidt, P.J., J.Poly.Sci., Part A-1, 1271 (1963).

31 Wolfram L.E., J.G. Grassel, J.L.Koenig, App. Spect.24, 263, (1970).

32 J.L. Koenig, S.W. Cornell, J. Macromol.Sci., B-1, 279 ,(1967).

33 Nomura, S., H.Kwai, I. Kimura and M. Kagiyama, J.Poly. Sci., A2, 5, 479 (1967).

34 Moseley, W.W., J. App. Poly. Sci., 3, 266 (1960).

35 Samuels, R.J., J. Poly. Sci., 31, 335, (1958)
Krieger publishing Co., N.Y. (1979).

36 Slayter, E.M., "Optical Methods in Biology", Wiley-Interscience, N.Y. (1970).

37 Page, L., N.E. Adams, "Electrodynamics", Van Nostrand, N.Y. (1940).

38 Gurnee, E.F., J.App.Poly.Phy., 25, 1232, (1954).

39 Onogi, Y., J.L.White, J.F. Fellers, J.N.Newt.FM., 7, 121 ,(1980).

40 Denbigh, K.G., Trans. Far.Soc. 121, 36, 936,(1940).

41 Bunn. C.W., R. Daubney, Trans. Far. Soc., 50, 1173 (1954)

42 Wang, S.N., J.Chem. Phy., 2, 1012 (1939).

43 Stein, R.S., J.Poly.Sci., Part A-2, 7, 1021 (1969).

44 Choi, K.J., J.E.Spruiell, J.L. White. Poly. Eng. Sci., 29, 1516, (1989).

45 Matsumoto, J.F.Fellers, J.L.White, J.App.Poly.Sci., 26, 85-96 (1981).

46 Stein, R.S., J. App. Phy., 32, 7, 1280 (1961).

47 Miligan, M.F., A.D. Gabaraayeva, I.I.Sishkin, Poly.Sci. USSR, 12, 513 (1970).

48 Matsumoto, K., I. Hirohiko, Sen.i-Gakkaish 35, 150 ,(1979).

49 Muller, F.H., Koll. Zeit., 95, 138,(1941).

50 Khun, Grun, Helv. Chim. Acta., 26, 1394 (1943).

51 Tech. Spec. Sheet, (Dylark and Dylene)ARCO Chemical Co.

52 Stein R.S., D.R. Paul, Poly. blends, Newmans Eds., Vol.1, Ch.9, Academic Press, N.Y. (1978).

53 Stein, R.S., F.H.Norris, J.Poly.Sci. 21, 381, (1956).

54 Brann, J.E., M.S.Thesis, University of Tennessee, Knoxville (1985).

55 Feynman, R. P., R. B. Leighton and M. Sands. "The Feynman lectures on Physics", Vol 1, Addison- Wesley Publishing Co. Inc. MA- (1963).

56 Hemsley, D.A., "Light Microscopy of Synthetic Polymers". Oxford Science Publications, (1984).

57 Choi, K. J., J.L. White and J.E. Spruiell, Poly. Eng. Sci., Vol 29, 21, 1516 (1989).

58 Ekio, I., H. Takashi, and H. Yasuji., J. App. Poly. Sci., Vol 22, 3193- 3201 (1978).

59 Ferry, J.D., J. Am. Chem. Soc. 64, 1330 (1942).

VITA

Naveen Bhojraj was born in Bangalore in the state of Karnataka in India on July 20, 1965. He entered the Department of Polymer Engineering in Maharashtra Institute of Technology (University of Poona) in August 1983 and received a Bachelor of Engineering in July of 1987 with distinction. He then worked as an Application Development Engineer- Plastics. at Siroplast Ltd, a subsidiary of a leading automotive corporation, for two and a half years. He joined the Polymer Engineering Program at the University of Tennessee, Knoxville in the spring of 1990 and received his Master of Science degree in August of 1992. He is also a current member of SPE.

Upon graduation he will be working at H-C industries, a division of ALCOA at Crawfordsville, Indiana as a Chemical Engineer - R&D and will be working in the area of polymer blends for closure applications in the beverage and related market segments.